Catalytic Asymmetric Alkylations of Latent Enolates

by

Michael J. Nardone

Bachelor of Science, The College of New Jersey, 2010

Submitted to the Graduate Faculty of

The Dietrich School of Arts and Sciences in partial fulfillment

of the requirements for the degree of

Doctor of Philosophy

University of Pittsburgh

2016

UNIVERSITY OF PITTSBURGH

DIETRICH SCHOOL OF ARTS AND SCIENCES

This dissertation was presented

by

Michael J. Nardone

It was defended on

January 5, 2016

and approved by

Peng Liu, PhD, Assistant Professor, Department of Chemistry

Lee A. McDermott, PhD, Assistant Professor, Department of Pharmaceutical Sciences

Tara Y. Meyer, PhD, Associate Professor, Department of Chemistry

Dissertation Advisor: Scott G. Nelson, PhD, Professor, Department of Chemistry

Catalytic Asymmetric Alkylations of Latent Enolates

Michael J. Nardone, PhD

University of Pittsburgh, 2016

Transition metal-catalyzed asymmetric allylic alkylations have become increasingly important in constructing highly versatile carbon-carbon and carbon-heteroatom bonds. However, diastereoselective allylic alkylations capable of setting vicinal stereocenters remain rare. The text herein describes a Ru(II)-catalyzed allylic alkylation that utilizes silyl enol ether nucleophiles to provide α,β-substituted-γ,δ-unsaturated acyl pyrroles in synthetically useful diastereoselectivities. To illustrate the value of the resulting products, the methodology was exploited to construct the core of a pharmacologically active target, actinoranone.

TABLE OF CONTENTS

LIST OF TABLES

LIST OF FIGURES

LIST OF SCHEMES

LIST OF ABBREVIATIONS

AAA…….Asymmetric Allylic Alkylation

Akt……...Protein Kinase B (PKB)

ATP…….Adenosine Triphosphate

BSA……..Bis(trimethylsilyl)acetamide

CDK…….....Cyclin-dependent Kinase

CNQ-027……Marine Actinobacterial Strain

COD……..Cyclooctadiene

COE……Cyclooctene

Cp…….....Cyclopentadienyl

Cp*……..Pentamethylcyclopentadienyl

CSA…….....Camphorsulfonic Acid

Cy……Cyclohexyl

DCE…….....Dichloroethane

DCM…….....Dichloromethane

DiBAlH…….....Diisobutylaluminum Hydride

DMAP……..4-Dimethylaminopyridine

DME……..Dimethoxyethane

DMF…….....*N,N*-Dimethylformamide

DMS…….Dimethylsulfide

DMSO……Dimethyl Sulfoxide

dr…….Diastereomer Ratio

EAS…….....Electrophilic Aromatic Substitution

ee……..Enantiomeric Excess

EI…….Electron Ionization

Equiv…….Equivalent

GC……Gas Chromatography

HCT-116……Human Colorectal Carcinoma Cell Line

HMPA……Hexamethylphosphoramide

HPLC…….....High Pressure Liquid Chromatography

HRMS……..High-Resolution Mass Spectrometry

IC_{50}……..Half Maximal Inhibitory Concentration

LA……Lewis Acid

LD_{50}…….....Median Lethal Dose

LDA…….Lithium Diisopropylamine

LiHMDS……Lithium Hexamethyldisilazide

mCPBA…….....3-Chloroperoxybenzoic Acid

MMP…….Matrix Metalloporteinase

MS……..Molecular Sieves

NaHMDS…….....Sodium Hexamethyldisilazide

NBS…….*N*-Bromosuccinimide

PDB……..Protein Data Bank

PPA……..Polyphosphoric Acid

RT…….....Ambient Temperature

TBAF……..Tetrabutylammonium Floride

TBD……..Triazabicyclodecene

TC……..Thiophene-2-carboxylate

Tf……..Trifluoromethanesulfonyl

THF……..Tetrahydrofuran

THIF……Trihydroxyisoflavone

TLC……..Thin Layer Chromatography

TMS……Trimethylsilyl

TMSCl……..Trimethylsilyl Chloride

PREFACE

The research presented here represents countless hours of experimentation on my part; yet, none of this work would be possible without the extensive support system from which I have obviously benefitted. While there are many individuals to whom I owe a debt of gratitude, I would like to take this opportunity to thank some of them here.

First, I would like to thank Prof. Scott G. Nelson, who brought me into his chemistry family, a generous act which has forever changed my life for the better and which I will unlikely be able to repay.

Many thanks to my graduate student mentor, Dr. Maryll E. Geherty who has taught me everything I know about practical organic chemistry. And, of course, Richard J. Liberatore, who for the past three years has been not only my collaborator, but also my friend. I owe the both of you a few rounds of beer.

I would also like to thank my family, especially Ronald and Janice Nardone and Julia and Eric Yoskowitz, who think that I'm a mad scientist, but have supported my dreams nonetheless.

Finally, I am forever indebted to Meagan McElroy, my partner in crime who moved with me to a strange city to start our lives together. I dedicate this document to you.

1.0 INTRODUCTION TO ASYMMETRIC ALLYLIC ALKYLATIONS

Asymmetric allylic alkylations (AAAs), the nucleophilic attack on a metal-bound allyl substrate, were first described in the mid-20th century.[1-4] Allylic alkylations attract synthetic chemists for their ability to access versatile carbon-carbon and carbon-heteroatom bond constructions (Figure 1).[5-9] Palladium(II) based systems, the seminal and most developed AAA reaction type, efficiently provide corresponding products with a high degree of selectivity; the linear regioisomer predominates under palladium-catalyzed conditions.[10,11] To access the branched regioisomer, other metal sources must be employed.[7, 8, 12-19] Reactions that favor branched isomer formation automatically establish an allylic stereocenter; achieving enantioselectivity at the newly formed bond proves critical for synthetic utility.

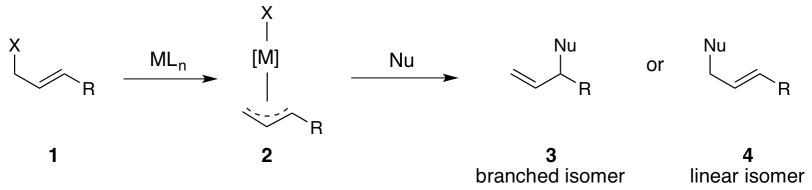

Figure 1: General Allylic Alkylation

Allylic alkylations traditionally employ simple, symmetrical nucleophiles, often 1,3-dicarbonyl enolates,[2] inherently limiting the reaction to setting only the allylic stereocenter. Utilizing prochiral nucleophiles establishes a second, vicinal stereocenter, building additional molecular complexity, but also introducing the need for diastereoselective control (Figure 2). Few reported methodologies explore allylic alkylations capable of setting vicinal stereocenters

with regio-, diastereo-, and enantioselectivity.[20] Establishing two vicinal tertiary stereocenters has proven particularly evasive due to the possibility of epimerization at the α-carbon under the reaction conditions.[20] Therefore establishing a novel allylic alkylation proficient in setting adjacent stereocenters with a high degree of diastereoselectivity presents a current synthetic need.

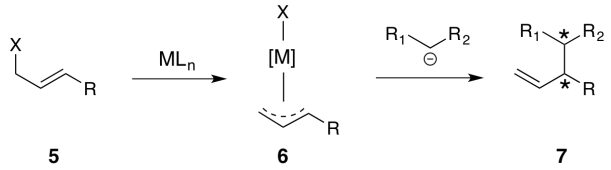

Figure 2: Diastereoselectivity Consequences of Prochiral Nucleophiles

1.1 ORIGINS OF TRANSITION METAL CATALYZED AAA

1.1.1 Palladium-catalyzed Allylic Alkylations

Electrophilic metal-allyl complexes appeared in 1965.[1] The foremost allylic alkylation reports the nucleophilic addition of diethyl sodiomalonate to allylpalladium(II) chloride complex (Scheme 1, Equation 1).[1] However, the required stoichiometric amount of palladium eclipsed the synthetic value of an electrophilic allyl ligand. Introducing phosphine ligands to the palladium(II) system circumvented this issue, allowing for a catalytic amount of metal to be used instead, thereby increasing reaction viability and ubiquity (Equation 2).[3] The early developments defined allylic alkylations. These studies established that soft nucleophiles, such as enolates, readily add into η^3-allyl ligands. Further, oxidative insertion into allylic halides or allylic

acetates provides the requisite metal-allyl complex. The precedent established allylic alkylations as a new reaction type.

Scheme 1: Seminal Allylic Alkylations

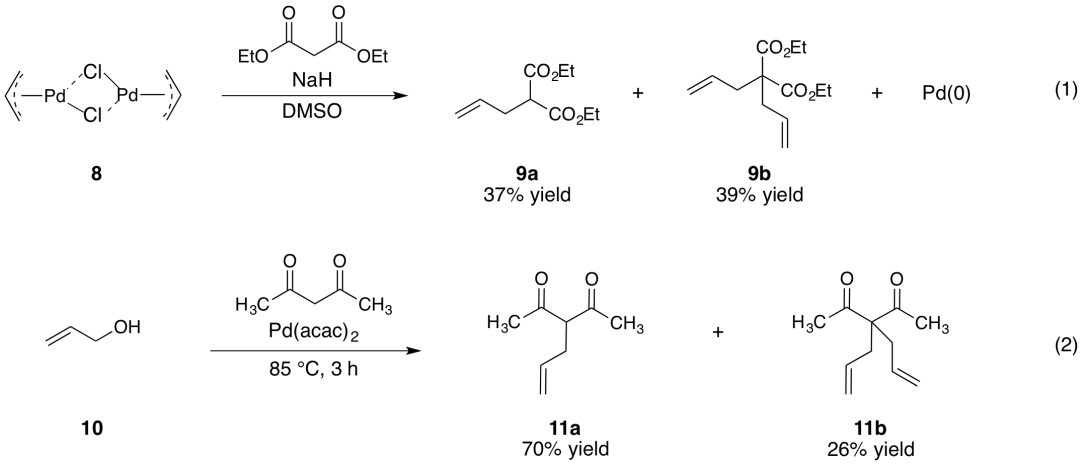

Utilizing unsymmetrical allylic substrates results in the formation of two possible regioisomeric products. Alkylation occurs at either the less or more substituted carbons of the π-allyl ligand, resulting in the linear and branched products respectively.[10] Palladium-catalyzed allylic alkylations usually yield the linear products regioselectively. For example, exposing di-μ-chlorobis(1-ethyl-2-propyl-π-allyl)dipalladium (**12**) to diethyl sodiomalonate and triphenylphosphine in THF favored the combined linear products 8:1 over the branched product (Scheme 2, Equation 3).[10] Cyclic electrophiles present the same selectivity (Equation 4). Consistently, when no strong electronic bias exists between carbons one (C_1) and three (C_3) on the π-allyl ligand, palladium-catalyzed reactions favor the linear product. Therefore, accessing the branched regioisomer requires metal centers more sensitive to subtle electronic differences.

Scheme 2: Regioselectivity of Palladium-catalyzed Allylic Alkylations

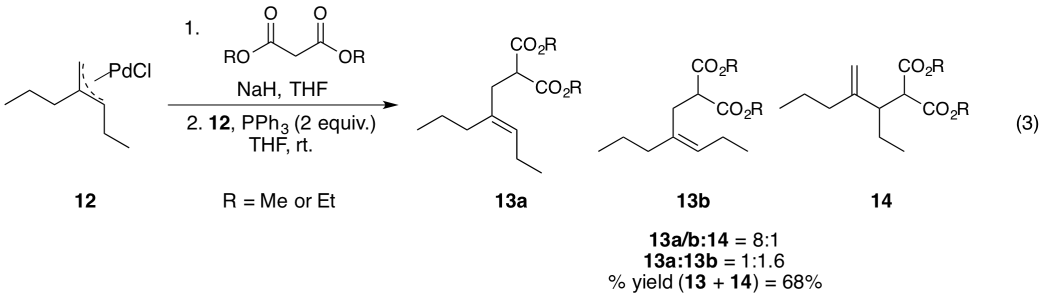

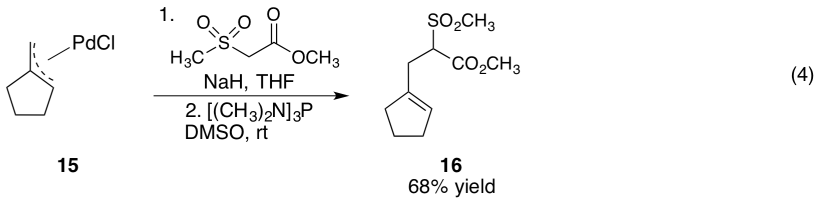

When neither C_1 nor C_3 of the palladium-allyl electrophile resides at the molecule's terminus, the resulting alkylation establishes an allylic stereogenic center. The seminal example induced enantioselectivity by utilizing a chiral phosphine rather than triphenylphosphine as the ligand source (Scheme 3, Equation 5).[4] Under these conditions, the product was obtained in 24% optical yield. Employing chiral phosphine ligands became standard procedure for achieving optically active products from allylic alkylations. Developing more structurally complex phosphine ligands with improved optical purities paralleled improvements in palladium-catalyzed allylic alkylations (Equations 6 and 7).[7, 21] Fortunately, this foundation directly translates to allylic alkylations with other metals.

Scheme 3: Examples of Asymmetric Palladium-catalyzed Allylic Alkylations

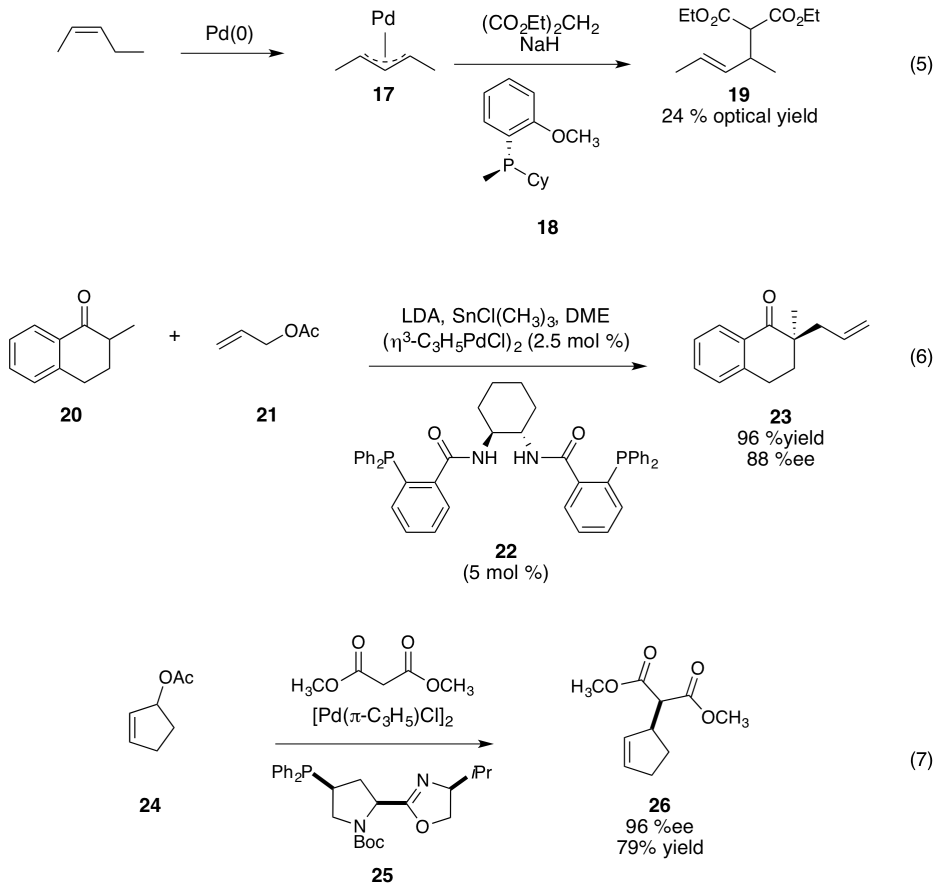

1.1.2 Branched Regioselectivity via Non-palladium Metals

A variety of metal sources have been used in allylic alkylation reactions, including molybdenum,[7, 8, 12, 13] tungsten,[8] copper,[7, 14] rhodium,[7, 16] iridium, [7, 8, 15] and ruthenium.[7, 17-19] In contrast to palladium, the alternative metal sources favor branched regioisomer formation under analogous conditions to the seminal asymmetric alkylations. For example, Mo(0) and methyl sodiomalonate alkylate methyl cinnamyl carbonate with complete regioselectivity (Scheme 4, Equation 8).[13] Similarly, Ir(I) catalyzes the alkylation of carbonate **27**, favoring the branched isomer 20:1 over the linear product (Equation 9).[22] The preference for branched product

formation becomes particularly apparent wherein the alkylation forms the quaternary carbon over the linear isomer under Rh(I) conditions (Equation 10).[23] Nucleophilic attack at the more substituted carbon of the allyl ligand establishes a stereogenic center. The above examples efficiently obtain complete enantioselectivity by employing chiral, sterically demanding ligands.

Scheme 4: Branched Regioisomer Formation via Alternative Metal Sources

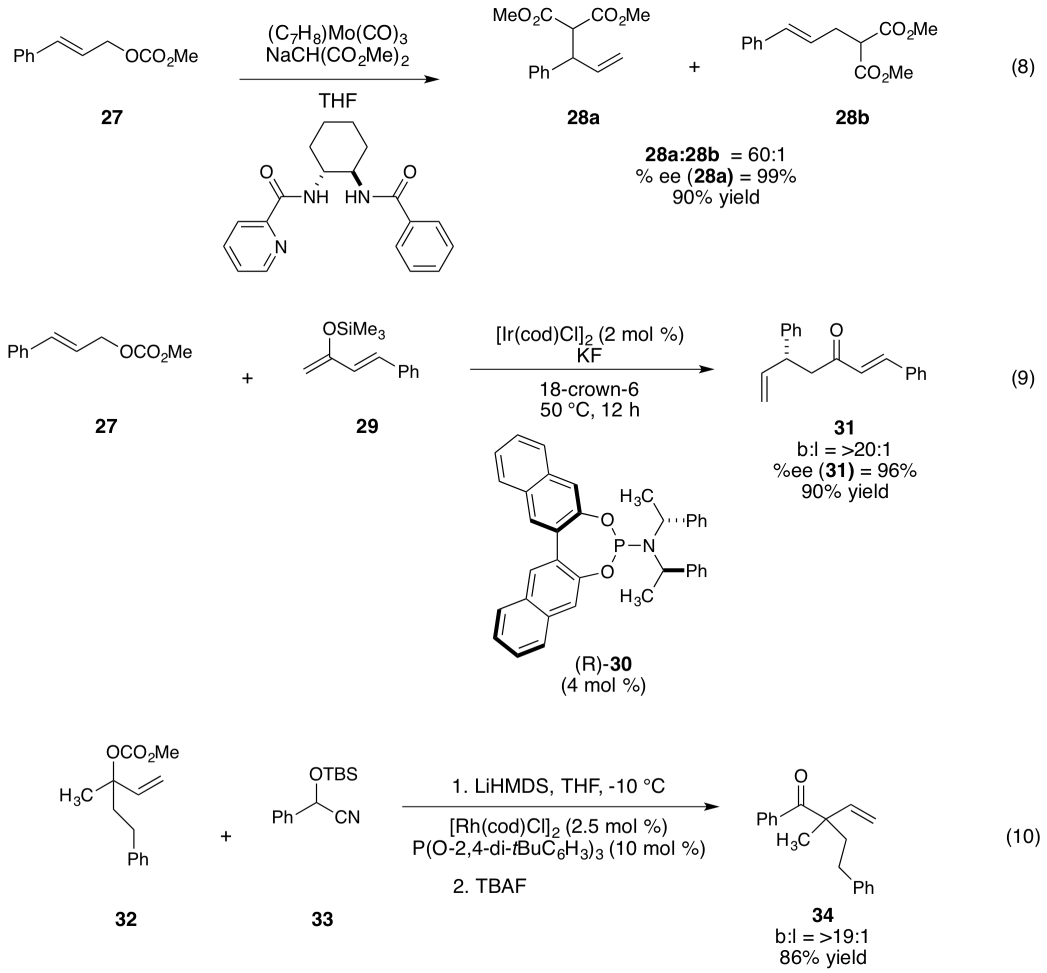

1.2 AN ASYMMETRIC CLAISEN REARRANGEMENT

In 2010, our group developed an asymmetric ruthenium(II)-catalyzed Claisen rearrangement of un-activated allyl vinyl ethers. Exposing the ethers to cyclopentadienyltris(acetonitrile)ruthenium(II) hexafluorophosphate ($[CpRu(CH_3CN)_3][PF_6]$), a chiral pyridyl aminoindanol ligand **36**, and a triphenylborate co-catalyst yielded α,β-substituted-γ,δ-unsaturated aldehydes (Equation 11).[24, 25] This method efficiently provides Claisen-type products with vicinal stereocenters in a single transformation. Further, the products contain two chemoselective handles, making them desirable intermediates in target-oriented synthesis. However, systematic probing of the reaction revealed vulnerabilities in the process. While enantioselectivity was consistent regardless of the substrate, the regio- and diastereoselectivities were substrate dependent and thereby limited the reaction scope. Understanding the origins of these limitations would allow for reaction modification, and hopefully, improvements in regio- and diastereoselectivity.

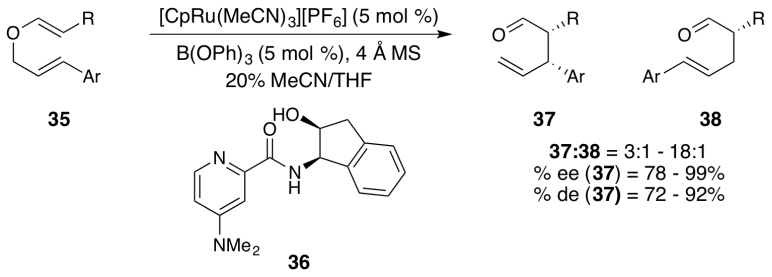

(11)

The regioselectivity of the asymmetric Claisen reaction depended highly on the electronic nature of the allyl fragment.[24, 25] Electron-rich aryl groups favored formation of the branched product by 14:1 (Figure 3). Conversely, electron-deficient aryl groups demonstrated only limited selectivity in favor of the branched isomer (4.7:1). It was discovered that an aromatic group was requisite for any regioselectivity; substitution of an alkyl group for an aryl group resulted in no

regioselective preference between the two isomers. A reaction modification, or the development of a new reaction mechanism, would expand the observed regioselectivity. Ideally, branched isomer formation would be independent of the electronic nature of the allyl ligand and capable of incorporating electron-deficient and alkyl derived groups into the reaction methodology.

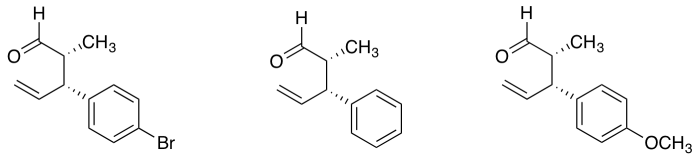

39
b:l = 4.7:1
anti:syn = 25:1
ee = 92%
92% yield

40
b:l = 5.3:1
anti:syn = 20:1
ee = 93%
91% yield

41
b:l = 14:1
anti:syn = 18:1
ee = 91%
86% yield

Figure 3: Electronic Effects on Alkylation Regioselectivity

Diastereoselectivity of the aforementioned catalyzed-Claisen rearrangement depends on the vinyl olefin, specifically, whether the double bond was set as the *E* or *Z* isomer.[25] The *E*-alkene provides the *anti*-diastereomer exclusively, while the *Z*-alkene yields the *syn*-diastereomer; therefore setting the double bond geometry of the vinyl portion of the ether was critical to reaction success. An iridium-catalyzed isomerization set the requisite vinyl alkene for the sigmatropic rearrangement. This method demonstrates complete selectivity for the *E*-alkene when the final R group was methyl. However, other alkyl chains, such as ethyl, showed no selectivity about the double bond and these isomers were inseparable by column chromatography (Equation 12). Therefore, the substrate scope was inherently limited at the cost of diastereoselectivity erosion. To eliminate this obstacle, two considerations needed to be evaluated: 1) the improved reaction would provide viable diastereoselectivities regardless of the double bond geometry of the vinyl fragment or 2) consistently provide the needed bond geometry independent of the substrate. By controlling either of these factors, consistent, synthetically useful diastereoselectivities were expected.

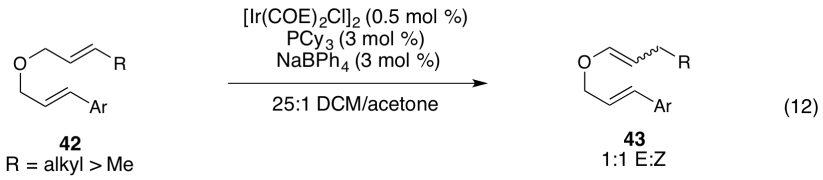

(12)

Mechanistic studies of the catalyzed-Claisen rearrangement indicated that the reaction was intramolecular in nature, but not a concerted process as is typical with traditional Claisen rearrangements.[25] Mechanism studies indicate a reassembly of the π-allyl and enolate fragments in an inner sphere mechanism (Figure 4). Therefore, the reaction more closely resembles an allylic alkylation where a preformed enolate captures a metal bound allyl ligand than the traditional sigmatropic rearrangement.

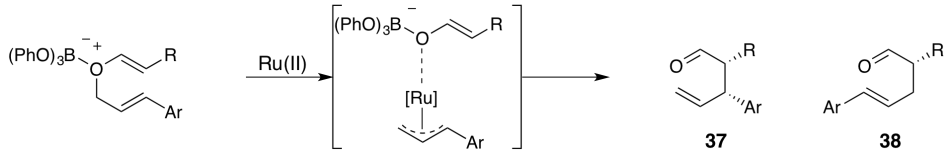

Figure 4: Asymmetric Claisen Reaction Inner Sphere Mechanism

Reimagining the Claisen rearrangement as an asymmetric allylic alkylation presents new possibilities for solving the regio- and diastereoselectivity limitations to the existing methodology (Figure 5). Generating the π-allyl fragment via oxidative insertion diversifies allyl precursors electronically, of which the regioselectivity was found to be dependent. More importantly, dividing the allyl vinyl ether into electrophilic and nucleophilic partners allows for an exploration of a variety of suitable nucleophilic enolates. Controlling the geometry of the nucleophile was expected to improve diastereoselectivity. By exploring the intermolecular reaction mechanism, the reaction scope could be expanded.

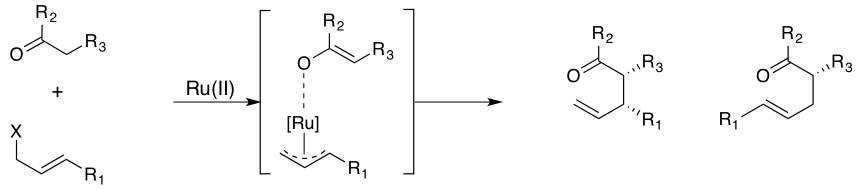

Figure 5: Examining the Claisen Rearrangement as an Allylic Alkylation

Wanting to use the Ru(II)-catalyzed Claisen rearrangement as a foundation from which to build the asymmetric allylic alkylation raised several concerns. For example, we hoped the current pre-catalyst would translate from the Claisen rearrangement to the allylic alkylation. However, ruthenium(II)-catalyzed allylic alkylations remain the least investigated AAA utilizing alternative metal sources. Further, accessing Claisen-type products via an allylic alkylation requires setting two tertiary vicinal stereocenters diastereoselectively. Diastereoselective allylic alkylations are exceedingly rare and few establish adjacent tertiary carbons. The link between the geometric structure and diastereoselectivity requires finding an appropriate and compatible nucleophile capable of setting the stereogenic center. Only by confronting these issues and improving the regio- and diastereoselectivities, would the proposed allylic alkylation succeed.

1.3 RUTHENIUM ALLYLIC ALKYLATION REGIOSELECTIVITY

Accessing the desired Claisen-type product via the proposed asymmetric allylic alkylation demands a system which favors both the branched regioisomer and has the ability to set the allylic stereocenter. When bonded to ruthenium, nonsymmetrical allylic ligands experience geometric and electronic distortions resulting in asymmetrical ruthenium-allyl complexes. [17, 18, 26, 27] Density functional theory (DFT) calculations reveal a shorter C_1 carbon-ruthenium bond (2.230 Å) compared to the C_3 carbon-ruthenium bond, 2.487 Å (Figure 6).[26] The bond

elongation, attributed to less efficient ruthenium d-electron backbonding to C_3 orbitals, causes less negative charge to develop on C_3 making nucleophilic attack more likely at C_3 than at C_1.[26] The lack of negative charge at C_3 suggests the preferential formation of the branched isomer under ruthenium-catalyzed allylic alkylation conditions.[26] At this time, despite showing an inherent preference towards the branched product, no regiospecific ruthenium allylic alkylation exists. The proposed allylic alkylation seeks complete regioselectivity by examining electronically diverse ligands. Ligands capable of amplifying the inherent asymmetric distortion present in the ruthenium-allyl complex should help to improve regioselectivity.

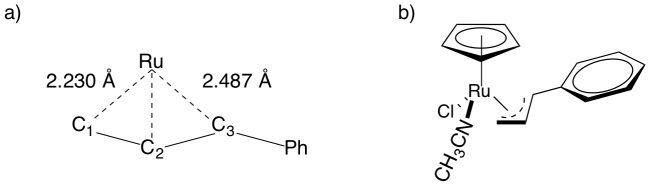

Figure 6: a) CpRu(II)-allyl DFT Calculations b) Complex from which Calculations are Based

While computational models indicate a preference for branched product formation, evidence suggests that the ligands and the ruthenium source play critical roles in determining regioselectivity. For example, a $Ru_3(CO)_{12}$ and aryl phosphine ligand **46** catalyst system favors linear product formation 99:1 over the branched isomer (Scheme 5, Equation 13).[28] Conversely, systems utilizing analogous ruthenium precatalysts to the Claisen rearrangement favor the branched regioisomer. Exposing allylic carbonates to malonate anions and pentamethylcyclopentadienyltris(acetonitrile)ruthenium(II) hexafluorophosphate ($[Cp^*Ru(CH_3CN)_3][PF_6]$) provides the branched regioisomer 12:1 over the linear product, supporting the theoretical predictions (Equation 14).[29] Similarly, an asymmetric Carroll rearrangement with $[CpRu(CH_3CN)_3][PF_6]$ provides 99:1 selectivity of the branched product (Equation 15).[30] Here, a pyridyl imine based ligand **51**, similar to pyridyl indanol ligand **36**, sets the required stereocenter with 70% ee. While the ligand and ruthenium source clearly influence

the regioselectivity of the reaction, this analysis suggests that the $[CpRu(CH_3CN)_3][PF_6]$ utilized in the Claisen rearrangement would translate to providing the branched isomer in the proposed allylic alkylation. Encouragingly, the asymmetric Carroll rearrangement indicates that pyridyl based ligands also favor branched product formation.[30] Therefore, it appears reasonable that the $[CpRu(CH_3CN)_3][PF_6]$ and pyridyl indanol ligand **36** would act as a proper foundation upon which to explore the desired allylic alkylation.

Scheme 5: Ruthenium-catalyzed Allylic Alkylations

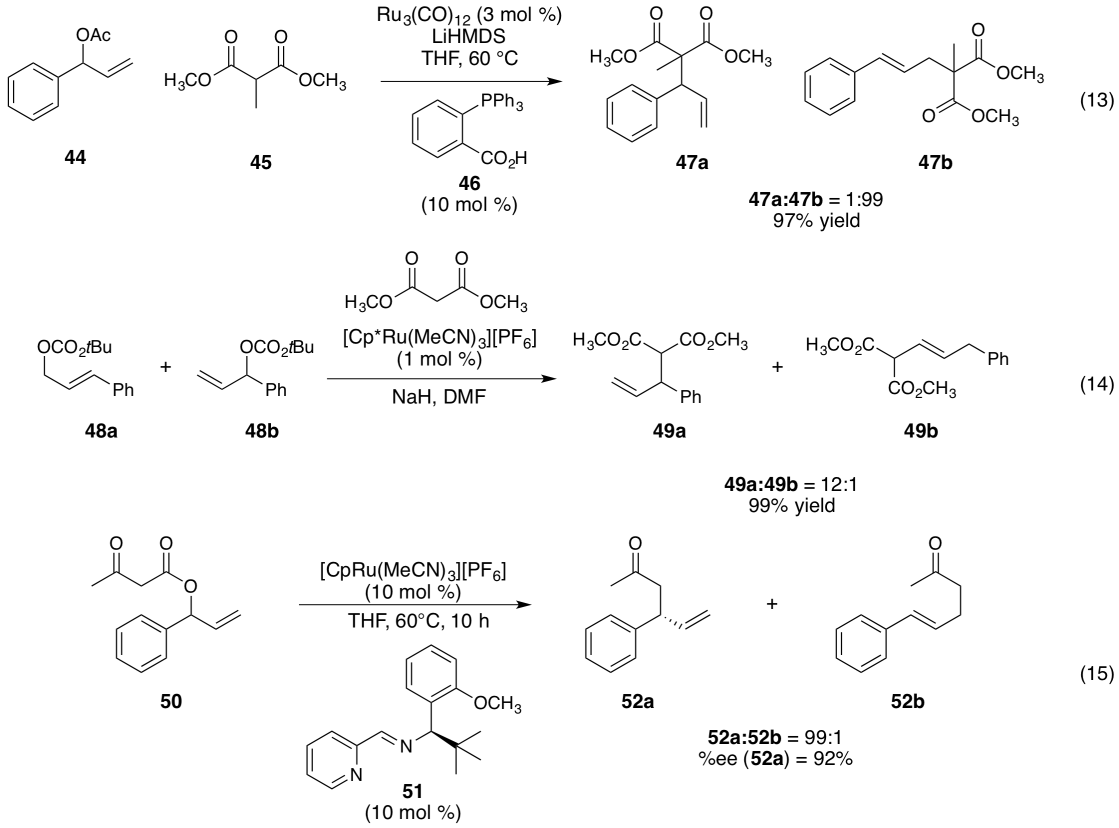

1.4 ESTABLISHING VICINAL STEREOCENTERS VIA AAA

1.4.1 Setting an Adjacent, Quaternary Stereocenter via AAAs

To gain access to synthetically useful Claisen-type products via an asymmetric allylic alkylation would require setting adjacent tertiary stereocenters in a diastereoselective manner. Introducing prochiral nucleophiles and establishing multiple stereocenters via allylic alkylations has traditionally proven difficult.[20] Several systems efficiently provide alkylated products with high selectivities while setting quaternary α-carbons.[31-34] The addition of cyanoester enolate (**53**) to a

Mo(II)(π-allyl) complex proceeds with ~17:1 diastereoselectivity (Scheme 6, Equation 16).[31] Ir(I)-catalyzed alkylation are more prevalent. Both cyclic and acyclic β-ketoesters exhibit high diastereoselectivities when exposed to $[Ir(cod)Cl]_2$ and phosphoramidite systems (Equation 17).[32, 33] Further, dual catalytic systems, which utilize Ir(I) and cinchona-alkaloid co-catalysts, prove capable of achieving both sets of diastereomers and enantiomers efficiently (Equation 18).[34, 35] These examples indicate that allylic substitutions can be rendered diastereoselective when setting a quaternary α-carbon. In addition, the described conditions depend on strong bases, NaH[31] and TBD,[32] and acids, trichloroacetic acid,[34] to generate the enolate nucleophile. Having a quaternary α-carbon prevents epimerization under the harsh reaction conditions.

Scheme 6: AAAs Capable of Setting Quaternary, Vicinal Stereocenters

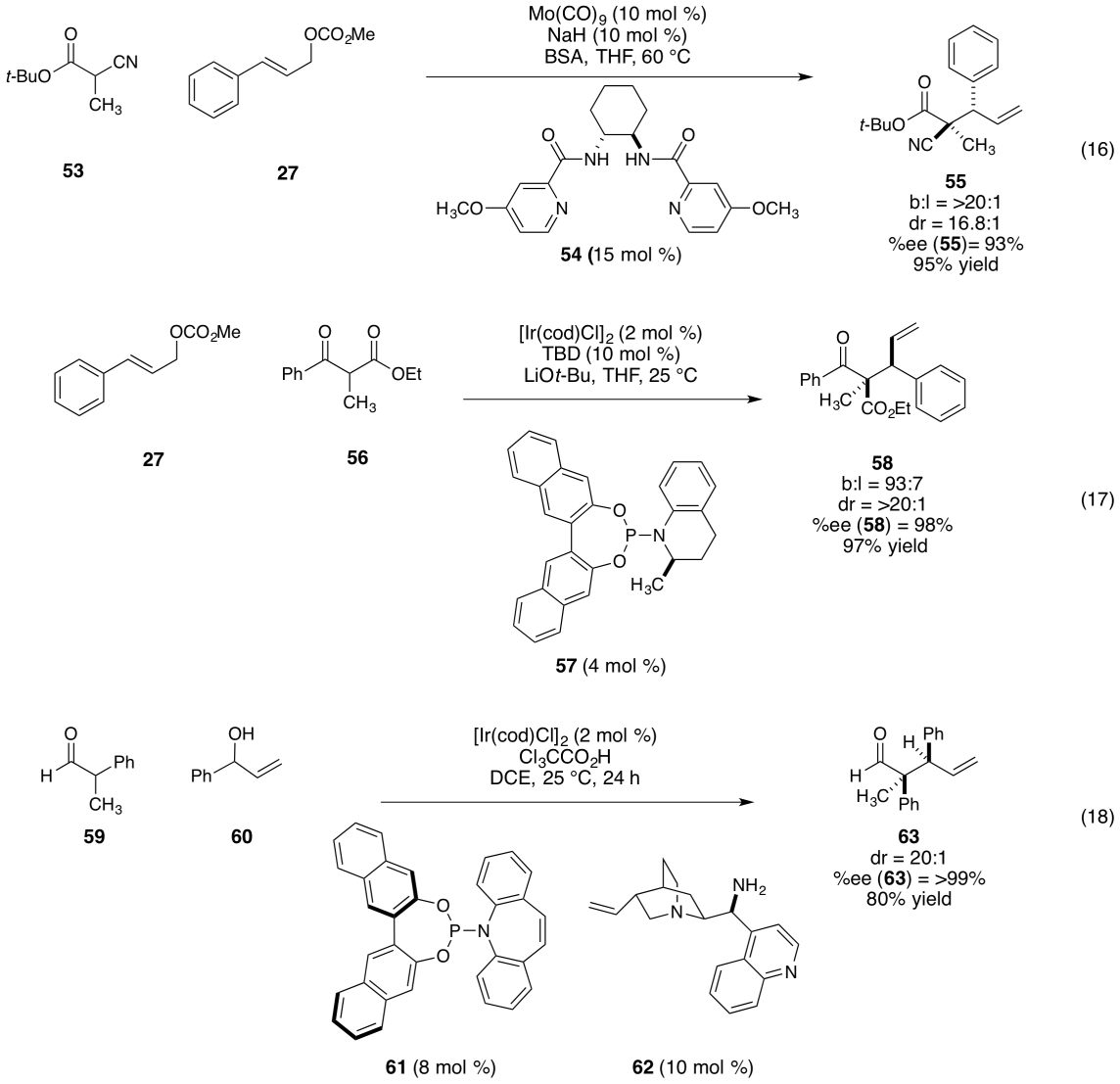

1.4.2 Setting Vicinal, Tertiary Stereocenters via AAAs

Setting vicinal tertiary carbons proves more difficult as the allylic alkylation must occur under mild conditions; utilizing strong acids or bases as described by methods which set quaternary α-carbons, erode the established diastereoselectivity via epimerization.[20] Keeping reaction conditions relatively neutral prevents product degradation, but severely limit the conditions for

generating the nucleophilic enolate. As a result, only two examples wherein an asymmetric allylic alkylation sets a tertiary, vicinal stereocenter are reported. Simple aldehydes were α-alkylated under Ir(I)-amine dual catalyst conditions to yield Claisen-equivalents in all possible isomers (Scheme 7, Equation 19).[35] However, the diastereoselectivity exhibits a dependence on the matched-mismatched nature of the catalytic system. In the second example, a diastereoselective Ru(II)-catalyzed allylic alkylation was reported (Equation 20).[20] Believed to occur via an inner-sphere mechanism, the reaction utilizes nonsymmetrical 1,3-diketones, activated by $NaHCO_3$, as the nucleophilic partner.[20] The diastereoselectivity proves dependent upon the structure of the nucleophile, providing a wide range of selectivities with 7:1 as the optimized case; employing stronger bases correlated to decreased diastereoselectivities.[20] Additionally, it appears that at least one of the two ketones must contain an aryl group. The only dialkyl substrate examined exhibits no diastereoselective preference.[20] The described methods reinforce the necessity of maintaining neutral reaction conditions in order to successfully establish the requisite stereocenters without diastereoselective erosion. The proposed allylic alkylation draws from both of these methodologies, seeking to provide products with only a single carbonyl while utilizing a Ru(II)-based catalyst. This combination would access a synthetically challenging substrate in a single transformation via an under utilized catalytic cycle.

Scheme 7: Reported AAAs Capable of Establishing Vicinal, Tertiary Stereocenters

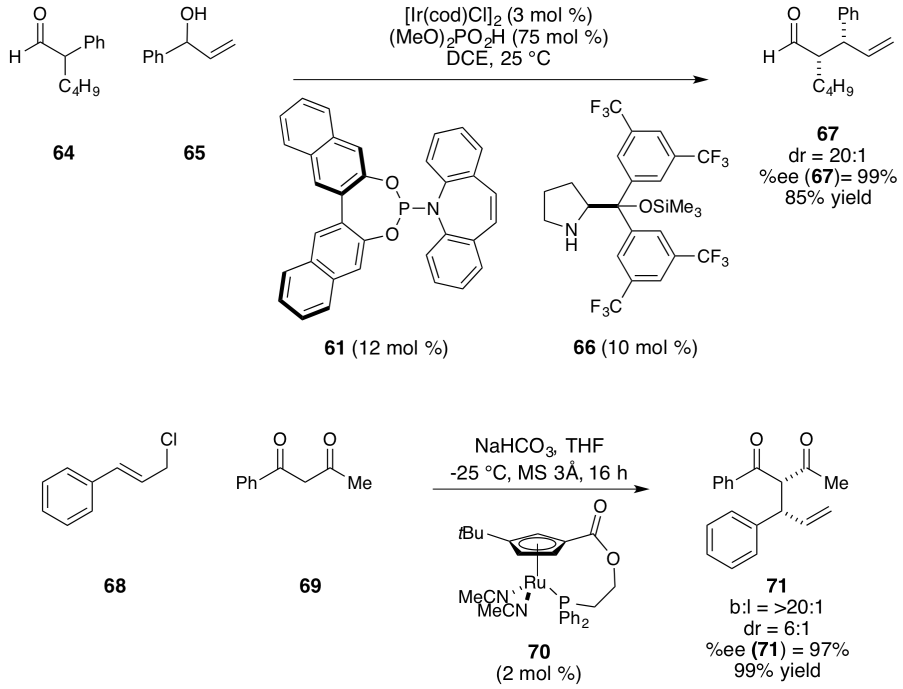

1.5 SILYL ENOLATE NUCLEOPHILES IN ALLYLIC ALKYLATIONS

The Ru(II)-catalyzed Claisen rearrangement indicated the diastereoselectivity was dependent upon the enolate nucleophile. The proposed allylic alkylation would require neutral reaction conditions to prevent product selectivity erosion, which greatly limits the conditions available for generating a strong nucleophile. Fortunately, during the synthesis of erythronolide-b, we found acyl pyrrole derived enol silanes (**73**) to be highly nucleophilic and capable of providing products diastereoselectively (Equation 21).[36, 37] Additionally, the preformed enol silanes require neither Brønsted acidic nor basic conditions to generate the active nucleophile *in situ*.[37] The promise of maintaining neutral reaction conditions and controlling a previously difficult diastereoselective variable was encouraging.

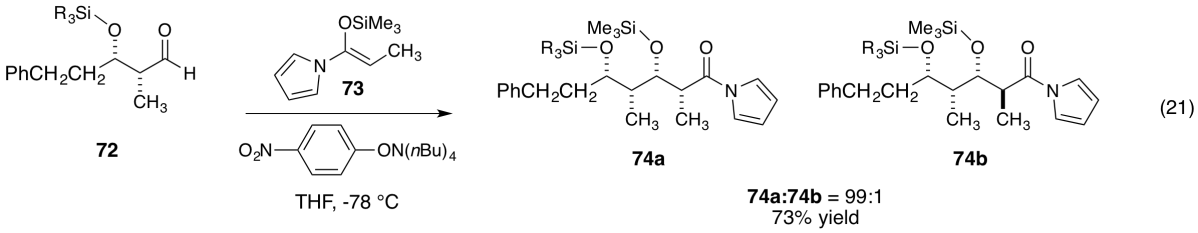

Despite their availability and extensive synthetic utility, silyl enol ether nucleophiles remain relatively rare in allylic alkylation reactions. However, enol silanes have proven utility in these processes (Scheme 8). An iridium-catalyzed allylic alkylation tolerates both aryl and alkyl based silyl enolate nucleophiles, producing the branched regioisomer in 91-96% enantioselectivity (Equation 22).[39] 2-Trimethyl-silyloxyfuran (**78**) alkylates cinnamyl acetate derivative **79** in the presence of palladium(0) enantioselectively and in 47% yield (Equation 23).[40] Evans-auxiliary silyl enol ether nucleophiles (**82**) also participate in allylic alkylations (Equation 24).[41] These examples, while limited, establish the participation of silyl enolates in asymmetric allylic alkylations with a high degree of selectivity. To date, no examples of acyl-pyrrole enol silanes in allylic alkylation have been reported despite their applicability.

Scheme 8: Silyl Enol Ether Nucleophiles in Metal-catalyzed Allylic Alkylations

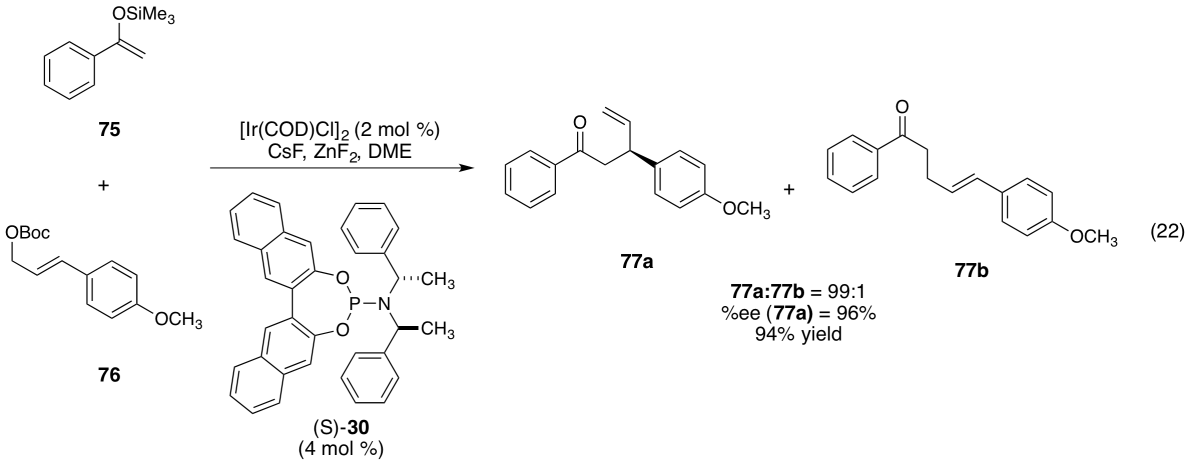

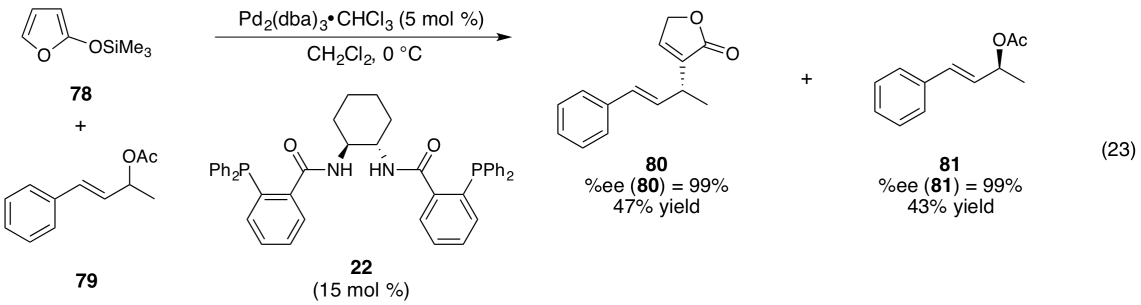

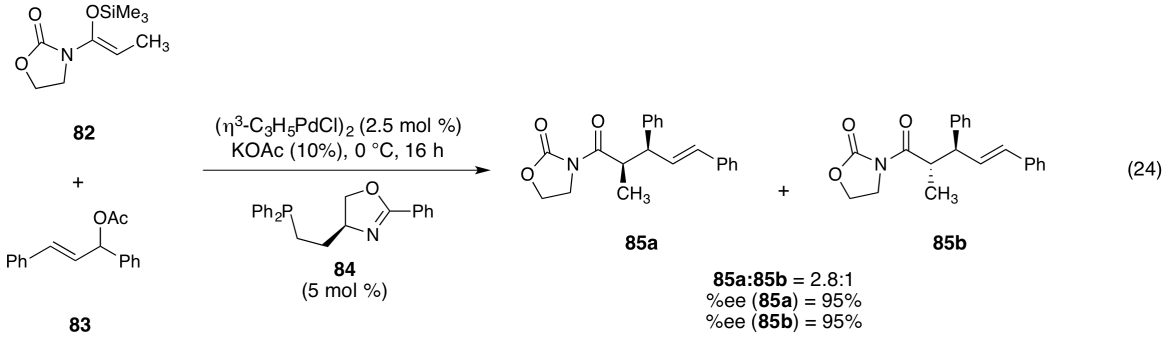

1.6 CONCLUSIONS

Re-imagining the Claisen rearrangement as an intermolecular allylic alkylation reaction would eliminate substrate constraints present in the previous methodology. A ruthenium-catalyzed oxidative insertion across an allylic precursor accesses the required π-allyl system. The ruthenium-based system and accompanying ligand are predicted to favor the formation of the desired branched regioisomer and establish high enantioselectivities. Nucleophilic capture of the η^3-allyl ligand by an *N*-acylpyrrole silyl enol ether provides a Claisen-type product under neutral reaction conditions with a high degree of diastereoselectivity. The resulting α,β-substituted-γ,δ-unsaturated acyl pyrrole (**88**) contains vicinal stereocenters and two chemoselective handles, like the Claisen-aldehydes. Facing few direct limitations, the substrate scope should expand the number of accessible products.

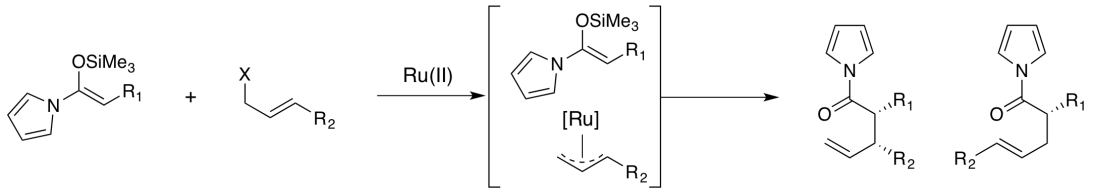

Figure 7: Envisioned Allylic Alkylation with a Silyl Enolate Nucleophile

2.0 A RU(II)-CATALYZED ALLYLIC ALKYLATION

Reaction optimization, including extensive ligand modification, rendered a regio-, diastereo-, and enantioselective Ru(II)-catalyzed asymmetric allylic alkylation. The reaction was found to be tolerant to diverse enolate nucleophiles and cinnamyl acetate derived electrophiles. Aliphatic-based electrophiles were only marginally successful under the optimized reaction conditions. The Claisen-type products now available greatly expanded the substrate scope of the previous methodology.

2.1 INITIAL EFFORTS TOWARDS A RUTHENIUM-CATALYZED ALLYLIC ALKYLATION

Building on what we learned during the development of the asymmetric Claisen chemistry, we began designing a ruthenium(II)-catalyzed allylic alkylation capable of yielding α,β-substituted-γ,δ-unsaturated acyl pyrroles. Utilizing allylic acetates as precursors to Ru(IV)(π-allyl) complexes has been well established[17-19, 30] and the proven nucleophilicity[38] of *N*-acyl pyrrole derived silyl enol ethers in Mukaiyama-Michael additions[36] led to our belief that the combination would provide the required reactivity in the desired allylic alkylation reaction. We sought to expose the allylic acetate-silyl enolate pairing to our Ru(II)-pyridyl indanol catalyst (Scheme 9,

entry A). After 24 hours, the reaction exhibited no signs of product formation, indicating either inefficient formation of the Ru(IV)(π-allyl) complex, the result of inefficient oxidative insertion into the allylic acetate, or poor nucleophilicity of the silyl enol ether (**91a**). We elected to investigate the oxidative insertion, understanding there were several opportunities to attain the desired reactivity, including introducing a Lewis acid co-catalyst or exchanging the acetate for a more effective leaving group.[42] Based upon our success in incorporating a phenylborate co-catalyst into the asymmetric Claisen rearrangement,[24, 25] which bonds to the allylic oxygen thereby weakening the carbon-oxygen bond and hastening the formation of the (ruthenium)(π-allyl) complex, we began by including this Lewis acid into the reaction design. Introducing triphenylborate ([PhO]$_3$B, 5 mol %) to the reaction produced the desired branched acyl pyrrole albeit in low yields (Scheme 9, entry B, 52% yield, **92a:93a** = 3.3:1, **92a**$_{anti}$**:93a**$_{syn}$ = 1.3:1, 40% ee **92a**). Therefore, cinnamyl acetates require sufficient Lewis acid activation to be suitable electrophilic precursors in the Ru(II)-catalyzed alkylation.

Scheme 9: Addition of Lewis Acid to the Allylic Alkylation

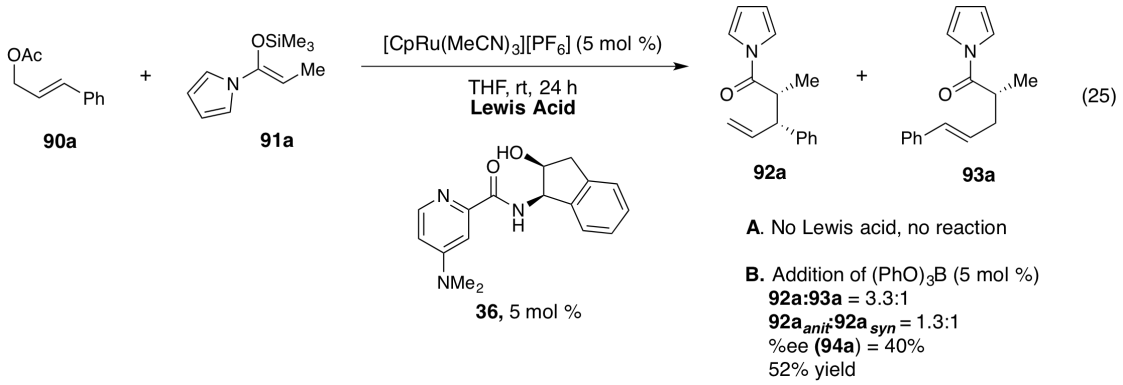

Preferential formation of the branched isomer encouraged efforts to improve reaction yields. Low yields were expected to be a symptom of either inefficient oxidative insertion or poor enolate nucleophilicity. Having demonstrated that allylic acetate activation toward oxidative insertion provided the desired reactivity, we chose to further probe the electrophilic

reactant. Exchanging the acetate for a more effective leaving group[42] or increasing the Lewis acidity of the borate co-catalyst were expected to further weaken the carbon-oxygen bond and allow for easier oxidative insertion. As both variables needed to be examined, we decided to first examine how the leaving group affected the reaction yields. Utilizing cinnamyl (4-nitrophenyl)carbonate (**94)** as the allyl precursor afforded the branched regioisomer in 86% yield (Table 1). However, the reaction exhibited no discernable diastereo- or enantioselectivity (86% yield, **92a:93a** = 3.4:1, **92a**$_{anti}$**:92a**$_{syn}$ = 1:1). The observed improvement in yields directly correlated to the ability to access the Ru(IV)(π-allyl) complex. However, affecting the oxidative insertion did not result in favorable reaction selectivities.

Needing to ensure the formation of the branched isomer, we sought to improve the reaction's regioselectivity. We suspected that ligand electronics dictated the reaction selectivity. Cinnamyl derived ruthenium-allyl complexes experience bond elongation between the metal and the C_3-allyl bond (Figure 6), resulting in ruthenium-based allylic alkylations favoring the branched regioisomer.[17, 18, 26, 27] We hypothesized that increasing the ligand's electron density would increase the electron density on the metal and further lengthen the metal-C_3 bond. By enhancing this existing phenomenon, we believed the regioselectivity would further favor the desired branched regioisomer. To test this hypothesis, a systematic examination of electron-rich ligands was conducted. Replacing the pyridyl indanol **36** with a pyridyl oxazoline **95**, capable of direct electron donation via resonance, in the catalytic reaction improved the regioselectivity as predicted. The diastereo- and enantioselectivity remained unaffected (Table 1, 95% yield, **92a:93a** = 10:1, **92a**$_{anti}$**:92a**$_{syn}$ = 1.3:1, 68% ee **92a**). Further increasing the electron density of the ligand was achieved by utilizing pyridyl imidazoline **96**.[43, 44] As the nitrogen better supports a positive charge in the corresponding resonance structure, **96** was expected to exhibit increased

selectivity favoring the branched isomer. However, pyridyl imidazoline **96** provided no additional regioselectivity improvements. Instead the diastereoselectivity and enantioselectivity improved (85% yield, **92a:93a** = 10:1, **92a**$_{anti}$**:92a**$_{syn}$ = 3:1, 88% ee **92a**). The improved selectivities, available from pyridyl imidazoline **96** indicated that this family of ligand was optimal for the desired alkylation.

Table 1: Allylic Alkylation with Carbonate Electrophiles

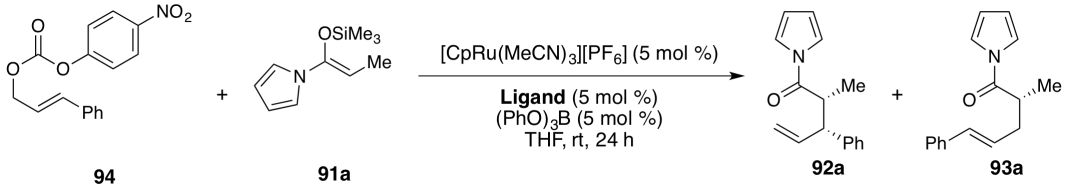

94 + **91a** → **92a** + **93a**

Ligand =	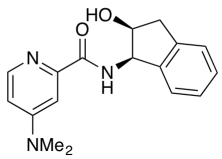 **36**	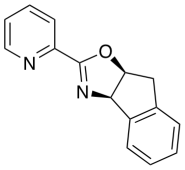 **95**	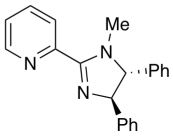 **96**
regio (**92a:93a**)[a]	3.4:1	10:1	10:1
anti:syn (**92a**)[a]	1:1	1.3:1	3:1
%ee (**92a**)[b]	0	68	88
% yield	86	95	85

[a] Determined by ^{1}H NMR; [b] Determined by chiral GC

We initially investigated allylic carbonates as one way to improve the reaction yields. However, the large *p*-nitrophenyl carbonate leaving group diminished the reaction's atom economy. Hoping to develop an atom efficient reaction, we decided to reevaluate allylic acetates in conjunction with more Lewis acidic phenyl borate. Appending electron-withdrawing groups to the aryl ring of the borate increases the Lewis acidity of the boron atom via induction; upon bonding to the allylic oxygen, a more Lewis acidic borate co-catalyst makes the acetate a better leaving group by further weakening the acetate's carbon-oxygen bond. Employing tri(4-

fluorophenyl)borate as the co-catalyst in the reaction conditions immediately improved yields and selectivities (Table 2, 86% yield, **92a:93a** = 13:1, **92a**$_{anti}$**:92a**$_{syn}$ = 7:1, 92% ee **92a**). However, reactions with stronger Lewis acids, $(4\text{-}CF_3C_6H_4O)_3B$ and $(4\text{-}NO_2C_6H_4O)_3B$, exhibited decreased diastereoselectivities, 4:1 (*anti:syn*) and 2.3:1 (*anti:syn*) respectively (Table 2). Incorporating tri(4-fluorophenyl)borate as the co-catalyst provided the greatest synthetic utility by improving yields while maintaining established diastereoselectivities (Table 2, entry a).

Table 2: Tuning Phenyl Borate Co-catalysts

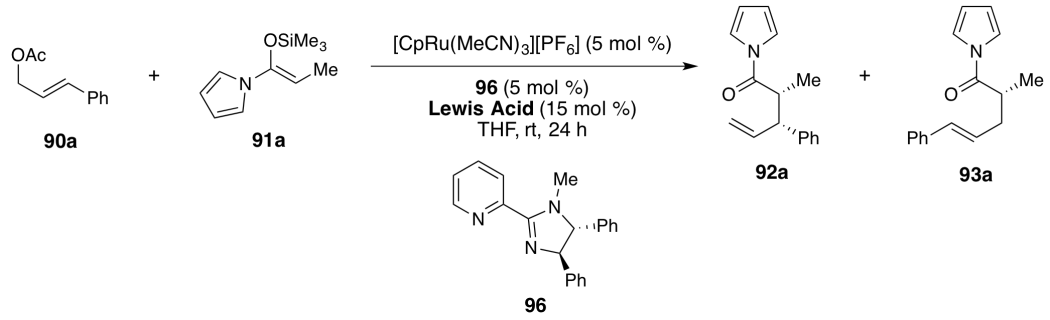

entry	Lewis Acid	Results
a	$(p\text{-}FC_6H_4O)_3B$	**92a:93a**[a] = 13: 1, **92a**[a] **(*anti:syn*)** = 7:1, %ee (**92a**)[b] = 92%, 86% yield
b	$(p\text{-}CF_3C_6H_4O)_3B$	**92a(*anti:syn*)** = 4:1
c	$(p\text{-}NO_2C_6H_4O)_3B$	**92a(*anti:syn)*** = 2.3:1

[a] Determined by ^{1}H NMR; [b] Determined by chiral GC; ND = not determined

2.2 LIGAND MODIFICATIONS

Pyridyl imidazolines were systematically modified to improve reaction selectivities. This examination led to two optimized ligands. Ligand **107** provided optimal diastereoselectivity while **111** provided consistently high regio- and enantioselectivities. As the ligands were seen a

complementary to each other, both were utilized in subsequent experimentation to determine the reaction's substrate scope.

2.2.1 Evaluation of Ligand Structure and Electronics

Having identified reaction variables that reliably produce Claisen-type products, we sought to optimize product selectivities via ligand modification. A structural analysis of the pyridyl imidazoline indicates three distinct regions that can be systematically modified: 1) the imidazoline protecting group 2) the pyridine ring 3) the ethylenediamine portion of the imidazoline ring (Table 3). Altering the N_{amine} alkyl group (Table 3, variable W) influences the stereoelectronics of the imidazoline ring which has been demonstrated to have a direct effect on catalytic activity and reaction selectivity.[43, 44] Structural modification to the pyridine ring (variables X and Y) would directly influence the Lewis-basicity (pKa) of $N_{pyridine}$. We predicted that a more Lewis-basic $N_{pyridine}$ would improve regioselectivity by enhancing the existing electronic distortion inherently present in Ru(IV)(π-allyl) complexes.[26] Finally, altering the functionality of the imidazoline ring (variables Z and Z') influences the trajectory of the incoming nucleophile by blocking one of the two faces of the allyl ligand. Larger groups more efficiently obstruct the electrophile and will improve diastereo- and enantioselectivities. A deliberate and rational modification of these regions was predicted to improve the overall selectivities of the developed allylic alkylation.

Table 3: Structural Variables on the Pyridyl Imidazoline Ligand and their Anticipated Effects

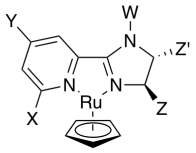

Variable/Region	Influence	Antipated Effect
W	Increase or decrease sterics at N_{amine}	Stereoelectronic effect that influcences enatioselectivity
X	Influence Lewis-basicity of $N_{pyridine}$	Influence binding of π-allyl ligand: regioselectivity
Y	Enhance electron donation to ruthenium	Influence regioselectivity through asymmetry in π-allyl system
Z	Increase steric environment of imidazoline ring	Influence binding of π–allyl system: enantioselectivity

A thorough investigation into the desired ligand modifications required an efficient synthesis of pyridyl imidazolines. Current methods build the ligands in two successive steps in good yields and high enantioselectivities (Equation 26). The pyridyl imidazoline core arises from the condensation of 2-pyridinecarboxaldehyde (**97**) and a chiral ethylenediamine (**98**) in the presence of *N*-bromosuccinimide (NBS). [45, 46] The simplicity of the condensation reaction allows for any available pyridinecarboxaldhyde and diamine to be utilized, thereby greatly expanding the number of pyridyl imidazoline cores available. Alkylating the N-H imidazoline under basic conditions with a variety of alkyl halides further expands ligand diversity. Utilizing the described synthetic strategy allowed for an efficient synthesis of a diverse family of pyridyl imidazoline ligands of varying steric and electronic properties, which were subsequently utilized in the developed allylic alkylation.

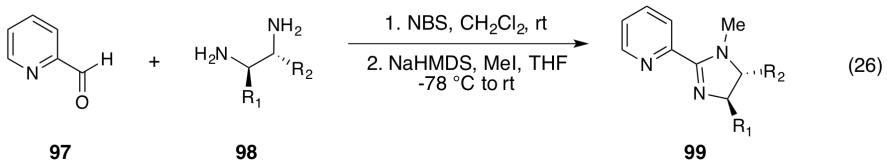

97 **98** **99** (26)

2.2.2 Stereoelectronic Modifications to the Imidazoline N_{amine}

Initial ligand modifications focused on altering the N_{amine} alkyl group. Previous studies indicated the N_{amine} alkyl group affects the electronic nature of the pyridyl imidazoline ligand, influencing catalyst activity and product selectivity.[43, 44] To this end, we directly compared three N_{amine} substitutions, including N-Me (**96),** to examine the effect the alkyl group had on the allylic alkylation. The N-H imidazoline (**100**) would examine whether a protecting group was required for reaction viability. Under the reaction conditions (Table 4), N-H **100** provided diminished conversions and regioselectivity when compared to the control **96** (50% conversion, **92a:93a** = 6.4:1, **92a**$_{anti}$**:92a**$_{syn}$ = 5:1, 81% ee **92a**). Sequestering the borate co-catalyst by the basic N_{amine} offers one possible explanation for the observed lack of reactivity. The benzyl-protected imidazoline **101** reacted comparably to the standard methyl-protected ligand, but demonstrated decreased regio- and diastereoselectivities (100% conversion, **92a:93a** = 11:1, **92a**$_{anti}$**:92a**$_{syn}$ = 5:1, 89% ee **92a**). The decreased selectivities suggest the increased sterics of the benzyl group causes less efficient electron-donating into the N_{imine} of the pyridylimidazoline.[43, 44] From this experimental set, **96** remained the optimized ligand for the allylic alkylation.

Table 4: Modification to the Pyridyl Imidazoline N_{amine}

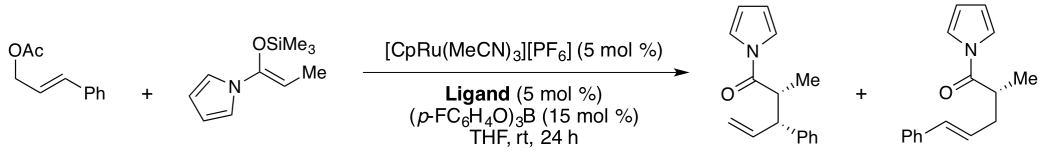

90a **91a** **92a** **93a**

Ligand =	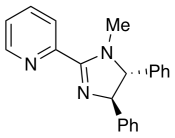 **96**	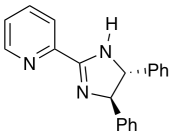 **100**	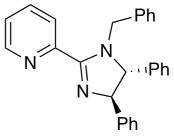 **101**
regio (**92a:93a**)[a]	13:1	6.4:1	11:1
anti:syn (**92a**)[a]	7:1	5:1	5:1
% ee (**92a**)[b]	92	81	88
% conversion	100	50	100
% yield	86	ND	ND

[a] Determined by ^{1}H NMR; [b] Determined by chiral GC; ND: not determined

2.2.3 Structural and Electronic Modifications to the Ligand's Pyridine Ring

Determining the ligand's mode of reactivity was critical before exploring a new subset of ligands. Pyridyl imidazolines typically act as bidentate ligands in transition-metal mediated catalysis.[45] However, it remained possible that only one of the two Lewis basic nitrogens remained bound during the catalytic cycle. If this were the case, altering the sterics and electronics of a non-bonding ring would have little to no effect on the reaction selectivity. To explore this possibility, we prepared a ligand wherein the pyridine ring was replaced with a phenyl substituent, thereby creating a monodentate ligand. Ligand **102** was obtained from the described condensation (Equation 26) between benzaldehyde and (1R,2R)-diphenylethelenediamine followed by subsequent methylation. Utilizing phenyl imidazoline **104** as the ligand under the allylic alkylation conditions (Equation 27, 5 mol %

[CpRu(MeCN)$_3$][PF$_6$], 15 mol % (4-FC$_6$H$_4$O)$_3$B, THF, rt, 24 h), yielded no reaction. The observed lack of reactivity indicated that the active catalyst consists of the bidentate pyridyl imidazoline-ruthenium complex. Therefore, modifying the sterics and electronics of the pyridine and imidazoline rings was warranted.

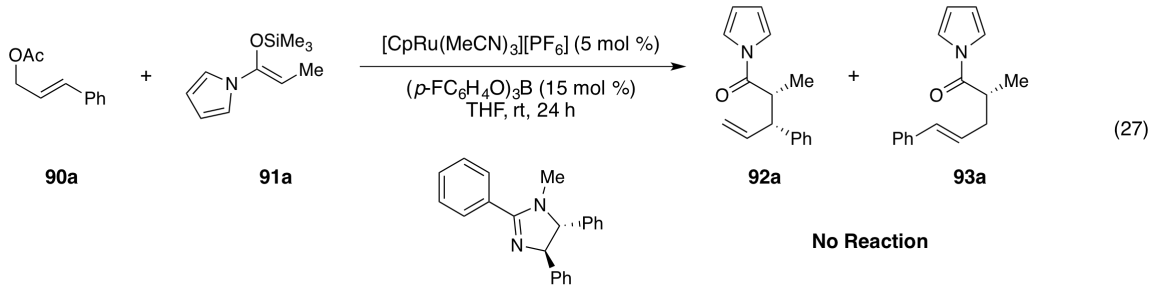

90a **91a** **92a** **93a** (27)

102, (5 mol %)

No Reaction

Knowing the ligand's pyridine ring was critical in generating the active catalyst, we sought to probe how structural modifications to the pyridine effected reaction selectivity. We understood that incorporating pyridine derivatives would directly affect the $N_{pyridine}$ pKa and hypothesized that tuning the nitrogen's basicity would influence ligand-ruthenium bonding. To examine this effect, two pyridine derivatives were synthesized and utilized in the established alkylation. 6-methylpyridyl imidazoline **103**, $N_{pyridine}$ pKa = 5.97,[47] exhibited regioselectivities consistent with the parent system, $N_{pyridine}$ = 5.14.[47] While enantioselectivities were also found to be similar, the observed diastereoselectivities were diminished (Table 5**,** 19% yield, **92a:93a** = 13:1, **92a**$_{anti}$**:92a**$_{syn}$ = 5:1, 88% ee **92a**). Unfortunately, the yield dropped below 20%, compared to the 86% yield achieved with ligand **96**. In contrast, utilizing quinolin imidazoline **104**, $N_{pyridine}$ pKa = 4.85,[47] exhibited lower regioselectivities than its counterpart (**103**) and the parent ligand (**96**) (50% yield, **92a:93a** = 10:1, **92a**$_{anti}$**:92a**$_{syn}$ = 2.5:1, 75% ee **92a**). Diastereo- and enantioselectivities were also diminished. The results from these experiments led to two conclusions: 1) the basicity of $N_{pyridine}$ directly effects the observed regioselectivity. Specifically, greater electron density on the pyridine nitrogen favors the formation of the branched

regioisomer. Both **96** and **103** have pKa values greater than 5.0, have the same branched-linear ratio. Comparatively, the weaker base **104** has a decreased branched-linear ratio. Further, the less basic nitrogen of **104** may also contribute to the modest yields (50%) due to less efficient ligand-ruthenium binding. 2) while **103** demonstrated a similar regioselectivity compared to the parent system, the yield was drastically lower. Since the pKa values between **96** and **103** are comparable, this decreased reactivity may be attributed to increased steric hindrance. Limited ligand-metal bonding could result in diminished catalyst efficacy (Figure 8, a). 2) Once formed, the now sterically strained catalyst could not efficiently bond the π-allyl ligand, resulting in poor reaction selectivities (Figure 8, b). From this set of experiments, it became clear that in order to further improve the regioselectivity, increasing the Lewis basicity of the $N_{pyridine}$ was required.

Table 5: Exploring the Lewis-basicity of $N_{pyridine}$

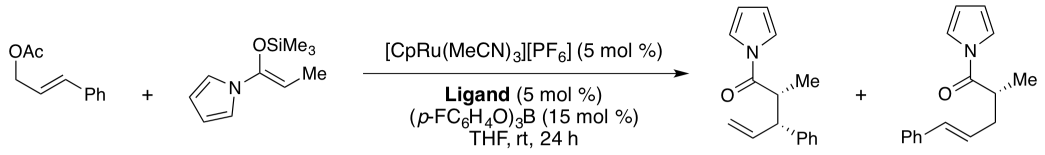

90a **91a** **92a** **93a**

Ligand =	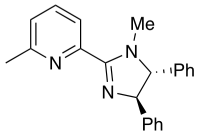 **103**	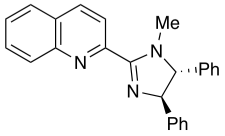 **104**
regio (**92a:93a**)[a]	13:1	10:1
anti:syn (**92a**)[a]	5:1	2.5:1
% ee (**92a**)[b]	88	75
% yield	19	50

[a] Determined by ^{1}H NMR; [b] Determined by chiral GC

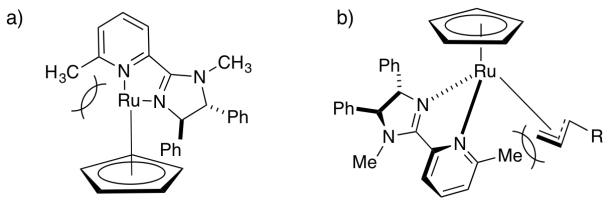

Figure 8: Sterically Congested Catalysts

From our experiments we discovered that increasing the σ-basicity of $N_{pyridine}$ improved the reaction's regioselectivity likely by enhancing the existing asymmetric distortion of the π-allyl ligand in the catalytic complex. Therefore, an investigation into further increasing the electron density of the pyridine nitrogen began. Three electron-rich pyridyl imidazolines were synthesized. Surprisingly, 4-chloro **105**[48], electron-donating by resonance and electron-withdrawing by induction and with a pKa = 3.88,[47] and 4-methoxypyridylimidazoline **108**[48], pKa = 6.62,[47] behaved similarly to the parent ligand (**96**) under the standard conditions (Table 6).

Further increasing the Lewis basicity of $N_{pyridine}$ was accomplished by incorporating a pyrrolidine ring (**107**), pKa >9.7.[47] An *N*-arylation installs a nitrogen atom to the 4-position of the pyridine ring via nucleophilic aromatic substitution. Since nitrogen is less electronegative than oxygen or chlorine, **107** contributes electron density to the pyridine ring through resonance better than its structural counterparts **106** and **106**. Applying ligand **107** to the allylic alkylation reaction provided improvements in both regio- and diastereoselectivity (88% yield, **92a:93a** = 18:1, **92a**$_{anti}$**:92a**$_{syn}$ = 9:1, 95% ee **92a**). We observed that increasing the electron density of the pyridine ring substantially improved the alkylations regioselectivity in favor the branched product. Increasing the electron density at $N_{pyridine}$ aligned with our expectations by improving the obtained regioselectivity.

Table 6: Additional Electronic Modification to the Ligand Pyridine Ring

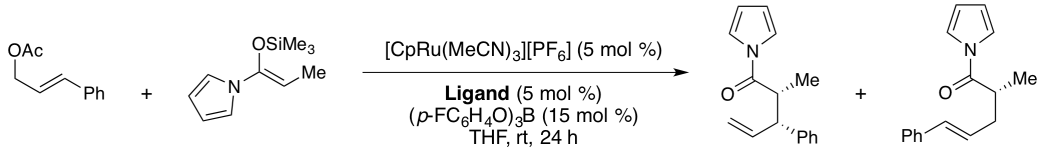

90a **91a** **92a** **93a**

Ligand =	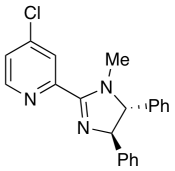 **105**	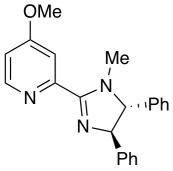 **106**	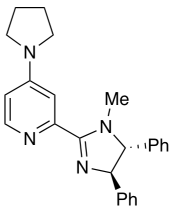 **107**
regio (**92a:93a**)[a]	13:1	13:1	18:1
anti:syn (**92a**)[a]	6.5	7:1	9:1
% ee (**93a**)[b]	88	90	95
% yield	92	82	88

[a] Determined by ^{1}H NMR; [b] Determined by chiral GC

Alterations to the pyridine ring offered valuable insights to reaction optimization. The pyridine ring was found to be critical for attaining an active Ru(II) catalyst, confirming the presence of a bidentate ligand during the allylic alkylation. Pyridine rings with less basic pyridine nitrogens exhibited decreased regioselectivities. However, increasing the σ-donating ability of the $N_{pyridine}$, improved the reaction's preference for the branched regioisomer. These studies provided evidence that an optimized ligand would require an electron-rich pyridine ring to ensure complete regioselectivity.

2.2.4 Examining Imidazoline Steric Contributions to Product Selectivity

Having explored the Lewis-basicity of the pyridine ring in comparison to **96** and having discovered a method for improving the allylic alkylation's regioselectivity, we investigated

structural modifications to the imidazoline portion of the ligand to further improve the product diastereo- and enantioselectivity. Specifically, we sought to examine two aspects of the imidazoline to affect the diastereo- and enantioselectivity: 1) whether a disubstituted imidazoline was optimal for the reaction design, and 2) what other alkyl groups on the imidazoline influence product selectivity. We predicted that mono-substituted imidazolines would be as efficient as their disubstituted counterparts. Additionally, we anticipated that alkyl groups larger than phenyl would further improve the diastereo- and enantioselectivities by directing nucleophile approach more effectively. Gaining access to synthetically useful diastereoselectivities and improved and consistent enantioselectivities would require dramatic structural alterations to the imidazoline ring.

Having only explored disubstituted imidazolines, we remained uncertain if the disubstituted imidazoline structure enhanced or limited the diastereo- and enantioselectivity of the allylic alkylation. We wondered if only the substituent at C_5 influenced the reaction selectivity. To determine this aspect of the catalyst's selectivity, monosubstituted ligands with a substitution at C_5 were required. As described, the pyridyl imidazolines were accessible via any available aldehyde and diamine condensation. Asymmetric monosubstituted diamines were derived from amino acids,[49] which offer substituents of varying in size. In this vein, three pyridyl imidazoline ligands were synthesized: mono-phenyl **108,** isopropyl **109**, and *t*-butyl **110**.

The control (**108**), analogous to **96** elucidated the importance of a substitution at C_5 of the imidazoline ring. In the standard reaction conditions, **108** maintained high yields (94% yield, Table 7). However, regioselectivity reverted to our initial, non-optimized conditions (Table 1) and the reaction exhibited little diastereoselectivity (94% yield, **92a:93a** = 3:1, **92a**$_{anti}$**:92a**$_{syn}$ = 1.5:1). This result indicated that the disubstituted imidazoline ring **96** better provided the product

in the desired selectivities than the monosubstituted imidazoline. However, the steric contribution of monosubstituted imidazolines would still provide critical data by using the (S)-4-phenylimidazoline **108** as a baseline from which to improve.

The steric contribution of the groups correlates to the corresponding A values and from which we predicted product selectivities. Isopropyl **109**, with an A_{value} of 2.21 kcal/mol,[50] was predicted to perform similarly to its phenyl counter part, with an A_{value} of 2.8 kcal/mol.[50] The larger *t*-butyl **110**, with an A_{value} of ~4.8 kcal/mol,[50] provides a greater steric contribution to the catalyst and was expected to provide better diastereo- and enantioselectivities. Utilizing ligand **109**, provided improved regio- and diastereoselectivities when compared to **108** (99% yield, **92a:93a** = 5:1, **92a**$_{anti}$**:92a**$_{syn}$ = 3:1). Ligand **110** exhibited comparable or improved selectivities compared to the 4-pyrrolidine **107** (67% yield, **92a:93a** = 20:1, **92a**$_{anti}$**:92a**$_{syn}$ = 8:1). The isopropyl ligand **109** exhibited better selectivities than predicted and *t*-butyl ligand **110** provided excellent regio- and diastereoselectivities. This led to the belief that incorporating greater sterics into a disubstituted pyridyl imidazoline ligand would further improve product selectivities, particularly the diastereoselectivity.

Table 7: Steric Modifications to the Ligand Imidazoline Ring

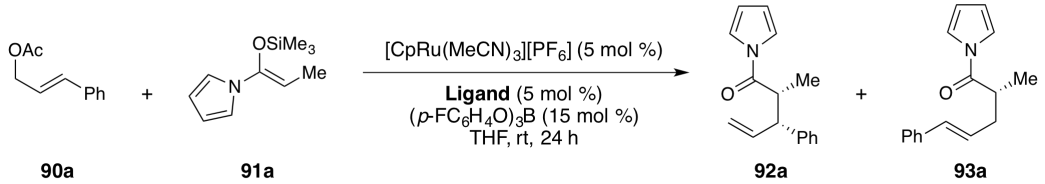

90a **91a** **92a** **93a**

Ligand =	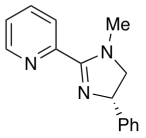 **108**	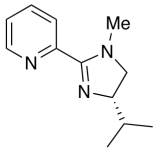 **109**	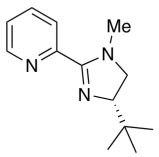 **110**
regio (**92a:93a**)[a]	3:1	5:1	20:1
anti:syn (**92a**)[a]	1.5:1	3:1	8:1
% yield	94	99	67

[a] Determined by ^{1}H NMR

The determined selectivities of the mono-substituted pyridyl imidazoline ligands indicated that a di-substituted pyridyl imidazoline with a greater steric profile than **96** would optimize reaction selectivities. Ideally, a di-*t*-butyl derived ligand would accomplish this goal; however, no current methods exist which synthesize the required diamine in the high diastereo- and enantioselectivities required for our needs. Instead, the sterically congested ligand **111** (A_{value} = 2.20 kcal/mol)[50] was synthesized from the known (1R,2R)-dicyclohexylethylenediamine.[51] Utilizing **111** in the standard reaction conditions yielded surprising results (Table 8, 89% yield, **92a:93a** = 20:1, **92a**$_{anti}$**:92a**$_{syn}$ = 5.4:1, 97% ee **92a**). The enantioselectivity surpassed all previous conditions, including direct comparison to ligand **107**. However, contrary to our predictions, the observed diastereoselectivity of ligand **110,** which exhibited synthetically useful diastereoselectivities, did not translate to ligand **111**. However, the regioselectivity reflected the branched-linear ratio achieved with ligand **110** (**92a:93a** = 20:1). Appending an alkyl group to C_5 of the imidazoline increases the basicity of N_{imine} via induction, which could contribute to the improved regioselectivity. However, other ligands with similarly capabilities, for example **109**,

exhibited no regioselective improvements. Therefore, we predicted that sterically congested, disubstituted imidazolines would exhibit vastly improved reaction selectivities.

If increasing the electron-density of the Ru(II)-complex in conjunction with a disubstituted ligand improved regioselectivity, further modification to **111** should lead to improved selectivities. Appending a pyrrolidine to the 4-posotion of the pyridine of ligand **111** would increase the σ-donating ability of pyridine ring and contribute additional electron density to the catalyst. Employing **112** as the ligand source under the standard allylic alkylation conditions rendered the reaction completely regioselective (**92a:93a** = 42:1). Additionally, the presence of the cyclohexyl rings produced the branched product in 95% ee (Table 8, 91% yield, **92a:93a** = 42:1, **92a**$_{anti}$**:92a**$_{syn}$ = 4.7:1, 95% ee **92a**). As with its structural counterpart, **112** further diminished the reaction's diastereoselectivity. The data suggested that electron-rich Ru(II)-complexes favor the formation of the branched product. Incorporating electron-donating groups on the pyridine ring via resonance dramatically increase the alkylation's preference for the branched regioisomer by increasing the Lewis-basicity of $N_{pyridine}$. However, the deterioration of the diastereoselectivity indicates that there exists a steric limit upon which the enantioselectivity could not be improved and the diastereoselectivity eroded.

Table 8: Investigation into Alkyl Derived Imidazoline Rings

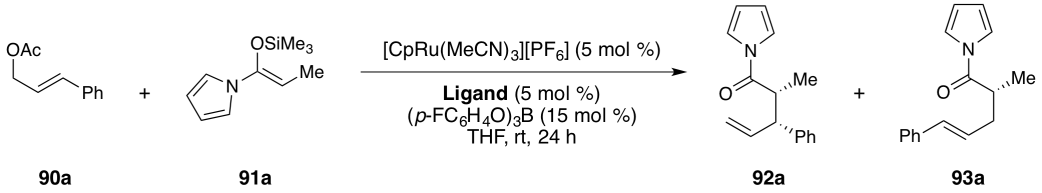

90a **91a** **92a** **93a**

Ligand =	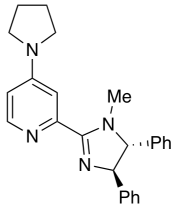 **107**	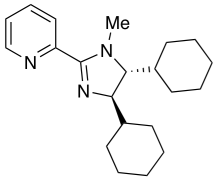 **111**	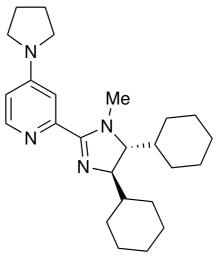 **112**
regio (**92a:93a**)[a]	18:1	20:1	42:1
anti:syn (**92a**)[a]	9:1	5.4:1	4.7
% ee (**92a**)[a]	95	97	95
% yield	88	89	91

[a] Determined by ^{1}H NMR; [b] Determined by chiral GC

Systematic examination of pyridyl imidazoline ligands failed to produce a singular optimized catalytic system. First, increasing the Lewis-basicity of $N_{pyridine}$ and thereby the electron density of the Ru(II)-imidazoline complex improved the alkylation's regioselectivity. The enantioselectivity of the reaction depended upon the steric contribution of the imidazoline and the diastereoselectivity followed no direct trend. Ultimately, 4-pyrrolidine ligand **107** yielded the greatest diastereoselectivity (**92a**$_{anti}$**:92a**$_{syn}$ = 9:1). As no single ligand provided uniformly high selectivities, both ligands **107** and **111** would need to be examined when exploring the allylic alkylation substrate scope.

2.2.5 Applying Cp*Ru(II)-catalyst to the Developed Allylic Alkylation

An investigation into the steric and electronic effects of the catalytic system included employing $[Cp^*Ru(CH_3CN)_3][PF_6]$ as the ruthenium(II) source. Historically, Cp*Ru(II)-catalyzed reactions exhibit improved product selectivities when compared to their CpRu(II) counterparts.[17-19, 27, 29, 30, 52] Therefore we anticipated improved reaction selectivities by employing $[Cp^*Ru(CH_3CN)_3][PF_6]$ as the ruthenium source. The reaction provided the desired branched regioisomer as the major product when ligands **96** and **111** were utilized (Table 9). Contrary to earlier observation where highly electron-rich metal-ligand complexes provided the best branched-linear ratios, the highly electron rich complexes Cp*Ru(II)-**107** and Cp*Ru(II)-**112** were completely unreactive. The observed lack of reactivity was attributed the increased Lewis basicity of the $N_{pyridine}$ ring. Simply, the active catalyst becomes too electron rich to effectively bond cinnamyl acetate. Ligand **111** provided the highest regioselectivity (**92a:93a** = 21:1) The branched regioisomer (**92a**) exhibited the opposite diastereo- and enantioselectivity relative to the reactions employing the CpRu(II)-derived catalyst. We currently hypothesize that the increased steric demands of the Cp* ligand completely block the approach available to the CpRu(II)-catalyzed reaction, resulting in the inverted diastereo- and enantioselectivity. The steric blocking of the Cp* ring likely causes the diminished diastereoselectivities as well (**92a**$_{anti}$**:92a**$_{syn}$ = 1:3); the observed diastereoselectivity falls far behind the CpRu(II)-catalyzed reaction previously explored. The determined trends in the CpRu(II)-catalyzed reactions did not translate to its Cp*Ru(II) counterpart.

Table 9: Effects of Cp*Ru(II) Derived Catalysts on the Allylic Alkylation

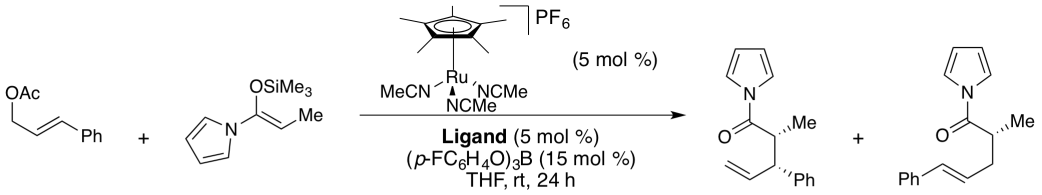

90a **91a** **92a** **93a**

Ligand =

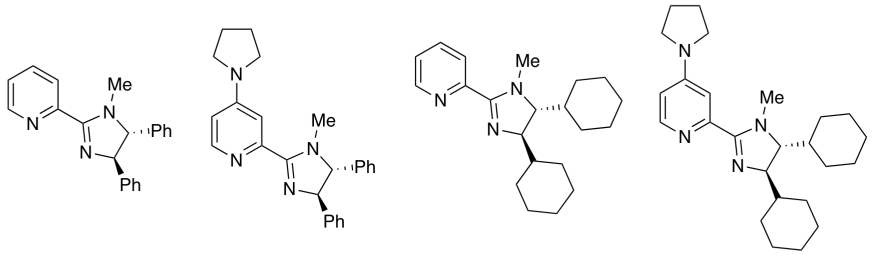

	96	**107**	**111**	**112**
regio (**92a:93a**)[a]	7:1	No Reaction	21:1	No Reaction
anti:syn (**92a**)[a]	1:3	ND	1:1.5	ND
% ee (**92a**)[b]	98	ND	ND	ND
% yield	81	ND	40	ND

[a] Determined by ^{1}H NMR; [b] Determined by chiral GC; ND: not determined

While the Cp*Ru(II) results were interesting, the reaction remained vastly limited. In contrast, the CpRu(II)-imidazoline catalysts easily provided the branched isomer in synthetically viable selectivities. However, no singular imidazoline ligand accomplished entirely optimized selectivities; ligand **107** yielded a higher diastereoselectivity while ligand **111** provided better regioselectivity and enantioselectivity. As a result, the investigation into expanding the substrate scope would explore both ligands to elucidate any additional reactivity differences.

2.3 EXPANDING SUBSTRATE SCOPE

Sterically and electronically diverse silyl enolates and cinnamyl acetate derivatives were subjected to the optimized reaction conditions. Consistently higher diastereoselectivities were achieved with **107**. Higher regio- and enantioselectivities were obtained when **111** was employed. The reaction was also found to be moderately tolerant to alkyl based electrophiles.

2.3.1 Introduction to Substrate Modification

Having identified two ligand-catalysts pairs (**109** and **114**) capable of producing Claisen-type products with good regio-, diastereo- and enantioselectivity, we sought to expand the structural complexity of the α,β-substituted-γ,δ-unsaturated acyl pyrroles by incorporating allylic acetates and silyl enolates of varying electronic and steric demands. The intermolecular mechanism allows for novel electrophile-nucleophile combinations. Synthetically, allylic acetates, available from aryl aldehydes, can be easily modified to include electron-donating and electron-withdrawing groups at any position on the benzene ring. We hypothesized the electronic nature of the resulting allyl ligand would influence the alkylation's regioselectivity. The silyl enol ether can include many diverse substituents as well. We anticipated the developed allylic alkylation would tolerate structurally complex enolates and easily expand upon the limited α-methylated Claisen products previously attainable. Generally, the enantioselectivity was expected to remain ligand dependent and consistently high regardless of the acetate-enolate combination. The developed allylic alkylation was anticipated to expand the number of accessible Claisen-type products with a high degree of regio-, diastereo- and enantioselectivity.

2.3.2 Reaction Scope

To fully elucidate the reactivity of the allylic alkylation, we sought to examine allylic acetates and silyl enol ethers of varying electronic and steric demands. Electronic modifications to the acetate would include appending electron-donating and electron-withdrawing groups to the aryl ring. Further, alkyl based allylic acetates were also to be examined. *ortho*-Substitutions on the acetate's phenyl ring examine the effect of increased sterics adjacent to the alkylation site. The silyl enol ethers could be modified similarly. Therefore, the reaction's nucleophilic tolerance could be determined. Additionally, enolates of varying alkyl chains were to be examined. We were particularly interested in alkyl chains greater than two carbons in length as well as branched enolates. To this end, a variety of aryl and heteroaryl allylic acetates and pyrrole silyl enol ethers were subjected to the optimized reaction conditions (Tables **10** and **11**).

Table 10: Asymmetric Allylic Alkylation Utilizing Ligand 107

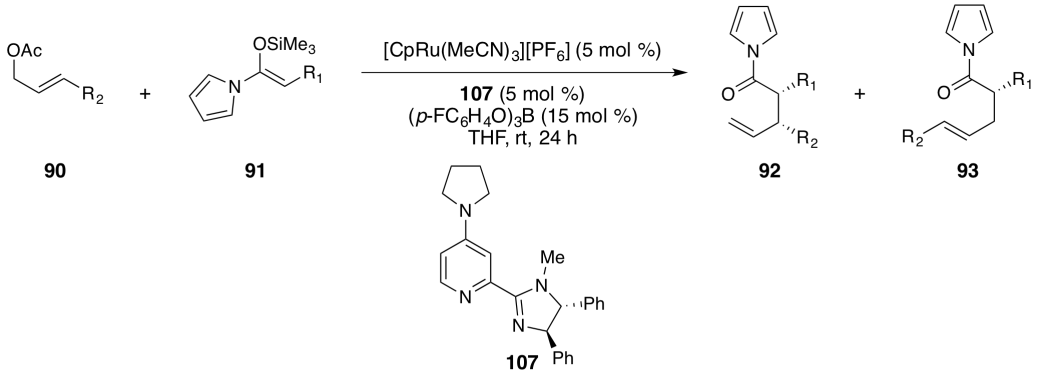

90 **91** **92** **93**

107

entry	R_1	R_2	**92:93**[a]	*anti:syn* (**92**)[a]	% ee (**92**)[b] (*anti, syn*)	% yield[c]
a	Me	Ph	18:1	9:1	95, 79	88
b	H	Ph	14:1	-	68	82
c[d]	*n*-propyl	Ph	13:1	7:1	89, 59	82
d	*i*-propyl	Ph	No Reaction	-	-	-
e	OBn	Ph	11:1	4:1	90, 53	80
f	Cl	Ph	32:1	1.3:1	34, -	21
f'	OAc	Ph	32:1	1.3:1	ND	5
g	Me	Ph, 4-OMe	>33:1	8:1	91, 67	92
h	Me	Ph, 2-OMe	8:1	4:1	89, 45	81
i	Me	2-furyl	17:1	8:1	89, 54	89
j	Me	Ph, 4-NO_2	4:1	5:1	88, 47	53

[a]Determined by ^{1}H NMR; [b]Determined by chiral GC; [c]Isolated yield after flash chromatography;
[d]1.0 equivalent (p-$FC_6H_4O)_3B$; ND = not determined

Table 11: Asymmetric Allylic Alkylation Utilizing Ligand 111

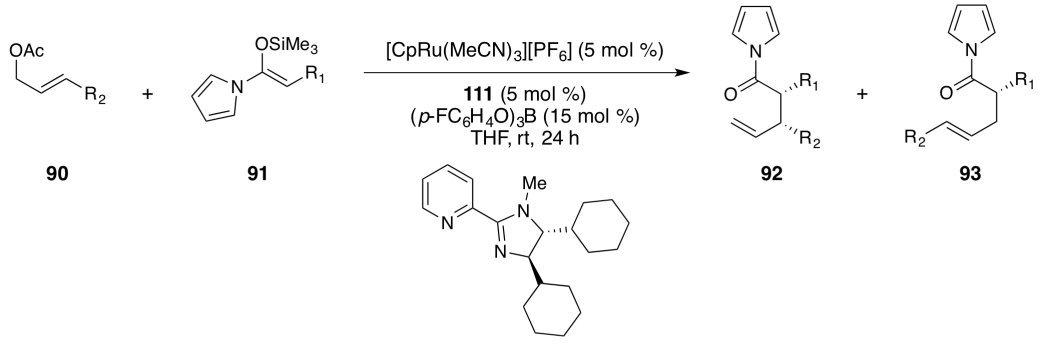

90 **91** **92** **93**

111

entry	R_1	R_2	**92:93**	*anit:syn* (**92**)[a]	% ee (**92**)[b] (*anti, syn*)	% yield[c]
a	Me	Ph	20:1	5.4:1	97, 91	89
b	H	Ph	25:1	-	95	82
c[d]	*n*-propyl	Ph	19:1	6:1	96, 97	82
d	*i*-propyl	Ph	No Reaction	-	-	-
e	OBn	Ph	>33:1	4:1	96, 89	75
f	Cl	Ph	32:1	1.3:1	97, ND	38
f'	OAc	Ph	16:1	2:1	99, 97	10
g	Me	Ph, 4-OMe	>33:1	5:1	94, 89	79
h	Me	Ph, 2-OMe	>33:1	3.3:1	98, 85	79
i	Me	2-furyl	20:1	4.3:1	95, 93	99
j	Me	Ph, 4-NO_2	5:1	4:1	94, 94	88

[a]Determined by ^{1}H NMR; [b]Determined by chiral GC; [c]Isolated yield after flash chromatography;
[d]1.0 equivalent (p-$FC_6H_4O)_3B$: ND = Not Determined

2.3.3 Limitations to Enolate Sterics

A primary goal of the developed methodology was to expand the structure of the α-substitutions available via the asymmetric Claisen rearrangement. This required employing structurally diverse enol silane nucleophiles in the developed allylic alkylation. While the reaction consistently afforded the desired Claisen-type product in high yields, three enolates exposed

limitations in the methodology. The *n*-propyl silyl enol ether (entries c) required additional borate co-catalyst (1.0 equivalents) for complete consumption of the allylic acetate to occur. Longer chain alkyl groups are known to substantially decrease enolate nucleophilicity. The additional borate may facilitate access to the Ru(IV)(π-allyl) complex which ensures that nucleophilic attack occurs more efficiently before catalyst death. The chlorine-substituted enol ether (entries f) provided the desired product in ~30% yield (average of both tables). Increasing the borate to a full equivalent proved ineffective in improving reaction yields, indicating that this substrate suffered from diminished nucleophilicity. Additionally, the chlorinated product was susceptible to displacement via an S_N2 mechanism by the acetate anion under the reaction conditions (entries f'). Although this lowered the yield of the desired product, it proves the facile derivatization at R_1 for this compound. Finally, the reaction proved intolerant to di-substitution at the α-position of the enol. The isopropyl derivative (entries d) afforded no reaction regardless of the ligand utilized or upon increasing the amount of borate to a full equivalent. The alkylation yields exhibited a dependence upon enolate structure. While larger alkyl chains were tolerated upon further activation, sterically congested enolates were proven incompatible under the reaction conditions. Further, a high degree of nucleophilicity was needed to maintain high yields. Overall, the reaction yields proved tolerant to structurally diverse silyl enolates.

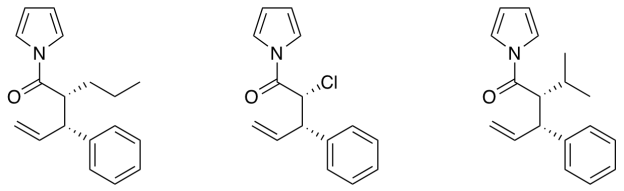

92c **92f** **92d**

Figure 9: Enolate Limitations in the Allylic Alkylation

2.3.4 Effects of Acetate Electronics on Observed Product Regioselectivity

Our ligand optimization efforts led to the hypothesis that catalyst electronics directly affected the allylic alkylation's regioselectivity. All tested reactions favored branched product formation (**92:93** = 4:1-33:1). Ligand **111** provided consistently higher, substrate independent regioselectivities than ligand **107**. Ligand **107** exhibited a greater dependence on the electronic nature of the allyl ligand. For example, electron-rich allylic acetates, such as *p*-methoxyphenyl (Table 10, entry g), exhibited increases in regiochemistry compared to the standard case (entry a). Conversely, the electron-deficient *p*-nitrophenyl allylic acetate provided considerably lower selectivities (Table 10, entry j, **92j:93j** = 4:1). This can be explained via the geometric and electronic distortion of the Ru(IV)(π-allyl) complex. Ruthenium-allyl complexes favor the branched product due to metal-C_3 bond elongation. As this bond lengthens, less negative charge develops on the benzylic carbon of the allyl ligand. Electron-rich aryl groups stabilize the benzylic carbon, thereby enhancing the bond elongation. However, the electron-deficient aryl groups cannot stabilize the benzylic carbon; as a result, the geometric distortion remains limited, and the branched product becomes less favored.

2.3.5 Silane Structure Affects Reaction's Diastereoselectivity

Ligand **107** provided higher diastereoselectivities than its counterpart (**111**). When maintaining cinnamyl acetate as the electrophilic partner, the diastereoselectivity ranged from 1.3:1 – 9:1 (**92**$_{anti}$**:92**$_{syn}$) when **107** was employed; in comparison the highest d.r. achieved with **111** was 6:1 (**92**$_{anti}$**:92**$_{syn}$, entry c). In both systems, chloro-substituted silyl enol ether (entries f) provided the lowest selectivity. However, this can be attributed to the epimerization of the stereocenter under

the conditions due to the relatively high acidity of the α-hydrogen due to the electron withdrawing abilities of the halide. Overall, the reaction demonstrated modest diastereoselectivities where **107** performed slightly better than **111**.

2.3.6 Ligand Effect on Enantioselectivity

Both tested ligands provided high enantioselectivities for the *anti*-diastereomer. Ligand **111** exhibited equally high %ee values for the *syn*-diastereomer. However, **107** demonstrated diminished %ee values for the *syn*-isomer (Table 10, entry a, %ee $\mathbf{92a_{anti}}$ = 95 %, %ee $\mathbf{92a_{syn}}$ = 79%). We attribute the success of **111** at maintaining high enantioselectivities regardless of the diastereomer to the increased steric contribution of the cyclohexane rings to the active catalyst. The larger rings better dictate enolate approach regardless of which trajectory is taken. Ligand **107** dictates the approach that provides the *anti*-diastereomer well, but is far less efficient at influencing the *syn*-trajectory. The two optimized ligands demonstrate complimentary selectivities, providing the opportunity to gain high regio- and enantioselectivities or diastereoselectivities depending upon synthetic needs.

2.4 ALLYLIC ALKYLATION OF AN ALKYL BASED ELECTROPHILE

The optimized allylic alkylation conditions tolerated electronically diverse cinnamyl acetate derivates. However, the methodology sought to expand the β-substitution of the Claisen-type products to include aliphatic groups. Utilizing crotyl acetate (**113**) as the electrophilic partner successfully produced the desired branched product **114** (Table 12). The reaction suffered from

chronically low yields regardless of the ligand utilized (~36%), indicating that the oxidative insertion across the alkyl acetate was less efficient that their aryl counterparts. Additionally, the aliphatic substrate directly impacted the regioselectivity. As previous studies indicated, ligand with the most Lewis-basic $N_{pyridine}$ (**112**) yielded the highest selectivities, providing the branched isomer 6:1 over the linear product. As Ru(IV) bonds to alkyl based π-allyl ligands in a more symmetrical fashion,[17] obtaining even a modest regioselectivity was an accomplishment. The diastereoselectivities correlated to those observed when ligand **107** was utilized with cinnamyl acetate based electrophiles (Table 10), yet the enantioselectivities fell below synthetic utility. As before, no case was found to provide uniformly high selectivities and even the best cases fell short of expectations. Other aliphatic substrates were not explored.

Table 12: Allylic Alkylation with Alkyl Based Electrophile

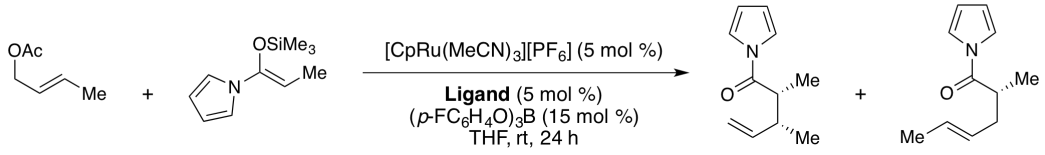

113 **91a** **114** **115**

Ligand =	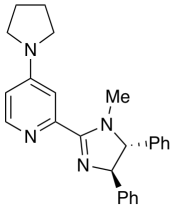	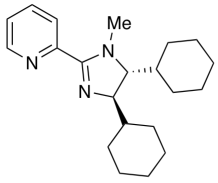	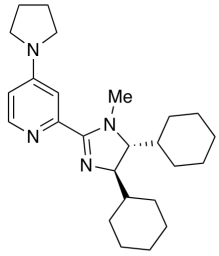
	107	**111**	**112**
regio (**117:118**)[a]	4:1	1.4:1	6:1
anti:syn (**118**)[a]	4:1	7:1	4:1
% ee (**117**)[b]	ND	67	80
% yield	36	37	37

[a]Determined by ^{1}H NMR; [b]Determined by chiral GC; ND: Not Determined

2.5 REACTION MECHANISM

2.5.1 A Proposed Tolman Cycle

Mechanistically, the reaction proceeds via allylic acetate association to active CpRu(II)-pyridyl imidazoline complex **118** (Figure 10) followed by oxidative insertion across the carbon-oxygen σ-bond with the assistance from the borate co-catalyst providing the requisite Ru(IV)(π-allyl) complex **120**. The resulting acetate leaving group activates the latent enolate towards nucleophilic attack via a Lewis acid-base interaction with the silicon residue.[36, 53] The reactive enolate adds into the activated allyl ligand with a bias for attack at the more substituted carbon forming Claisen-type products **92a** with a preference for the *anti*-diastereomer.

Establishing two tertiary, vicinal stereocenters without epimerization requires maintaining neutral reaction conditions.[20] Using allylic acetates as the allyl precursor generates an equivalent of acetate anion, whose basicity could deprotonate the α-position of the acyl pyrrole product. The proposed mechanism prevents the undesired reactivity by sequestering the acetate ion. First, allyl acetate activation by the borate Lewis acid produces an equivalent of borate ester upon oxidative insertion (**119**). Subsequent activation of the silyl enolate by the acetate generates trimethylsilyl acetate (**122**). Therefore at no time during the reaction process is there a significant population of acetate anion present to cause epimerization. Ultimately, the reaction's success relies upon rendering the acetate ion inert.

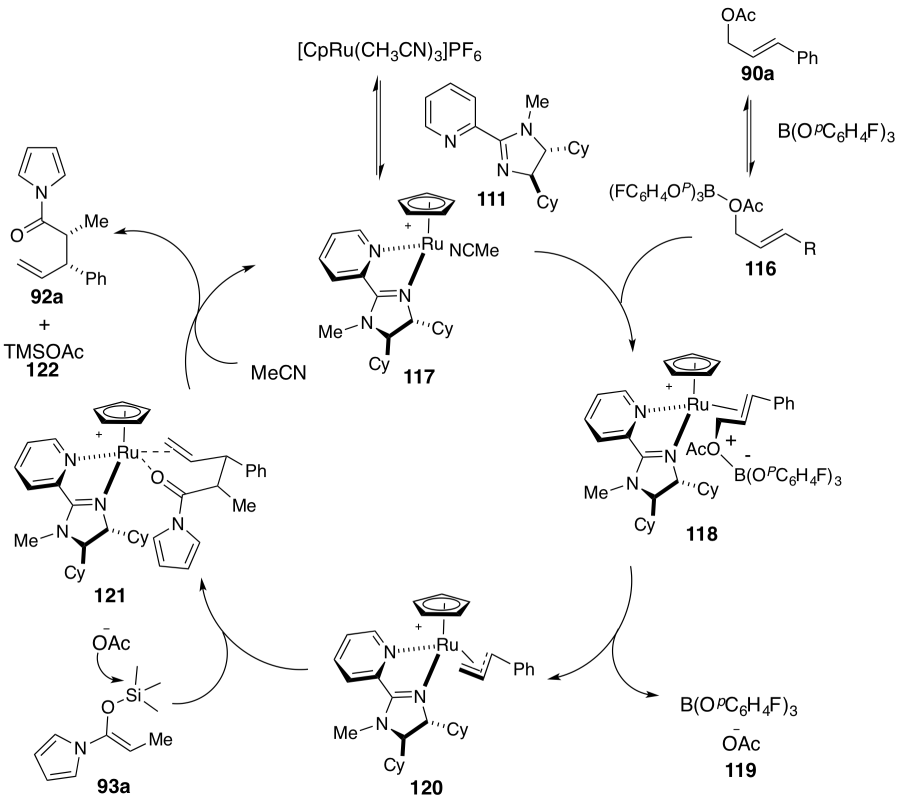

Figure 10: Proposed Reaction Mechanism

2.5.2 Evidence of a Ru(IV)(π-allyl) Intermediate

Allylic alkylation chemistry mechanisms depend upon the formation of a π-allyl complex as the key intermediate. Although the proposed mechanism incorporates a Ru(IV)-allyl complex, a metal-mediated S_N2' reaction cannot be fully disproven.[54] To provide further evidence in support of the η^3-allyl complex, we sought to subject the branched allylic acetate **90a'** to the optimized reaction conditions. If the reaction undergoes an S_N2' mechanism, the branched acetate would favor the linear product; however, if the branched product remained dominant, than a common intermediate is supported. Employing the branched allylic acetate under the optimized reaction conditions (Figure 11), produced the identical regioselectivity as the linear allylic acetate,

supporting the formation of an Ru(IV)-allyl complex. While it remains possible that the branched substrate undergoes a rearrangement to form the linear allylic acetate followed by subsequent S_N2' substitution, we can conclude that the standard π-allyl complex is the most likely mechanism.

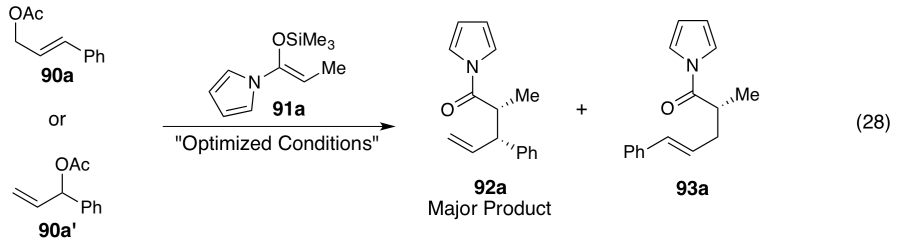

Figure 11: Evidence of a Ru(IV)-allyl intermediate

2.5.3 Diastereoselectivity Models

The asymmetric Claisen chemistry controlled the diastereoselectivity via an inner sphere mechanism dictated by a hydrogen bond with the pyridyl indanol ligand **36** (Figure 12).[24, 25] However, the pyridyl imidazoline ligands utilized in the allylic alkylation are incapable of hydrogen bonding in this manner. Therefore, an alternate explanation of the observed diastereoselectivity is required.

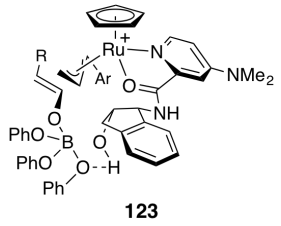

Figure 12: Hydrogen Bonding Capabilities of Pyridyl Indanol Ligand 36

Examination of the Newman projections of the pyrrole silyl enol ether nucleophiles provided valuable insight. As orientation of the enol ether dictates the diastereoselectivity, both possibilities were examined. Two stable conformations, one of which provides the desired *anti*-

diastereomer and the other the *syn*-diastereomer, were elucidated. Upon initial examination, it appears that both conformations are equally stable. However, a more detailed analysis reveals that three gauche interactions are present in the *syn*-clinal model, but there are only two such interactions in the *anti*-periplanar model. This explains the preference, but highly variable selectivity, towards the *anti*-product.

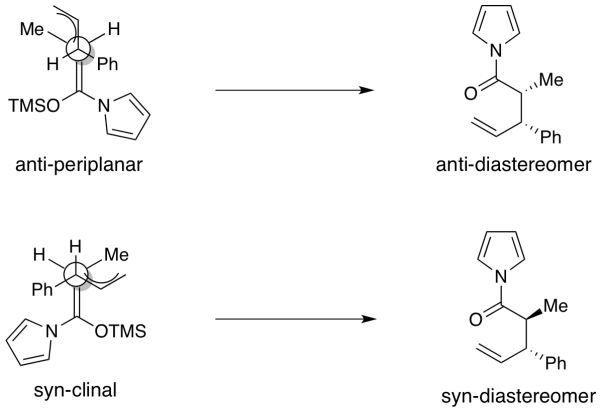

Figure 13: Diastereoselectivity Models

2.6 CONCLUSIONS

A highly regioselective, diastereoselective, and enantioselective ruthenium(II)-catalyzed allylic alkylation which utilizes pyrrole silyl enol ether nucleophiles has been developed. This reaction tolerates a variety of aromatic allylic acetate electrophiles and enol silane nucleophiles. Under the optimized reaction conditions described, Claisen-type products previously inaccessible due to prior starting material limitations were readily synthesized. In addition, all possible combinations of allylic acetates and pyrrole silyl enol ethers contained herein are synthetically feasible to provide a greater scope than summarized in the above tables. The acyl pyrrole products contain

two chemoselective handles, which further increase utility, especially in the lens of natural product synthesis.

3.0 EFFORTS TOWARDS THE TOTAL SYNTHESIS OF ACTINORANONE

We sought to exemplify the utility of our Ru(II)-catalyzed asymmetric allylic alkylation by designing a efficient natural product synthesis. Actinoranone was chosen as the target for our efforts due to its biological activity against human colon cancer cells (HCT-116). The asymmetric allylic alkylation sets the key benzylic stereocenter in the naphthalone core. The penultimate compound was achieved over five steps in 7.11% yield. However, difficulties in synthesizing the terpenoid fragment enantioselectively prevented our ability to achieve the total synthesis.

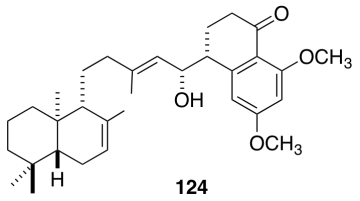

124

Figure 14: Actinoranone

3.1 MOLECULAR STRUCTURE

Actinoranone (**124**) was isolated as a pale yellow oil from a marine actinomycete (strain CNQ-027) related to *Strepomyces marinus* in limited yields.[54] An initial evaluation of the structure reveals a C_1-C_{14} octahydronapthalene and a $C_{1'}$-C_{15} tetrahydronaphthalene subunits linked by a

functionalized alkyl chain (Figure 15). The bicyclic diterpenoid contains three contiguous stereogenic centers including a quaternary stereocenter at C_{10}. The $C_{1'}$-C_{15} subunit contains two contiguous stereogenic centers including the C_{15} alcohol. Our interest in actinoranone resides in its biological activity and its potential as a drug scaffold.

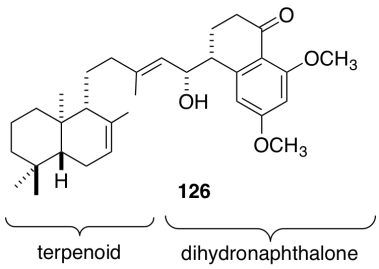

Figure 15: Actinoranone Subunits

3.2 ACTINORANONE: A POTENTIAL COLON CANCER DRUG SCAFFOLD

Colorectal cancer ranks third in annual cancer deaths in the United States and fourth globally.[56] While surgery effectively treats early detection cases, metastasis in later stages remains essentially incurable.[57] Providing a therapeutic strategy for late stage colon cancer remains a focus of clinical research. Actinoranone demonstrates a high efficacy against a human colon cancer cell-based assay (HCT-116) with a measured LD_{50} = 2.0 μg/mL.[55] Given the limited availability from natural sources, a synthesis of actinoranone would provide an important supply of the material for further biological investigation and possibly lay the foundation for pharmaceutical development.

The precise mode of action against the HCT-116 cell line remains undetermined and not well understood as there are several possible available pathways; determining the most effective protein target for small molecule inhibition remains under investigation.[57, 58] Actinoranone's

structure, coupled with its effectiveness against colon cancer cells, led to an inference about its biological activity. We speculated that the observed cytotoxicity is due to the dihydronaphthalenone core while the "labdane" half acts as a structural anchor, filling a lipophilic protein pocket. With this structure-function hypothesis, we sought an efficient synthesis of actinoranone's core via our ruthenium(II)-catalyzed asymmetric allylic alkylation.

3.3 RETROSYNTHETIC ANALYSIS

Retrosynthetic analysis of actinoranone divides the molecule into its C_1-C_{14} and $C_{1'}$-C_{15} subunits. Union of the synthons was envisioned as proceeding by an aluminum-mediated addition of the decalin system (**125**) into aldehyde **126** (Figure 18a). The reaction would observe Felkin-Anh selectivity to set the carbinol stereocenter (Figure 18b). Aldehyde **126** would be obtained via oxidative cleavage of vinyl moiety **127**, the product of a Friedel-Crafts acylation. Carboxylic acid **128** would derive from acyl pyrrole **130**, obtainable via the ruthenium(II)-catalyzed asymmetric allylic alkylation.

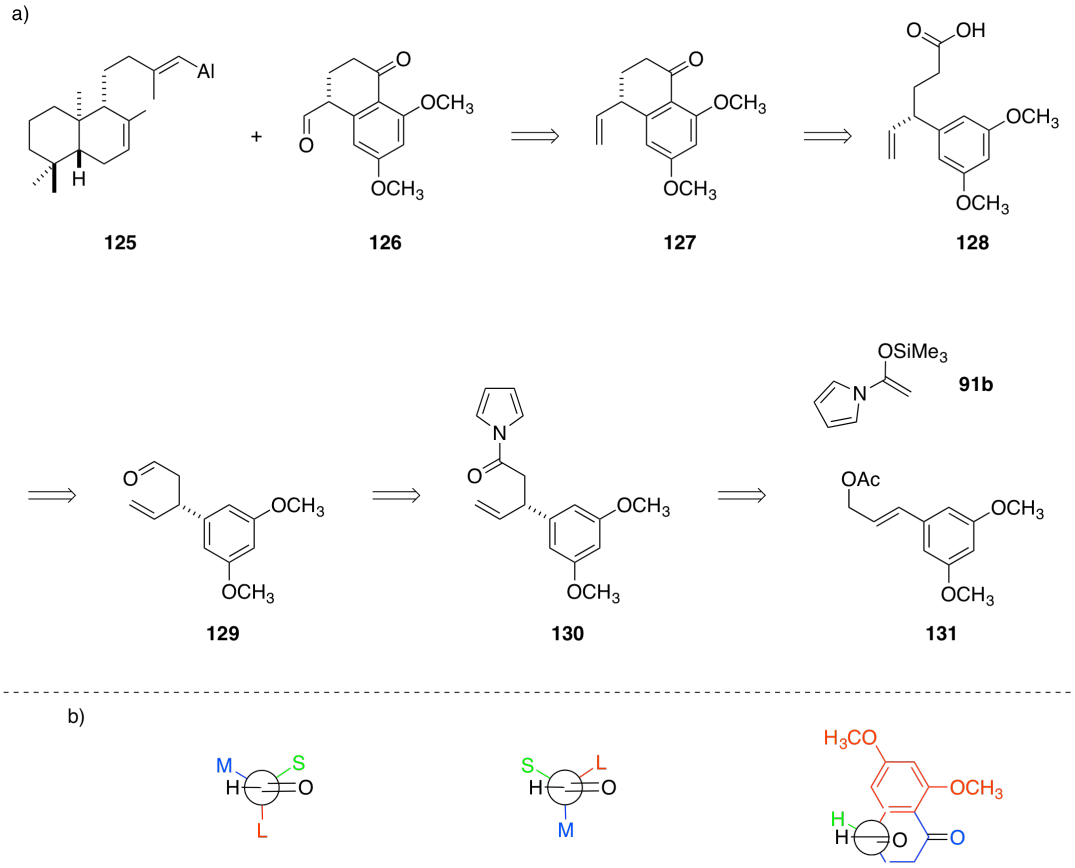

Figure 16: a) Retrosynthesis of the $C_{1'}$-C_{15} Subunit; b) Felkin-Anh Model of Aldehyde 126

Vinyl aluminum **125** would be obtainable from the *syn*-addition of Me_3Al across the terminal alkyne (**132**). We envisioned that alkyne **132** would be formed via a copper-mediated 1,4-addition into ketone **133**. We envisioned that the key intermediate (**133**) would result from an asymmetric Ir(I)-catalyzed isomerization of β,γ-unsaturated ketone **134**. A Birch reduction of bicyclic *m*-anisole derivative **135** would provide ketone **134**. Acid-catalyzed dehydration of tertiary alcohol **136** precipitates ring closure, the materials for which would be obtainable from commercially available carboxylic acid **137**. The proposed convergent route would access actinoranone efficiently while highlighting the novel allylic substitution chemistry.

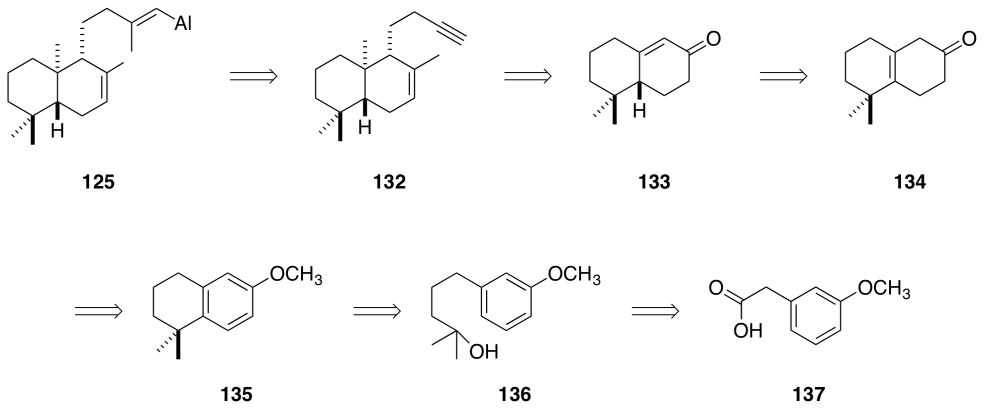

125 132 133 134

135 136 137

Figure 17: Retrosynthesis of the Terpenoid Subunit

3.4 SYNTHESIS OF THE NAPHTHALONE CORE

Our efforts towards the synthesis of actinoranone commenced with the naphthalone core. Using the previous asymmetric allylic alkylations as a model (Table 10), we made predictions about the required, previously unexplored substrate. Specifically, we expected a high degree of regioselectivity when employing ligand **107** due to the highly electron-rich allylic acetate. Specifically, the enantiomeric excess was expected to be approximately 70% ee based upon the unsubstituted silyl enol ether nucleophile required (Table 10, entry b). Exposing silyl enol ether **91b** to dimethoxy allyl acetate **131** in the ruthenium(II)-catalyzed asymmetric allylic alkylation conditions produced β-substituted acyl pyrrole **130** (Equation 29**,** 86% yield, **130:130a** = >40:1, 72% ee **130**). As anticipated, the highly electron-rich allyl ligand rendered the reaction regioselective, surpassing the >33:1 (b:l) regioselectivity observed when 4-methoxy acetate was the substrate in the ruthenium(II)-catalyzed allylic alkylation (see Table 10, entry g). Similarly, the enantioselectivity 72% ee was in the anticipated range based upon previous allylic alkylations with silyl enolate **91b**. While a 72% ee is not ideal for asymmetric synthesis, we

understood that this value could be improved by employing the more sterically congested ligand **111**. However, facing the difficulty in producing ligand **111** on large scale, we thought it expedient to continue to explore the synthesis with the limited enantioselectivity.

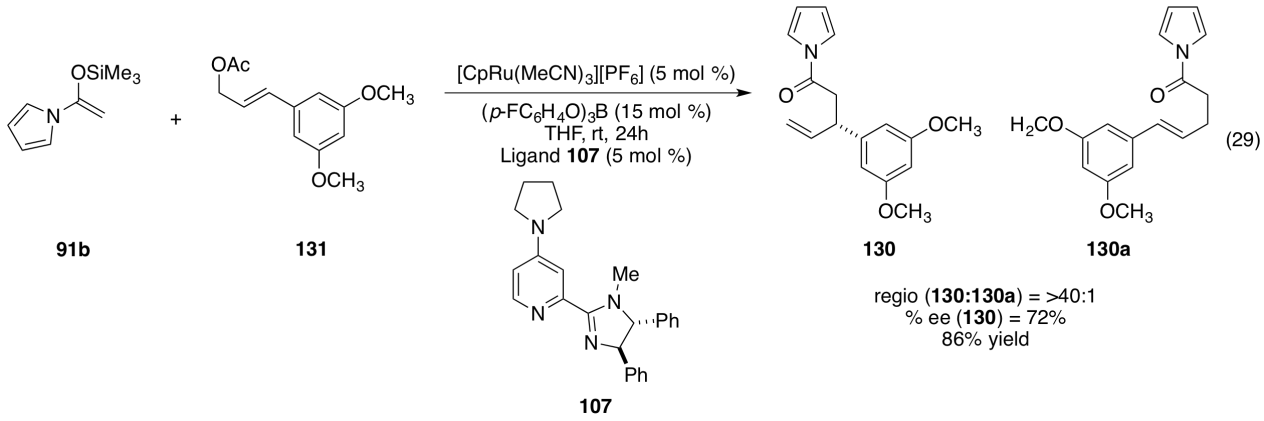

In order to access the six-six fused ring system, a homologation of the acyl pyrrole (**130**) between C_1 and C_2 was required. Initially, a reduction of the acyl pyrrole to the corresponding aldehyde was believed to be necessary in order to perform the subsequent Wittig homologation oxidation.[59] To access the aldehyde, a direct reduction of the acyl pyrrole with DiBAlH was conducted. However, this strategy yielded the stable hemiaminal (Equation 30). This indicated that the reactivity of the acyl pyrrole more closely resembled an aldehyde or ketone rather than a traditional amide, the reduction of which typically yields an amine. To circumvent this undesired reactivity, it was proposed that converting the pyrrole to the methyl ester followed by a single reduction to aldehyde would be most efficient.

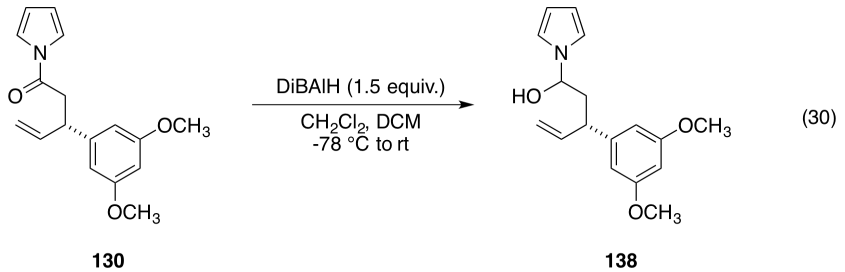

Precedent indicated that exposing an acyl pyrrole to nucleophilic base would provide the desired ester. Exposing **130** to anhydrous sodium methoxide in methanol/THF proceeded in 70% yield (Equation 31).[25] Subsequent experimentation indicated that removing the solvent in vacuo prior to acidic work-up resulted in quantitative yields.

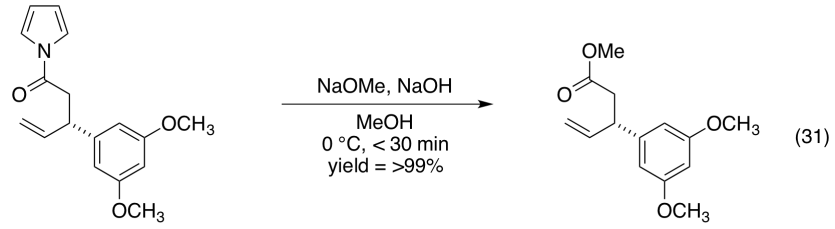

130 **139** (31)

The Wittig homologation-oxidation requires an aldehyde electrophilic partner. To install the aldehyde, a single reduction of the methyl ester was conducted (Equation 32). Attempted homologation of aldehyde **129** utilizing (methoxymethyl)triphenylphosphine chloride (**140**) proved incompatible with the substrate as the conditions provided the decalin (**146**) rather than aldehyde **141** (Scheme 10). The decalin product **146** results from hydrolysis of methyl-vinyl ether **142** with dilute HCl generating the oxocarbenium ion **143**. The highly electron-rich aromatic ring system directly attacks the oxocarbenium ion, closing the bicyclic ring system (**144**), which, upon elimination of methanol, extends conjugation. While this reaction pathway did not lead to the desired tetrahydronaphthalene (**127**), the observed reactivity indicated that the substrate would readily undergo a Friedel-Crafts acylation. As we sought to close the ring system via this exact mechanism in the next transformation, it was predicted that the Friedel-Crafts acylation would occur readily. Therefore, while this process was incompatible with intermediate **129**, it verified the viability of the proposed synthesis plan.

Scheme 10: Intramolecular Cyclization via Wittig Homologation

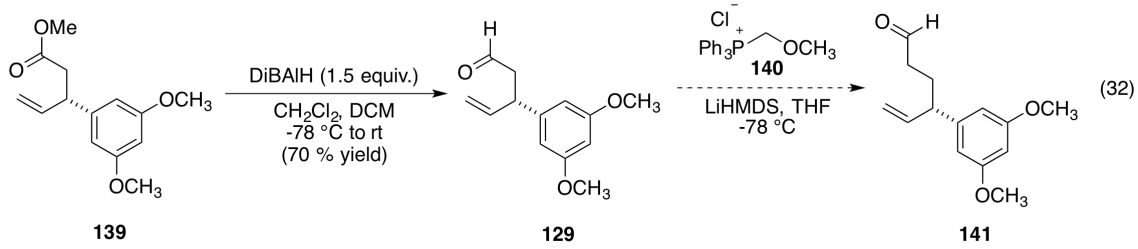

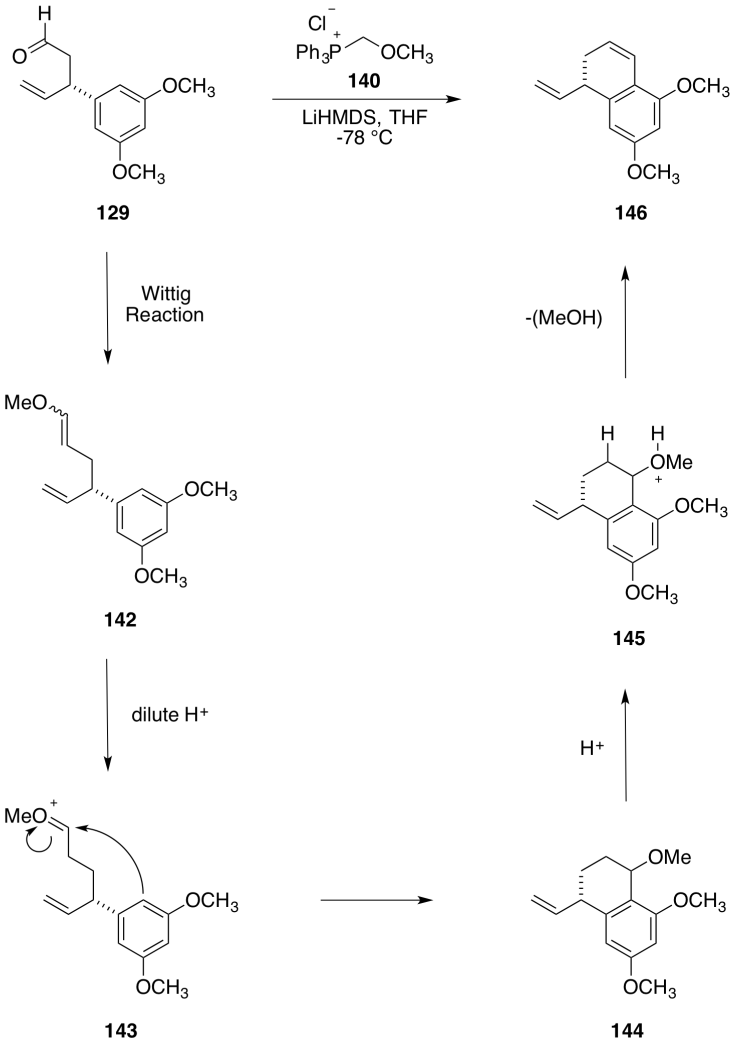

Actinoranone contains a carbonyl at C_1, which we sought to establish via a Friedel-Crafts acylation. However, aldehyde **129** demonstrated that the carbonyl would be lost with this substrate. To avoid the undesired reactivity, we required a homologation that provided a carbonyl of a higher oxidation state. A higher oxidation state carbonyl, while still capable of

direct cyclization, would maintain the carbon-oxygen double bond rather than establishing a carbon-carbon double bond via elimination. To accomplish this goal, an initial investigation focused on installing a second methyl-vinyl ether functionality (**148,** Scheme 11).[60] Under strongly basic conditions, *n*-BuLi in THF, a dialkyl phosphate (**147**) reacted with aldehyde **129** yielding **148**. Exposing **148** to dilute acid generated the oxocarbenium ion, whereupon elimination of solvent would maintain the carbonyl adjacent to the aromatic ring upon ring closing (Scheme 11). However, the EAS reaction was far slower than the previously observed case (Scheme 10) and as a result, methyl ester **149** was consistently isolated instead of naphthalone **127** (Scheme 11). Since methyl ester **149** cannot participate in the ring-closing Friedel-Crafts acylation, to utilize the ester in the designed route would require a subsequent transformation to the carboxylic acid. While this sequence yielded the desired homologation-oxidation, we chose to investigate other pathways that could potentially result in direct cycylized product.

Scheme 11: Initial Oxidative Homologation

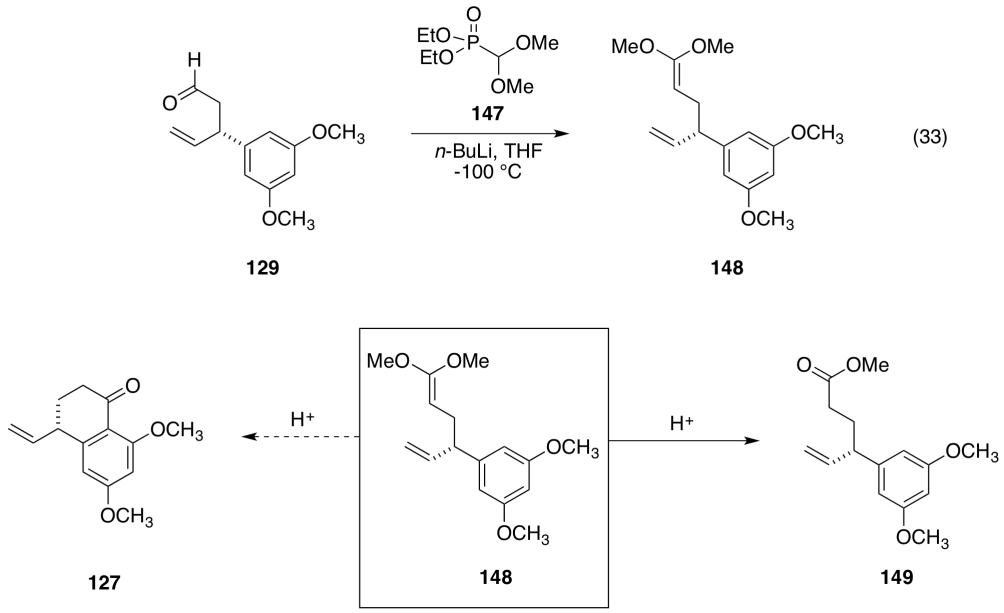

A second homologation-oxidation method utilizes trimethylsilyl(methoxy)benzotriazol-1-ylmethane (**150**) as the nucleophilic source.[61] The strongly Brønsted and Lewis conditions ($ZnBr_2$, HCl, in refluxing dioxane), in the second synthetic step guarantees the formation of carboxylic acid **128** which we anticipated would undergo direct Friedel-Crafts acylation resulting in the bicyclic ring system (**127**). Under the conditions (**156**, *n*-BuLi, THF, -78 °C, Scheme 12),[61] the homologated carboxylic acid **128** and the naphthalone **127** were isolated, favoring the acyclic product. The production of the bicyclic product was encouraging, proving that when **153** is sufficiently activated, the intramolecular ring closure occurs. However, the reaction conditions could not be altered to provide solely bicycle **127** or the acid **128** and the products needed to be separated before subsequent experimentation. Therefore, while we needed **127** in our synthetic route, we wanted to explore one additional procedure capable of producing acyclic acid **128** selectively.

Scheme 12: Benzotriazole Mediated Homologation-Oxidation

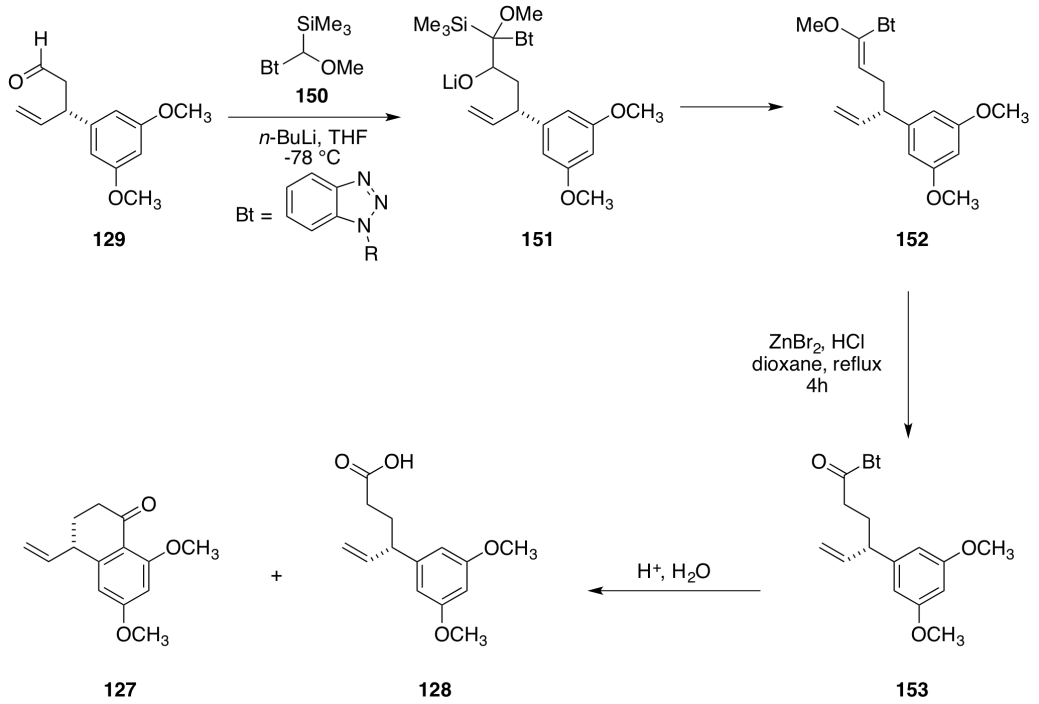

While the benzotriazole method presented a viable option for obtaining bicycle **127** and acyclic acid **128** as a mixture, we wanted to explore a third homologation-oxidation procedure capable of producing solely the desired acid. The alternative method utilizes nucleophilic chloroform in a Jocic-type reaction as the carbon source under aqueous basic conditions (Scheme 13).[62] Previous experimentation from other groups successfully implemented this reaction procedure to homologate benzaldehyde derivatives in small molecule syntheses.[63] We were encouraged by this precedent and remained confident that any side products would be easily removed by standard purification methods. We exposed aldehyde **129** to chloroform in aqueous KOH immediately followed by *in situ* exposure of **154** to $NaBH_4$ in *tert*-butanol (Equation 34). The resultant acid chloride hydrolyzes under the reaction conditions to provide **128** in 35% yield over two steps. Under the basic conditions, neither the acid chloride nor acid **128** were sufficiently activated toward electrophilic aromatic substitution. Thus, direct intramolecular ring closure cannot take place and bicycle product **127** was not detected in the crude reaction mixture. Having successfully obtained the acid as the major product in good yields without producing bicycle **127**, we chose to apply this method in our total synthesis.

Scheme 13: Jocic-type Homologation-Oxidation

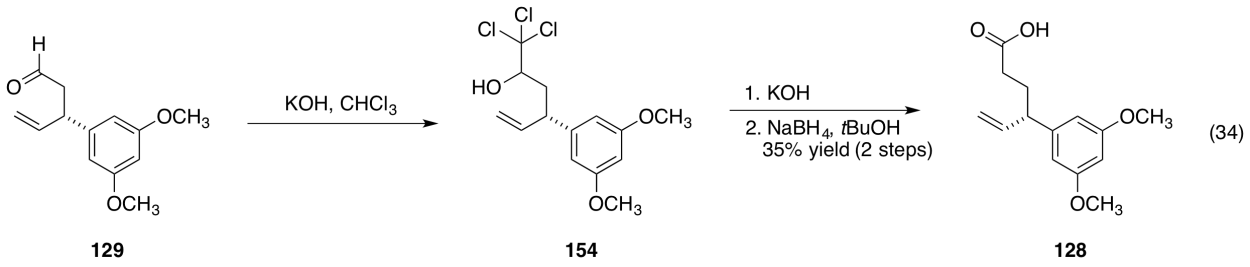

129 **154** **128** (34)

Friedel-Crafts acylations necessitate an activated electrophile and suitably electron-rich nucleophile. Having inadvertently proven that the aromatic ring was exceedingly capable of undergoing the desired intramolecular ring closure, efforts focused on activating the latent carbonyl. Standard conditions suggest accessing the acid chloride followed by subjection to a

strong Lewis acid. However, carbonyl activation with electron-deficient anhydrides, such as TFAA, occurs under milder conditions and, in many cases, in the absence of solvent.[64] Further, the reaction rates occur on the scale of minutes rather than hours. To this end, acyclic acid **128** was subjected to triflic anhydride in minimal THF (Equation 35). These conditions provided the desired naphthalone **127** in 75% yield. Currently efforts are underway to determine the ideal conditions necessary for achieving the oxidative cleave of the terminal olefin.

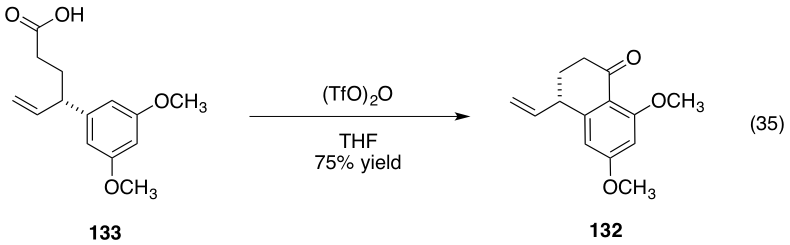

133 **132** (35)

From these efforts, an asymmetric synthesis of bicycle **127** was achieved in five synthetic steps and 7.11% overall yield. This material was produced with moderate enantioselectivity, 72% ee. Future efforts may be capable of improving the enantioselectivity by utilizing bulkier ligand **111** during the asymmetric allylic alkylation. Based on our previous efforts, this ligand may be capable of producing **130** in 95% ee.

3.5 INITIAL SYNTHESIS OF THE TERPENOID SUBUNIT

The initial synthetic effort towards the terpenoid fragment of actinoranone utilized a commercially available *m*-anisole derivative (**137**, Scheme 14a). Reduction of carboxylic acid **137** with BH_3•DMS complex to primary alcohol **155** proceeded in quantitative yields.[65] Subsequent conversion of the alcohol to the corresponding Grignard precursor (**156**).[66] Exposing **156** to magnesium metal in diethyl ether yielded the Grignard reagent, to which was added 1,1-

dimethyloxirane.[67] Despite the simplicity of this reaction, the recorded yields of the tertiary alcohol were highly inconsistent. Under the reaction conditions, Wurtz coupling predominated (Scheme 14b). To improve yields and limit side reactivity, we exchanged the bromide leaving group for the related iodide believing that by increasing the rate of oxidative insertion, dimerization would be suppressed. However, this modification did not stabilize the yields. No optimization of this reaction took place.

Scheme 14: a) Synthesis of 136 via a Grignard Reaction b) Competing Wurtz Coupling

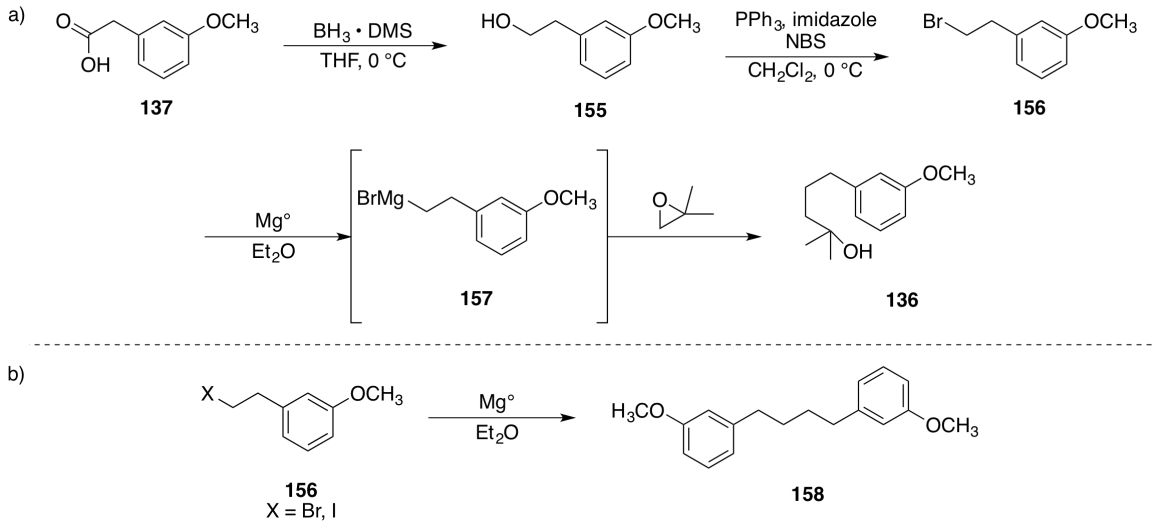

Dehydrating tertiary alcohol **136** provides a stable tertiary carbocation which immediately undergoes intramolecular ring closure. However, the structure of this material establishes competing ring closings between two regioisomers, of which only the *para*-isomer could lead to the natural product. In order to discern the optimal conditions for complete regioselectivity, several conditions were examined. Lewis acid activation of the alcohol by $Bi(OTf)_3$[68] and Amberlyst® 15 hydrogen form[69] showed minimal preference for the desired product, exhibiting 1.5:1 and 2.5:1 selectivity (**135:135a**) in favor of *para*-product **135**. Utilizing dehydrating polyphosphoric acid (PPA), which has a large counterion, consistently exhibits

complete selectivity for **135** in 70% yields.[67, 70] The steric acid proved most efficient in terms of yield and selectivity in yielding the desired bicycle.

Table 13: Intramolecular Ring Closing Regioselectivity

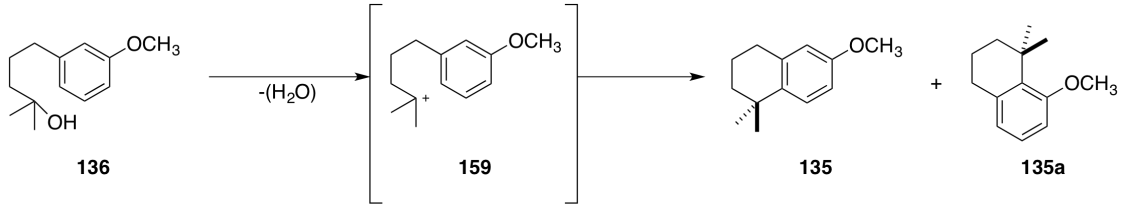

136 **159** **135** **135a**

entry	reagent	**135:135a**	% yield
a	$Bi(OTf)_3$	1.5:1	94%
b	Amberlyst 15	2.5:1	NA
c	Polyphosphoric Acid (PPA)	100:1	70%

[a] Determined by ^1H NMR; NA = Not Available

The β,γ-unsaturated ketone **134** derived from naphthalene **135** via a Birch reduction with complete regioselectivity in 70% yield (Equation 36).[67, 71] The observed reaction conversions were inefficient, typically falling between 70% and 80% conversion. Adding excess lithium metal in several portions over the course of the reaction failed to improve conversions and isolated yields. Reexposing the unreacted starting materials to the Birch conditions became restrictive in terms of time and resources.

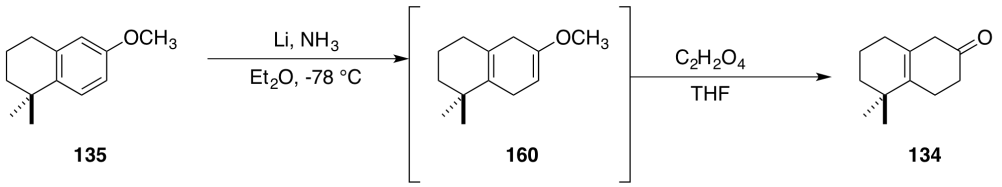

135 **160** **134** (36)

Enone **134** proved relatively labile. Prolonged exposure to ambient light converts the β,γ-unsaturated ketone to the thermodynamically more stable α,β-unsaturated ketone (**133**). This observation was both encouraging and problematic as it indicates that the desired isomerization would occur readily, controlling the mode of isomerization could prove difficult. We sought to

utilize our previously developed Ir(I)-catalyzed conditions to control the isomerization.[72] Initial results were encouraging; both TLC and ^{1}HNMR indicated a successful isomerization to the α,β-unsaturated ketone. The desired product was isolated in 37% yield (Table 14). Although the initial test conditions indicated a successful reaction, subsequent isomerization reactions consistently failed to yield the desired product (**133)**. Knowing the isomerization to be sensitive to the metal to phosphine-ligand ratio, we conducted a small methodological study to determine what conditions promoted the desired isomerization. The initial reaction results were never replicated despite numerous efforts. This suggested the presence of an unforeseen anomaly in the initial conditions; likely, this reaction was a false positive where the substrate isomerized either photolytically or thermally during the reaction.

Table 14: Ir(I)-catalyzed Isomerization of Enone 134

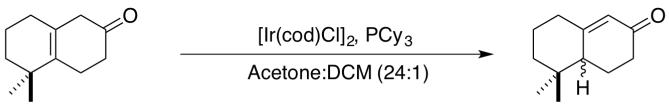

134 **133**

entry	$[Ir(cod)Cl]_2$ (equiv.)	PCy_3 (equiv.)	% yield (**133**)
a	1.0	1.0	37%[a]
b	1.0	2.0	0%
c	1.0	3.0	0%
d	1.0	4.0	0%

[a] Represents only one experiment

The proposed synthetic route to the decalin system faced several challenges cumulating in the failed isomerization, the key step that differentiated it from previous studies. Decreased yields from undesired side reactions and incomplete conversions plagued this route from its initial steps. With these obstacles in mind, it was decided that a redesign of the half was required.

3.6 APPROACHING THE TERPENOID VIA AN ASYMMETRIC 1,4-ADDITION INTO A STERICALLY CONGESTED ENONE

A new examination of the terpenoid subunit indicates the relationship between the three continuous stereocenters ensures the greatest stability in the bicyclic system. The C_{10}-Me and the C_5-H establish the *trans*-decalin ring system (Figure 20). By comparison to the *cis*-decalin isomer, the thermodynamic stability of the *trans*-isomer becomes obvious. Further, the *cis*-relationship between C_{10}-Me and C_9-alkyl ensures that the alkyl-linker occupies an equatorial position on the ring. Having the advantage of a thermodynamic product, we explored a route designed to take advantage of the inherent stability: setting a single stereocenter could potentially control the stereochemistry of the remaining two stereogenic centers. To this end, decalin-ester **161** was chosen as the new key intermediate in the terpenoid synthesis. **162** sets the quaternary methyl group as the anchor stereocenter, while the remaining stereocenters are made pliable by installing two adjacent carbonyl groups. By increasing the acidity of H_5 and H_9, the stereocenters become enolizable when exposed to mild acid or base. Therefore, setting the stereocenter at C_{10} and exposing **162** to thermodynamic control should achieve the most stable bicyclic ring system (**161**).

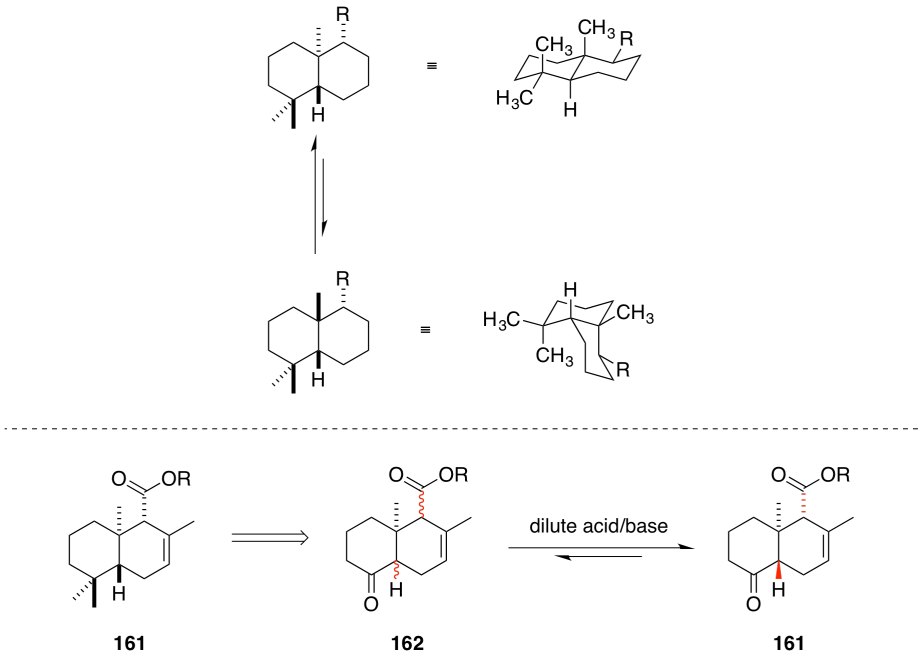

Figure 18: Trans Decalin Stability

3.6.1 Retrosynthetic Analysis

A retrosynthetic route from **125** that incorporates intermediate **161** installs the alkyne via a standard S_N2 reaction from protected alcohol **163** (Figure 21).[73] The alcohol (**163**) derives from a reduction of keto-ester **161**. A Reetz alkylation converts the C_4 carbonyl to the geminal dimethyl group under strongly Lewis acidic conditions.[74] Accessing the trisubstituted alkene would be achieved via a Au(I)-catalyzed ring closure with the silyl acetal derivative of **164**.[75] A Michael addition of an enolate to 3-methyl-2-cyclohexenone **167** followed by direct trapping[76] of the resultant enolate with 4-bromo-1-butyne provides the needed cyclization precursor.

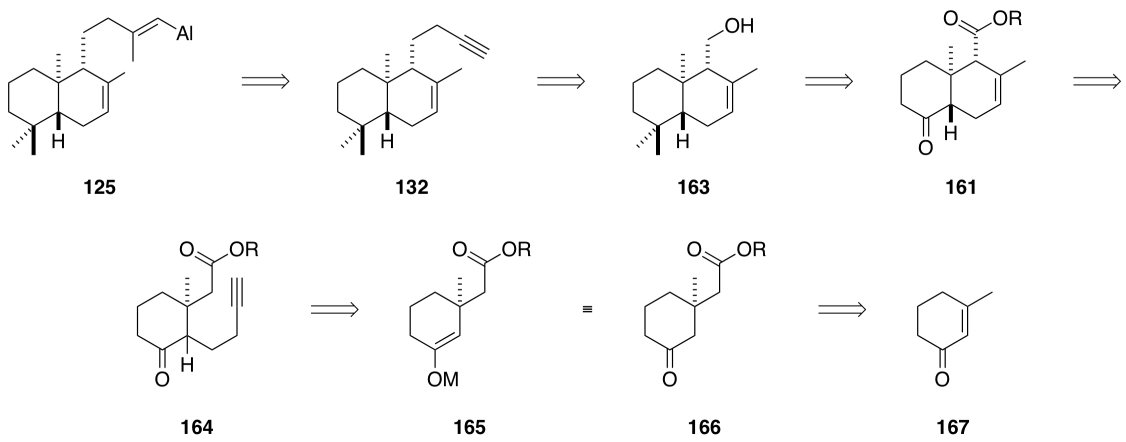

Figure 19: Retrosynthetic Analysis of the Terpenoid Incorporating Trans Decalin 161

3.6.2 Aluminum Mediated 1,4-additions into Sterically Hindered Enones

The terpenoid synthesis began by establishing the critical quaternary carbon. Enolates, relatively soft nucleophiles, generally participate in 1,4-additions to α,β-unsaturated ketones. The addition of a zinc enolate (Scheme 15, Equation 37) to 3-methyl-2-cyclohexenone (**167**) was expected to yield keto-ester **166**. However, the reaction yielded only the 1,2-additon product (**168**). Further, typical Gilman reagents demonstrated the same reactivity (Equation 38). Therefore, it was concluded that steric hindrance of the methyl group prevented nucleophilic addition into C_3. The substrate demanded specialized conditions to attain the desired intermediate.

Scheme 15: Enolate Additions into 3-methyl-2-cyclohexenone

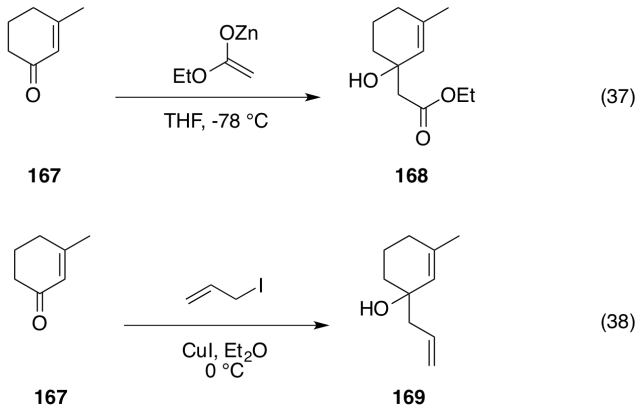

Alkylating sterically congested enones requires additional activation of the substrate by a strong Lewis acid. One such set of conditions includes utilizing suprastoichiometric amounts of alkyl aluminum in the presence of copper(I) salts.[77] The aluminum provides twofold reactivity. The strong covalent interaction between the carbonyl oxygen and the alkyl aluminum activates the enone towards nucleophilic attack. A second equivalent of the aluminum source alkylates the copper(I)-catalyst; the Cu(I) species then performs 1,4-addition through the established six-membered transition state. The addition of a chiral phosphoramidite ligand renders the reaction highly enantioselective.[77] For example, the enantioselective alkylation of 3-methylcyclohexenone occurs when exposed to triethylaluminum (Et_3Al), copper thiophene carboxylate (CuTC), and phorphoramidite ligand **170** (Scheme 16, Equation 39).[77a] Changing the copper(I) source allows for the alkylation of highly sterically congested substrates (Equation 40). However, no examples of introducing enolates with this methodology have been documented. Therefore, in order to be applicable in the actinoranone synthesis, the quaternary methyl group would need to be introduced to keto-ester **166**,[78] a substrate that had yet to be explored with this chemistry.

Scheme 16: Alkyl Aluminum Mediated 1,4-additions into Sterically Congested Enones

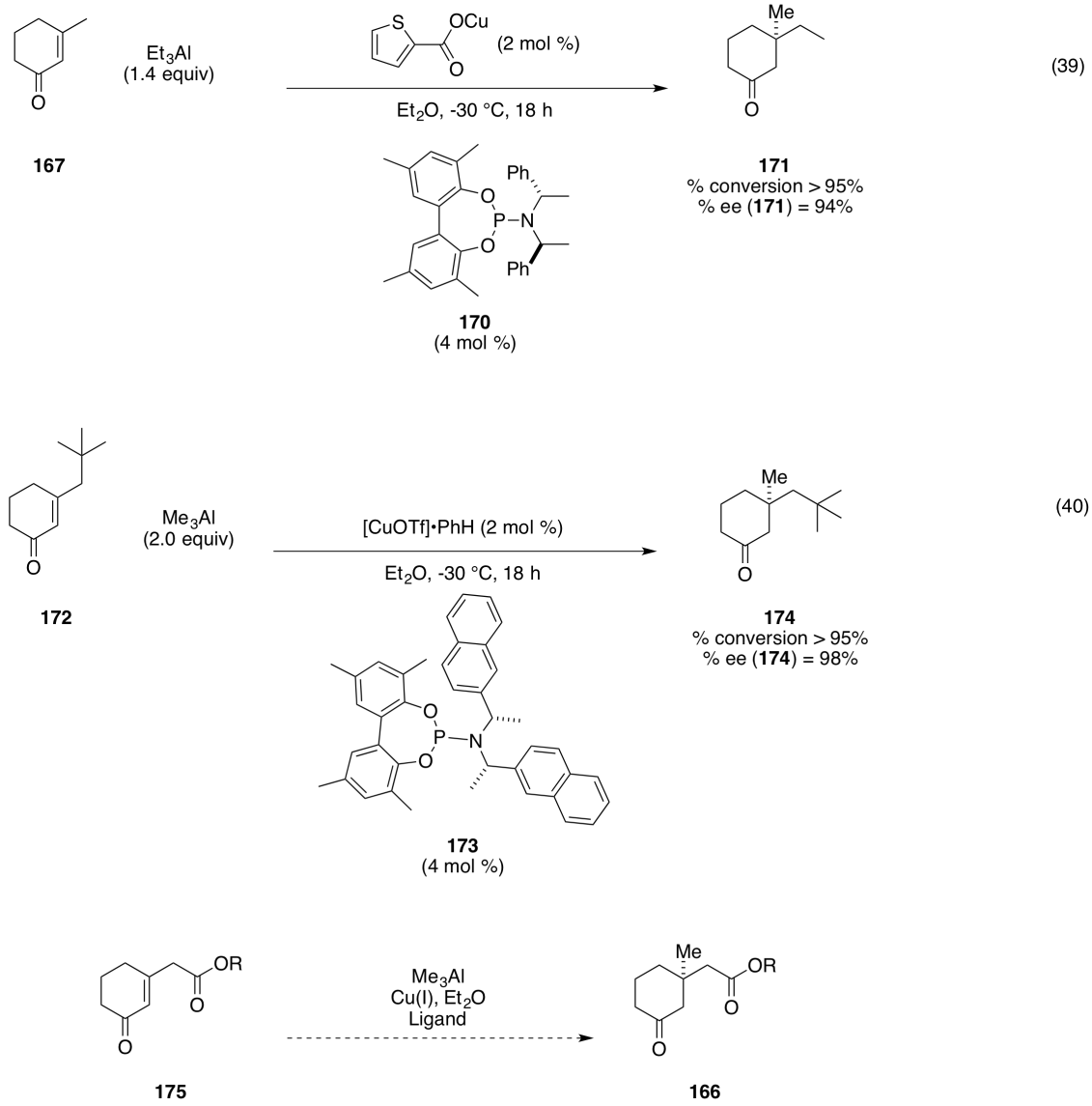

Utilizing the conditions applicable to the most hindered substrate, 3-isobutylcyclohex-2-en-1-one,[77a] as a template (Table 15, entry a) and R-MonoPhos (**176**) as the ligand, keto-ester **175** provided the alkylated product in 26% yield. The reaction failed to consume all of the keto-ester starting material resulting in poor reaction conversions. The precedent indicates the alkylation yields depend on the ligand utilized;[77a] MonoPhos derived ligands were not explored. A ligand screen would determine the reaction's tolerance to other available phosphoramidites ligands.[79] Employing ligand **177** led to complete consumption of the starting materials. Further,

ligand **30** improved the enantioselectivity to a modest 55% ee. Ligands that lacked chiral amines, such as **178** and **179**, maintained reaction conversions, but exhibited diminished enantioselectivities, indicating the amine portion of the phosphoramidite was essential to render the reaction enantioselective. We also observed that increasing the sterics of the α,β-unsaturated enone improved yields and enantioselectivities. Critically, *tert*-butylketo-ester yielded the best results, providing the desired ketone in 68% yield and 64% ee (entry e), exemplifying the most optimized reaction conditions to date. We hope that further investigation into additional ligands, particularly ones with highly congested amines, further improve enantioselectivities. In summary, this work expands upon the previously disclosed methodology by establishing a quaternary stereocenter in more complex substrates.

Table 15: Asymmetric Methylations into Sterically Hindered Substrates

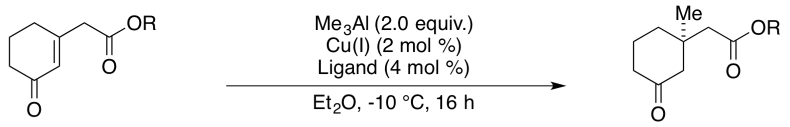

175 **166**

entry	R	Cu(I)X	Ligand	% conversion[a] (% yield)	% ee[b]
a	Et	CuTC	**176**	40 % (26 %)	14%
b	Et	$(CuOTf)_2$•PhH	**176**	50 %	ND
c	Et	$(CuOTf)_2$•PhH	**177**	100 % (47 %)	36%
d	Et	$(CuOTf)_2$•PhH	**30**	100 %	55%
e	*t*Bu	$(CuOTf)_2$•PhH	**30**	100 % (68%)	64 %
f	Et	$(CuOTf)_2$•PhH	**178**	100 %	27%
g	*t*Bu	$(CuOTf)_2$•PhH	**179**	ND	36%
h	Et	$(CuOTf)_2$•PhH	**180**	100 % (70 %)	0%

Ligands

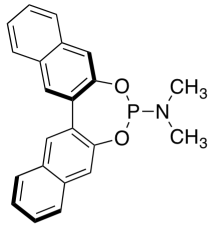

176

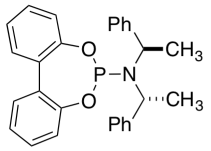

177

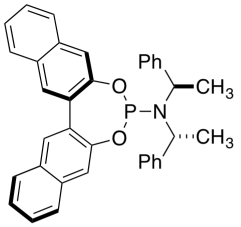

30

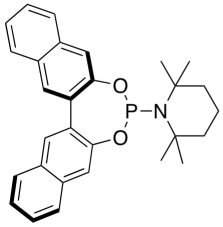

178

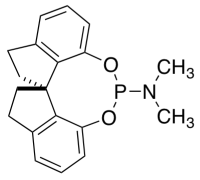

179

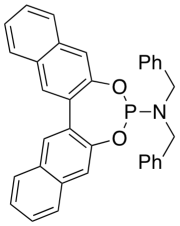

180

[a] Determined by ^1H NMR; [b] Determined by chiral GC; ND: not determined

Having found a method that reliably set the quaternary stereocenter, albeit in modest enantioselectivity, the enone α-carbon required functionalization. Ideally, the α-alkylation would be carried out *in situ* from the Michael addition conditions.[76] However, the strong aluminum-

oxygen bond stabilizes the enolate and renders it nonreactive toward electrophiles. Due to the lack of reactivity, converting aluminum enolates into the reactive lithium enolate typifies most current efforts.[77a] Aluminum-lithium transmetallation has been accomplished by adding an equivalent of methyllithium to the aluminum enolate[77a] and, in some cases, a strong coordinating solvent such as HMPA.[76] While successful with simple substrates, we believed that adding a strong nucleophile would prove incompatible with this particular enolate due to a lack of chemoselectivity. Therefore, we sought to limit substrate exposure to strongly nucleophilic conditions. A direct lithiation of aluminum enolate by the addition of MeLi•LiBr, followed by the addition of allyl iodide, failed to yield the desired alkylation (Equation 41).

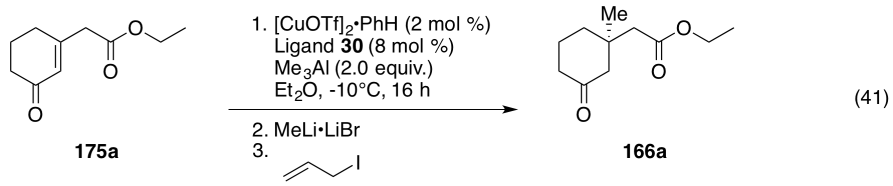

175a **166a** (41)

Convinced the aluminum enolate would not be coaxed into direct alkylation, an alternative solution was sought. Protecting the aluminum enolate could be accomplished utilizing reactive electrophiles under mild reaction conditions. Aluminum enolates undergo *O*-alkylation when exposed to acetic anhydride, providing vinyl acetate **165a** (Figure 22).[77a] Similarly, TMSOTf generates the enol silane (**165b**) under analogous conditions.[77a] While structurally related, the compounds differ in terms of stability and reactivity. Acetate **165a** was expected to be easily isolatable compared to the silyl enol ether, but deprotection would require harsher conditions. Conversely, the reactivity of enol silane **165b** would make isolation more difficult, yet more deprotection conditions were available. Ultimately, both pathways were simultaneously explored to determine which was more compatible with later chemistry.

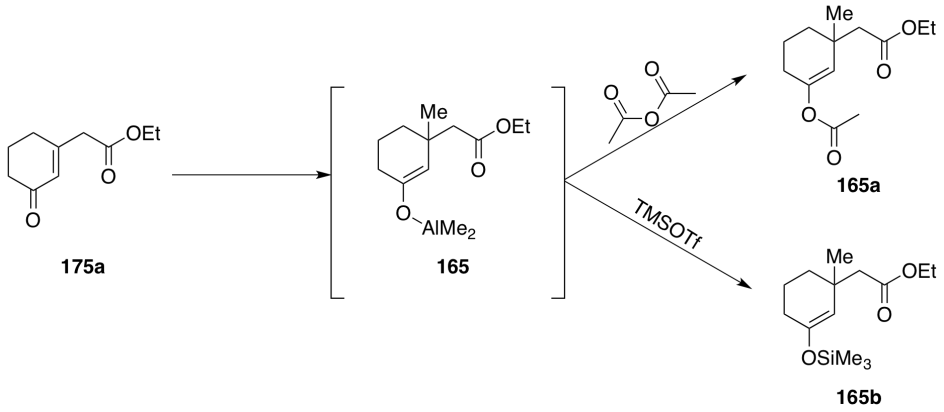

Figure 20: Direct Trapping of the Aluminum Enolate

3.6.3 Utilizing Vinyl Acetates as Critical Intermediates

Adding acetic anhydride to the established alkylation conditions provided vinyl acetate **165a** in good yields (68% yield, Equation 42). Accessing the nucleophilic lithium enolate requires two equivalents of LiMe•LiBr complex.[77a] The excess reagent suppresses undesired side reactions. However, the addition of excess nucleophile was expected to incur chemoselectivity issues; specifically, addition-elimination reactions into the ester are well documented and predicted to be non-orthogonal under these conditions. To explore this reactivity, a single equivalent of LiMe•LiBr was added to vinyl acetate **165a** followed by an equivalent of allyl iodide. These conditions provided the desired product and, surprisingly, the dialkylated product (Table 16**,** entry a). The undesired side product results from establishing an equilibrium as a result of only using only a single equivalent of LiMe•LiBr. No indication of nucleophilic addition into the ester was observed.

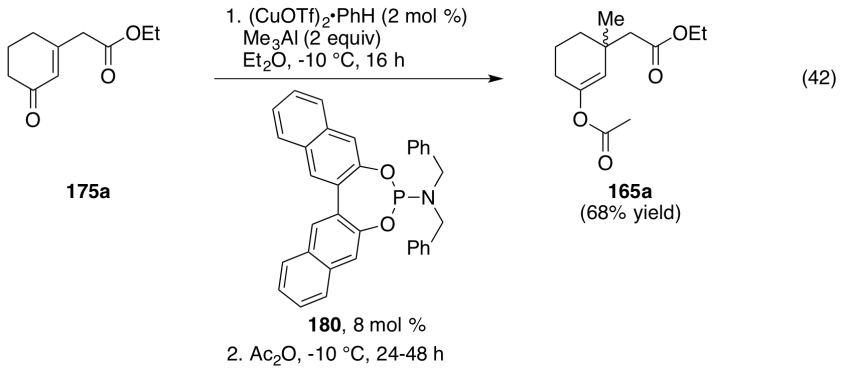

(42)

While encouraged by the preliminary results, attempts to install the required alkyne proved difficult. Exposing homopropargyl iodide (**182**, entry b) to the test conditions failed to produce the α-substituted product. Under the basic reaction conditions, we believe that the electrophile undergoes an elimination reaction to produce but-1-en-3-yne, a volatile and inert gas. To prevent this reactivity, the iodide leaving group was exchanged for a tosyl protected alcohol (**183**, entry c). While the material did not decompose under the basic reaction conditions, the material was completely nonreactive towards alkylation. To suppress elimination and maintain a strong leaving group, internal alkyne isomer **184** (entry d) was employed. Under the reaction conditions, this reagent underwent the desired alkylation to provide **186a**; however, product **185** predominated, the result of nucleophilic addition into the ester portion of the substrate.

Table 16: Alpha Alkylation of Vinyl Acetate 165a

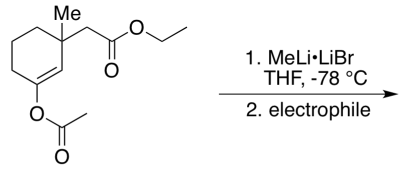

165a

entry	electrophile		products
a			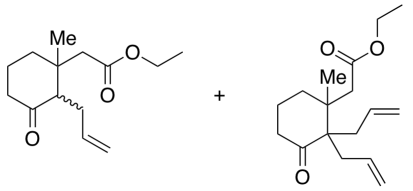 **181a** + **181b**
b	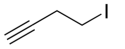	**182**	No Reaction
c	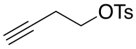	**183**	No Reaction
d	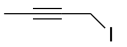	**184**	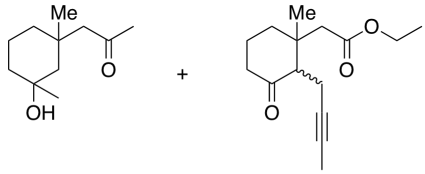 **185** + **186a**

Examining keto-ester **175b** under identical reaction conditions (Scheme 17) provided the desired product **187b** with high fidelity as no side product was detected (78% yield, 51% yield from **165a'**). Isolating sterically congested cyclohexanone **187b** revealed the alkylation occurred with no diastereoselective preference (Scheme 17). The ester functionality was predicted to exhibit greater steric blocking towards the approaching electrophile than the neighboring methyl group. However, the formation of both isomers in equal amounts proved that both groups exhibit near equal steric contributions during the alkylation reaction. Evaluating the relevant A values for methyl (1.74 kcal/mol)[50] and methelene derivatives (CH_2, 1.79 kcal/mol)[50] confirmed that comparatively, neither group demonstrates a preference for the equatorial position of the resulting chair conformation (Scheme 17).

Scheme 17: Alpha Alkylation with Internal Alkynyl Iodide

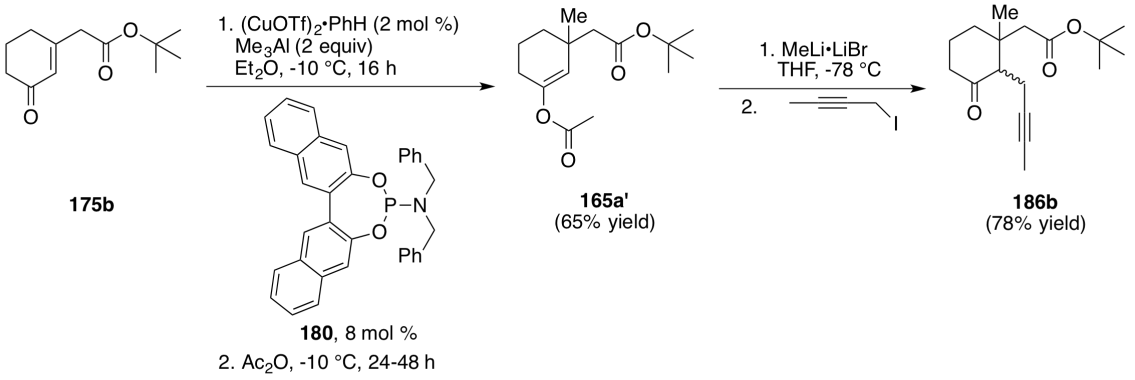

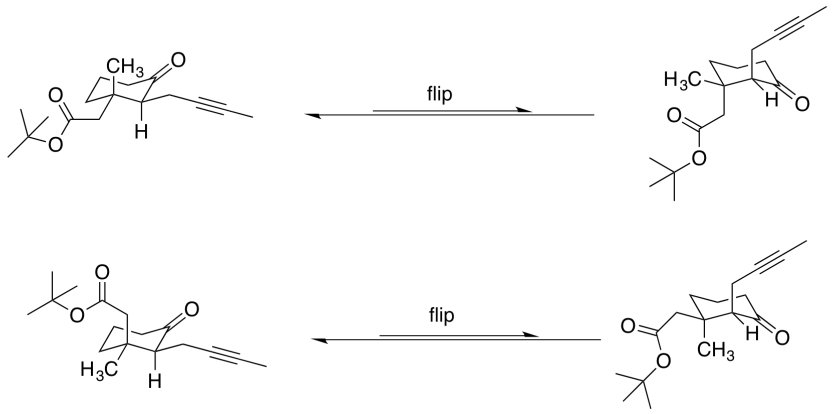

Achieving a successful alkylation, we sought to attain the bicycle via the Au(I)-catalyzed ring closing. However, having adjusted the alkylation to incorporate the internal alkyne prevented direct exposure to the ring closing reaction. Thermodynamics dictate the products obtained from the Au(I)-catalyzed ring closure.[75] The internal alkyne establishes a direct competition between a 5-exo-dig and a 6-endo-dig cyclizations, both of which are favorable under Baldwin's rules (Scheme 18).[80] The terpenoid requires the six-six bicycle, yet direct cyclization of the internal alkyne would generate the six-five system because kinetics favor the five-membered ring closure.[75b] However, an isomerization of the internal alkyne to the terminal alkyne would create a competition between a 6-exo-dig and a 7-endo-dig cyclization; while both pathways are also Baldwin favored, kinetics favors the 6-exo-dig cyclization and would provide the desired product. To isomerize, the alkyne zipper reaction takes advantage of C_{sp}-H basicity to

generate the terminal alkyne from the related internal alkyne.[81] Unfortunately, exposing **186b** to the strongly basic isomerization conditions consistently led to starting material decomposition, the exact products of which were not determined.

Scheme 18: a) Available Baldwin Cyclizations b) Alkyne Zipper Reaction

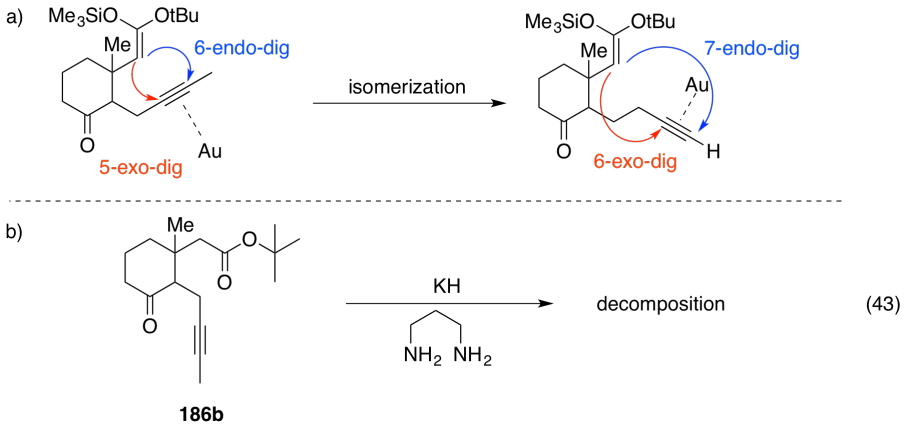

While the isomerization results were discouraging, we sought to explore other isomerization options to obtain the terminal alkyne. However, scaling up earlier synthetic steps revealed a serious deficiency in this route. Producing large quantities of 1-iodobut-2-yne (**184**) proved unfeasible for several reasons. As expected, the halide proved highly sensitive to ambient light, decomposing via a radical pathway; storage in the freezer slowed this process, but failed to halt it completely. More critically, the alkyne was incredible volatile. Separating the material from triphenylphosphine and triphenylphosphine oxide, side products of its synthesis, could not be achieved. When purified by flash chromatography, pentanes, the most volatile solvent available, could not be removed from the material with any efficiency under vacuum. Simple and fractional distillation as well as kugelrohr distillation proved the material to be thermally unstable. Therefore, reactions predicted to provide grams of material only provided hundreds of milligrams of material as dilute solutions in pentanes. Clearly unsustainable, this route fell victim to an inability to sufficiently fulfill the supply chain.

3.6.4 Examining a Silyl Enolate Intermediate

Protecting the aluminum enolate **165** as the enol silane (**165b**) provided alternate reaction pathways unavailable to the vinyl acetate. Specifically, a variety of mild conditions are available for removing silane protecting groups. Subjecting **165** to standard methylation conditions followed by TMSOTf afforded the silyl protected enolate **165b** in good yields (Equation 44).[77a] Standard conditions for generating a reactive enolate from the silyl precursor require the addition of methyl lithium in order to form the lithio enolate. However, our previous work determined that the presence of the ester moiety caused chemoselectivity issues regarding directed methylation equilibration of the keto-enolate to the corresponding, undesired ester-enolate. Instead, we investigated alternative conditions investigated to afford a reactive enolate (Table 17). Formation of the strong Si-F bond promotes the removal of alkyl silanes to form alcohols; in this vein, TBAF was utilized with hopes that the ammonium enolate would prove nucleophilic. From previous laboratory experience, enol silanes have been activated towards nucleophilicity with chlorine and acetate anions. If LiCl promoted silane deprotection, this would provide an alternate route to the lithio enolate. Similarly, NaOAc would access the nucleophilic sodium enolate. Under identical conditions, only the TBAF successful promoted removal of the silane group. This was determined by the detection of known keto-ester **166a** by TLC. However, the addition of allyl iodide to this reaction failed to form the allylated product, confirming the lack of nucleophilicity of ammonium enolates.

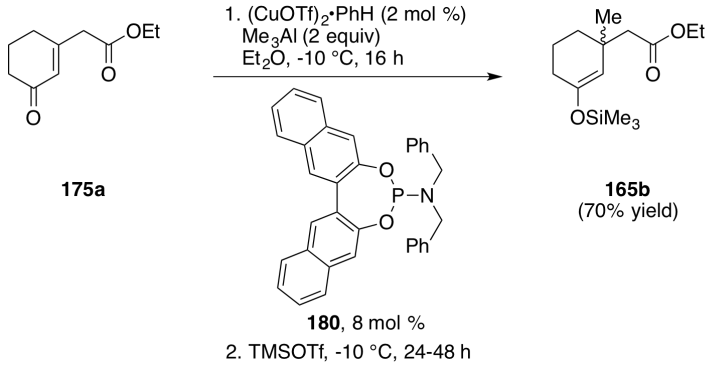

(44)

Table 17: Examination of Trimethylsilane Deprotection and Subsequent Nucleophilicity

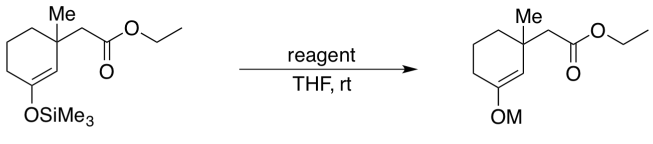

165b **165**

entry	reagent	notes
a	MeLi•LiBr	decomposition
b	TBAF	successful deprotection; exposure to allyl iodide gave no alkylation prodcuts
c	LiCl	no reaction
d	NaOAc	no reaction

3.6.5 A Cross-Coupling Approach

Rather than attempting direct alkylation of the enol silane, installing a functional group to act as chemical handle would also be advantageous. This method would guarantee the alkylation would occur selectively, adjacent to the quaternary center. Specifically, establishing a halide or halide equivalent at the α-position would allow for a variety of reactions, including transition-metal mediated cross-couplings to install the alkyl group. The Rubottom oxidation converts silyl enol ethers to α-hydroxy ketones upon the addition of peroxyacids such as mCPBA.[82] This method takes advantage of the enol silane intermediate and incorporates a secondary alcohol, which upon

protection, would act as a halide surrogate. For this method to be truly successful, the α-hydroxy ketone would have to directly precede alkynyl intermediate **164a** without further modification, making a cross-coupling reaction particularly attractive.

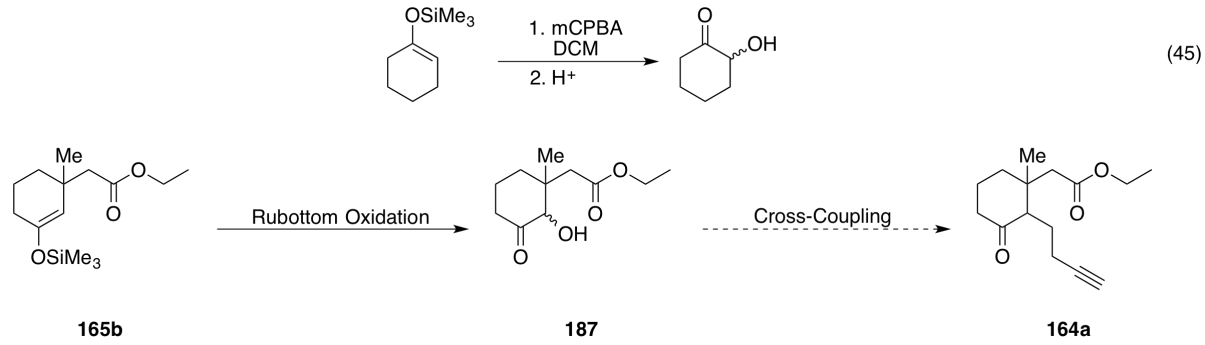

Figure 21: Synthetic Analysis Incorporating a Rubottom Oxidation

Incorporating an alkyne via a cross-coupling reaction immediately implicated a Sonogashira reaction. However, this procedure would establish the alkyne adjacent to the carbonyl (Scheme 19). This material requires isomerization to the terminal alkyne to undergo the Au(I)-catalyzed cyclization, which we sought to avoid. Instead, a Suzuki cross-coupling utilizing alkyl borate ester **188** would be more advantageous. Protection of the α-hydroxy ketone as a triflate would provide the coupling partner. In this manner, we predicted that the desired intermediate would be available in two synthetic steps.

Scheme 19: Accessing Cyclic Precursor via a Suzuki Cross-Coupling

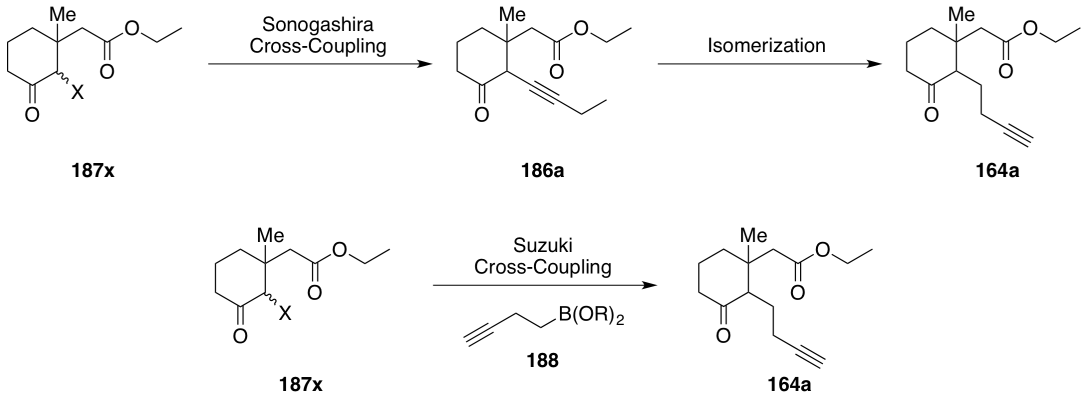

A Rubottom oxidation of enol silane **165b** yielded the desired α-hydroxy ketone upon acidic workup (**187**, Scheme 20). Experimentation revealed this particular substrate required 2 equivalents of mCPBA added sequentially during the reaction to afford moderate yields (~60%). This compound, as its predecessors, exhibited no inherent diastereoselectivity. The alcohol was protected with triflic anhydride under neutral conditions ($[TfO]_2O$, THF). Predictably, this compound proved to be highly unstable and decomposed easily upon exposure to ambient light and silica gel. Subjecting **189** to standard Suzuki conditions[83] with borate **190**[84] led to several decomposition pathways: the basic conditions cleaved the C_{sp}-$SiMe_3$ bond and hydrolyzed both the triflate and the borate ester. The lack of compatibility of these compounds under typical Suzuki conditions proved that this too was not a viable pathway to actinoranone.

Scheme 20: Suzuki Cross-Coupling

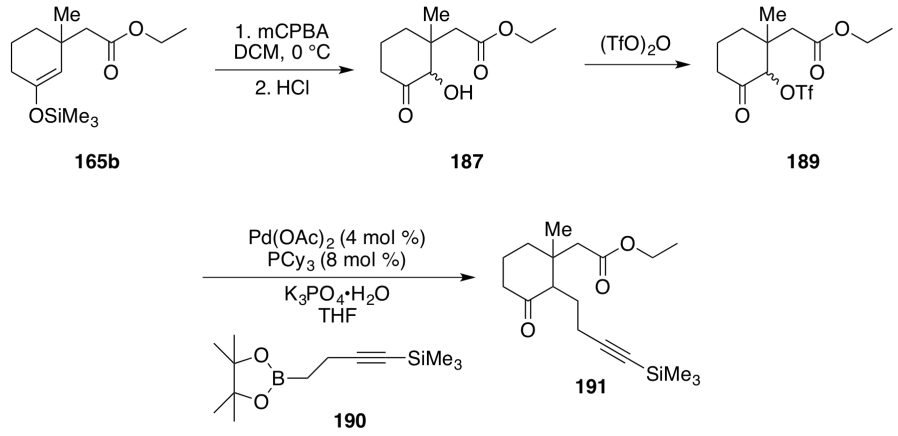

The efforts to produce the terpenoid half of actinoranone via a Au(I)-catalyzed cyclization ultimately proved unfruitful. The determined reactions and intermediates faced many obstacles some of which were insurmountable despite innovative steps taken to reconcile unpredicted reactivity with synthetic requirements. Unfortunately, the decalin system was never achieved via this synthetic pathway.

3.6.6 Future Work

Our hypothesis regarding the structure of actinoranone stated that the naphthalone core (**127**) was responsible for the observed cytotoxicity, whereas the terpenoid half acts primarily as a molecular anchor. If correct, than the precise structure of the terpenoid, while critical for achieving the total synthesis, would be unimportant to the reactivity. To this end, several efforts could be made to further explore the activity of actinoranone if unnatural isomers or chemical derivatives more readily accessible.

Efforts launched to explore how other researchers approached similar terpenoids revealed several methods. Many endeavors follow racemic pathways and later perform resolution to extract the needed enantiomer.[85] Of course such methods prove wasteful, inefficient, and frankly, uninteresting. Perhaps more noteworthy were examples that avoided chiral resolution, but also did not conduct any asymmetric synthesis. To this end, the syntheses utilized chiral, commercially available sclareolide (**192**).[86] This material contains the bicyclic ring system and all of the requisite stereocenters. However, **192** cannot be used in the total synthesis of actinoranone as it is the opposite enantiomer. From a medicinal chemistry perspective, this enantiomer would be an excellent surrogate to elucidate reactivity. Future work could focus on optimizing the terpenoid portion via structure simplification.

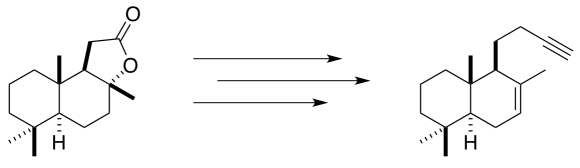

192 ent-**132**

Figure 22: Sclareolide as a Chiral Pool Starting Material

3.7 CONCLUSIONS

The work herein presented discloses the current efforts underway to synthesize the natural product actinoranone. The terpenoid half proved unobtainable via the described methods. The molecular core, certainly responsible for the observed cytotoxicity in human colorectal cells, was successfully synthesized via a novel asymmetric allylic alkylation reaction between a Ru(IV)(π-allyl) ligand and a stabilized silyl enol ether. This exemplifies the utility of this method to efficiently construct complex molecular skeletons.

4.0 EXPERIMENTAL

4.1 RUTHENIUM(II)-CATALYZED ASYMMETRIC ALLYLIC ALKYLATION

General Information: Unless otherwise indicated, all reactions were performed in dry glassware under an atmosphere of oxygen-free nitrogen using standard inert atmosphere techniques for the manipulation of both solvents and reagents. Anhydrous solvents were obtained by passage through successive alumina- and Q5-packed columns on a solvent purification system. $[CpRu(CH_3CN)_3]PF_6$ was synthesized according to the published procedure[87] and was stored and weighed out in a nitrogen-filled glove box. NMR spectra were recorded at the indicated magnetic field strengths with chemical shifts reported relative to residual C**H**Cl_3 (7.26 ppm) for ^1H and **C**DCl_3 (77.0 ppm) for ^{13}C spectra. Analytical thin layer chromatography (TLC) was performed on 0.25 mm silica gel 60-F plates. Flash chromatography was performed over silica gel (230-240 mesh). Analytical gas chromatography (GC) was performed using a flame ionization detector and split mode capillary injection system using Varian Chirasil-Dex CB WCOT fused silica 25 m x 0.25 mm column (CP 7502). Analytical high-performance liquid chromatography (HPLC) was performed using a variable wavelength UV detector (deuterium lamp, 190-600 nm) using a Chiracel OD-H column and HPLC-grade isopropanol and hexanes as the eluting solvents. Melting points were obtained on a Laboratory Devices Mel-Temp apparatus and are uncorrected.

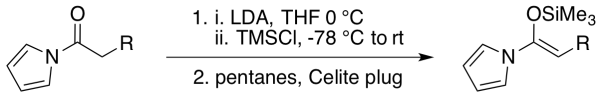

General Procedure A. Synthesis of pyrrole silyl enol ethers 91a – 91f: To a 0 °C solution of diisopropylamine (1.0 equiv) in THF (1.6M relative to diisopropylamine) was added a solution of 1.6M *n*-BuLi in hexanes (1.1 equiv). The reaction was allowed to stir at 0 °C for 10 min and then cooled to -78 °C. Next, a 0.8M solution of acylpyrrole (1.0 equiv) in THF was added dropwise to the reaction vessel over 5 min and the resulting solution was allowed to stir at -78 °C for 30 min. TMSCl (1.1 equiv) was added dropwise over 5 min, and the reaction was allowed to stir an additional 20 min at -78 °C. The dry ice/acetone bath was removed and the reaction was allowed to stir for an additional 1 h. Next, the reaction was diluted with pentane (4x the reaction volume), and the heterogeneous mixture was filtered through a plug of Celite and concentrated. The final product was purified via kugelrohr distillation.

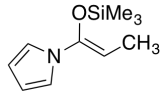

(Z)-1-{1-[(Trimethylsilyl)oxy]prop-1-en-1-yl}-1*H*-pyrrole (91fa): Characterization materials match the data provided in the following publication: Evans, D. A.; Johnson, D. S. *Org. Lett.* **1999**, *1*, 595-598.

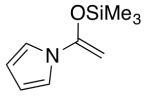

1-{1-[(Trimethylsilyl)oxy]vinyl}-1*H*-pyrrole (91b): Characterization materials match the data provided in the following publication: Frick, U.; Simchen, G. *Liebigs Ann.* 1987, *10*, 839-845.

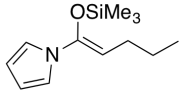

(Z)-1-{1-[(Trimethylsilyl)oxy]pent-1-en-1-yl}-1*H*-pyrrole (91c): General procedure A was followed employing 1.87 mL of diisopropylamine (13.2 mmol), 9.07 mL of 1.6 M *n*-BuLi (14.52 mmol), 2.0 g 1-(1*H*-pyrrol-1-yl)- 1-pentanone (13.2

mmol), 1.84 mL TMSCl (1.1 mmol) in 30 mL THF. The reaction was purified via kugelrohr distillation at 1 mm Hg. The product distilled between 70 and 80 ^{o}C (2.14 g, 73%) as a clear colorless oil. ^{1}H NMR (500 MHz, $CDCl_3$): δ 6.86 (t, *J* = 2.0 Hz, 2H), 6.16 (t, *J* = 2.0 Hz, 2H), 4.68 (t, *J* = 7.5 Hz, 1H), 2.09 (q, *J* = 7.5 Hz, 2H), 1.43 (sextet, *J* = 7.5 Hz, 2H), 0.96 (t, *J* = 7.5 Hz, 3H), 0.15 (s, 9H); ^{13}C NMR (125 MHz, $CDCl_3$): δ 143.0, 119.0, 108.8, 97.8, 27.4, 23.1, 13.8, -0.15; IR ν_{max}^{neat} cm^{-1}: 2959, 2932, 2871, 1682, 1478, 1368, 1254, 1155, 1101, 1078, 1040, 960, 849, 737, 726; HRMS (EI) *m/z* calcd for $C_{12}H_{21}NOSi$ $(M + H)^+$: 224.1471; found: 224.1480.

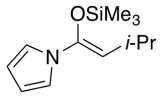

(Z)-1-{3-Methyl-1-[(trimethylsilyl)oxy]but-1-en-1-yl}-1*H*-pyrrole (91d): Characterization materials match the data provided in the following publication: Evans, D. A.; Johnson, D. S. *Org. Lett.* **1999**, *1*, 595-598.

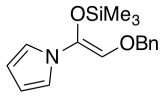

(Z)-1-{2-(Benzyloxy)-1-[(trimethylsilyl)oxy]vinyl}-1*H*-pyrrole (91e): Characterization materials match the data provided in the following publication: Evans, D. A.; Scheidt, K. A.; Johnson, J. N.; Willis, M. C. *J. Am. Chem. Soc.* **2001**, *123*, 4480-4491.

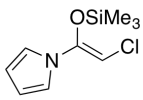

(Z)-1-{2-chloro-1-[(trimethylsilyl)oxy]vinyl}-1*H*-pyrrole (91f): General procedure A was followed employing 1.49 mL of diisopropylamine (10.5 mmol), 7.19 mL of 1.6 M *n*-BuLi (11.5 mmol), 1.5 g 2-chloro-1-(1*H*-pyrrol-1-yl)-ethanone (10.5 mmol), 1.46 mL TMSCl in 30 mL THF. The reaction was purified via kugelrohr distillation at 1 mm Hg. The product distilled between 75 and 80 ^{o}C (1.85 g, 82%) as a clear colorless oil. ^{1}H NMR (500 MHz, $CDCl_3$): δ 6.85 (t, *J* = 2.0 Hz, 2H), 6.23 (t, *J* = 2.0 Hz, 2H), 5.53 (s, 1H), 0.27

(s, 9H); ^{13}C NMR (125 MHz, $CDCl_3$): δ 145.3, 118.9, 110.1, 89.0, 0.06; IR ν_{max}^{neat} cm^{-1}: 3108, 2961, 2900, 1723, 1655, 1562, 1475, 1353, 1258, 1134, 1078, 961, 887, 789, 728; HRMS (EI) *m/z* calcd for $C_9H_{14}ClNOSi$ $(M + H)^+$: 216.0611; found: 216.0619.

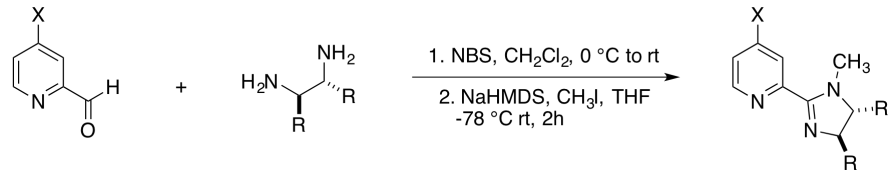

General Procedure B. Synthesis of imidazolylpyridine ligands 96, 100-112: To a solution of picolinaldehyde (1.0 equiv) in CH_2Cl_2 (0.10 M relative to picolinaldehyde) was added the diamine (1.05 equiv). The reaction was allowed to stir for 30 min before N-bromosuccinimide (1.05 equiv) was added as a solid. The resulting solution was stirred overnight. The reaction was quenched with 10% NaOH/H_2O solution of equivalent volume. Organics were extracted with CH_2Cl_2 (3x the reaction volume), dried with $MgSO_4$, and concentrated in vacuo. The crude product was then subjected to methylation conditions without purification. A solution of the crude product in THF (0.10 M) was cooled to -78ºC. To this was added sodium bis(trimethylsilyl)amide (NaHMDS) as a 1.0M solution in THF (1.3 equiv). After stirring for 30 min, iodomethane (1.1 equiv) was added. The reaction flask was then allowed to warm to room temperature and stir for 2 h. Next, the reaction was quenched with an equivalent volume of H_2O and the organics were extracted with CH_2Cl_2 (3x the reaction volume). The extract was dried with $MgSO_4$ and concentrated in vacuo. The product mixture was purified by column chromatography.

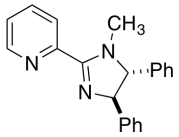

2-[(4R,5R)-4,5-Diphenyl-4,5-dihydro-1*H*-imidazol-2-yl]pyridine (96): Characterization materials match the data provided in the following publication: Bastero, A.; Claver, C.; Ruiz, A.; Castillon, S.; Daura, E.; Bo, C.; Zangrando, E.; *Chem. Eur. J.* **2004**, *10*, 3747-3760.

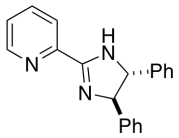

2-[(4*R*,5*R*)-4,5-Diphenyl-4,5-dihydro-1*H*-imidazol-2-yl]pyridine (100): Characterization materials match the data provided in the following publication: Bastero, A.; Claver, C.; Ruiz, A.; Castillon, S.; Daura, E.; Bo, C.; Zangrando, E. *Chem. Eur. J.* **2004**, *10*, 3747-3760.

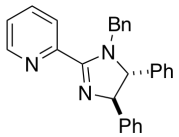

2-[(4R,5R)-1-Benzyl-4,5-diphenyl-4,5-dihydro-1*H*-imidazole (101): Characterization materials match the data provided in the following publication: Bastero, A.; Claver, C.; Ruiz, A.; Castillon, S.; Daura, E.; Bo, C.; Zangrando, E.; *Chem. Eur. J.* **2004**, *10*, 3747-3760.

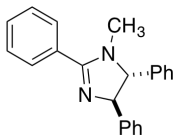

(4R,5R)-1-Methyl-2,4,5-triphenyl-4,5-dihydro-1*H*-imidazole (102): Characterization materials match the data provided in the following publication: Busacca, C. A.; Bartholomeyzik, T.; Cheekoori, S.; Grinberg, N.; Lee, H.; Ma, S.; Saha, A.; Shen, S.; Senanayake, C. H.; *J. Org. Chem.* **2008**, *73*, 9756-9761.

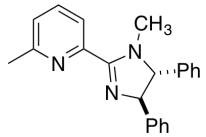

2-Methyl-6-[(4R,5R)-1-methyl-4,5-diphenyl-4,5-dihydro-1*H*-imidazole-2-yl]pyridine (103): General procedure B was followed employing 163 mg of 6-methylpicolinaldehyde (1.34 mmol), 300 mg (1R,2R)-diphenylethylenediamine (1.41 mmol),

252 mg N-bromosuccinimide (1.41 mmol), in 13 mL CH_2Cl_2. After workup, 429 mg (1.37 mmol) crude product was recovered. The crude product was then subjected to methylation conditions employing 1.78 mL of NaHMDS (1.0M in THF, 1.78 mmol) and 94 μL iodomethane (1.51 mmol) in 13 mL THF. The reaction mixture was purified by column chromatography (SiO_2, 5% MeOH/CH_2Cl_2) to afford 256 mg (57%) of the title compound as a pale brown oil: $[a]_D^{19}$ +0.209 (*c* 4.12, $CHCl_3$); ^{1}H NMR (500 MHz, $CDCl_3$): δ 7.93 (d, *J*= 7.5 Hz, 1H), 7.69 (t, *J*= 8.0 Hz, 1H), 7.42-7.22 (m, 11H), 5.00 (d, *J* = 10.5 Hz, 1H), 4.39 (d, *J* = 10.5 Hz, 1H), 3.00 (s, 3H), 2.64 (s, 3H); ^{13}C NMR (125 MHz, $CDCl_3$): δ164.3, 157.5, 149.8, 143.3, 140.8, 136.8, 128.8, 128.4, 127.9, 127.4, 127,1, 126.9, 124.2, 122.0, 34.2, 24.5; IR ν_{max}^{neat} cm^{-1}:3060, 2922, 1591, 1569, 1453, 1388, 1302, 1277, 1222, 1156, 1080, 913, 808, 752; HRMS (EI) *m/z* calcd for $C_{22}H_{21}N_3$ $(M + H)^+$: 328.1814; found: 328.1813.

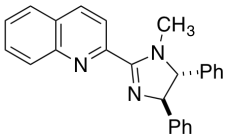

2-[(4R,5R)-1-Methyl-4,5-diphenyl-4,5-dihydro-1H-imidzol-2-yl)quinoline (104): General procedure B was followed employing 106 mg of quinoline-2-carbaldehyde (0.67 mmol), 150 mg (1R,2R)-diphenylethylenediamine (0.71 mmol), 125 mg N-bromosuccinimide (0.70 mmol), in 7 mL CH_2Cl_2. After workup, 104 mg (0.30 mmol) crude product was recovered. The crude product was then subjected to methylation conditions employing 0.39 mL of NaHMDS (1.0M in THF, 0.39 mmol) and 24 μL iodomethane (0.33 mmol) in 3 mL THF. The reaction mixture was purified by column chromatography (SiO_2, 5% MeOH/CH_2Cl_2) to afford 94 mg (86%) of the title compound as a pale brown oil: $[a]_D^{19}$ -1.86 (*c* 2.01, $CHCl_3$); ^{1}H NMR (500 MHz, $CDCl_3$): δ 8.27 (dd, *J* = 14.5, 9.0 Hz, 2H), 8.20 (d, *J* = 8.5 Hz, 1H), 7.88 (d, *J* = 8.5 Hz, 1H), 7.77 (ddd, *J* = 8.5, 7.0, 1.5 Hz, 1H), 7.61 (ddd, *J* = 8.0, 1.0 Hz, 1H), 7.44-7.28 (m, 10H), 5.06 (d, *J* = 10.5 Hz, 1H), 4.44 (d, *J* = 10.5 Hz, 1H), 3.20 (s, 3H); ^{13}C

NMR (125 MHz, $CDCl_3$): δ 164.0, 150.5, 147.0, 143.3, 140.9, 136.4, 129.9, 129.7, 128.8, 128.5, 128.2, 127.9, 127.6, 127.4, 127.2, 127.1, 122.1, 79.2, 77.4, 34.6; IR ν_{max}^{neat} cm^{-1}: 3059, 3028, 2926, 1600, 1555, 1491, 1392, 1277, 1067, 839, 755; HRMS (EI) *m/z* calcd for $C_{25}H_{21}N_3$ $(M + H)^+$: 364.1814; found: 364.1808.

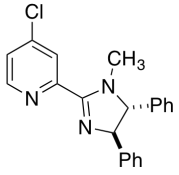

4-Chloro-2-[(4R,5R)-1-methyl-4,5-diphenyl-4,5-dihydro-1H-imidazol-2-yl]pyridine (105): General procedure B was followed employing 222.8 mg of 4-chloropicolinaldehyde (1.57 mmol), 350.8 mg 1R,2R-diphenylethylenediamine (1.65 mmol), 294.1 mg N-bromosuccinimide (1.65 mmol), in 15 mL CH_2Cl_2. After workup, 590.3 mg (1.74 mmol) crude product was recovered. Then the crude product was subjected to methylation employing 2.30 mL of NaHMDS (1.0M in THF, 2.26 mmol) and 121 μL iodomethane (1.91 mmol) in 18 mL THF. The reaction mixture was purified by column chromatography (SiO_2, 0-2% MeOH/CH_2Cl_2 gradient) to afford 440.0 mg (72%) of the title compound as a pale brown oil: $[a]_D^{19}$ +0.369 (*c* 2.22, $CHCl_3$); ^1H NMR (500 MHz, $CDCl_3$): δ 8.59 (dd, *J* = 5.0, 0.5 Hz, 1H), 8.19 (d, *J* = 1.5 Hz, 1H), 7.41-7.33 (m, 11H), 4.99 (d, *J* = 10.5 Hz, 1H), 4.38 (d, *J* = 10.5 Hz, 1H), 3.01 (s, 3H); ^{13}C NMR (125 MHz, $CDCl_3$): δ 163.2, 152.0, 149.3, 144.8, 143.1, 140.7, 128.9, 128.5, 127.9, 127.3, 127.2, 126.9, 125.3, 124.9, 79.0, 77.5, 34.3; IR ν_{max}^{neat} cm^{-1}:3059, 3028, 2855, 1575, 1550, 1491, 1407, 1343, 1277, 1075, 972, 834; HRMS (EI) *m/z* calcd for $C_{21}H_{18}ClN_3$ $(M + H)^+$: 348.1268; found: 348.1250.

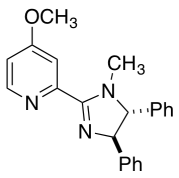

4-Methoxy-2-[(4R,5R)-1-methyl-4,5-diphenyl-4,5-dihydro-1*H*-imidazol-2-yl]pyridine (106): General procedure B was followed employing 355 mg of 4-methoxypicolinaldehyde (2.59 mmol), 577 mg (1R,2R)-

diphenylethylenediamine (2.59 mmol), 461 mg N-bromosuccinimide (2.59 mmol), in 26 mL CH_2Cl_2. After workup, 861 mg (2.61 mmol) crude product was recovered. The crude product was then subjected to methylation conditions employing 3.40 mL of NaHMDS (1.0M in THF, 3.40 mmol) and 42 μL iodomethane (0.67mmol) in 6 mL THF. The reaction mixture was purified by column chromatography (SiO_2, 0-2% MeOH/CH_2Cl_2 gradient) to afford 836 mg (72%) of the title compound as a pale brown oil: $[a]_D^{22}$ +0.995 (*c* 2.21, $CHCl_3$); ^{1}H NMR (500 MHz, $CDCl_3$): δ 8.50 (d, *J* = 5.5 Hz, 1H), 7.68 (d, *J* = 2.5 Hz, 1H), 7.40-7.26 (m, 10H), 6.91 (dd, *J* = 6.0, 2.5 Hz, 1H), 4.99 (d, *J* = 10.5 Hz, 1H), 4.39 (d, *J* = 10.5 Hz, 1H), 3.93 (s, 3H), 3.01 (s, 3H); ^{13}C NMR (125 MHz, $CDCl_3$): δ 166.2, 164.3, 151.8, 149.8, 143.0, 140.6, 128.8, 126.9, 111.9, 110.2, 78.8, 76.9, 55.5, 34.3; IR ν_{max}^{neat} cm^{-1}: 3060, 2939, 1593, 1562, 1474, 1435, 1376, 1304, 1280, 1190, 1070, 977, 866, 756; HRMS (EI) *m/z* calcd for $C_{22}H_{21}N_3O$ $(M + H)^+$: 344.1763; found: 344.1765.

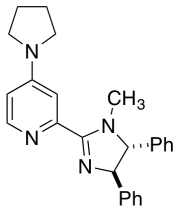

2-[(4R,5R)-1-Methyl-4,5-diphenyl-4,5-dihydro-1*H*-imidazol-2-yl]-4-(pyrrolidin-1-yl)pyridine (107): Compound **105**, 440.0 mg (1.27 mmol) was added to a medium pressure reaction vessel along with 4.2 mL neat pyrrolidine (50.6 mmol). The vessel was sealed and heated to 90°C for 24 h. At this time the reaction vessel was removed from the oil bath and allowed to cool to ambient temperature and then concentrated in vacuo. The crude reaction mixture was purified by column chromatography (SiO_2, 2-10% MeOH/CH_2Cl_2 gradient) to afford 256.4 mg (53%) of the title compound as an off-white solid: decomposition 62-65°C; $[a]_D^{19}$ -1.57 (*c* 1.08, $CHCl_3$); ^{1}H NMR (500 MHz, $CDCl_3$): δ 8.28 (d, *J* = 5.5 Hz, 1H), 7.38-7.26 (m, 10H), 7.19 (br s, 1H), 6.44 (dd, *J* = 6.0, 2.5 Hz, 1H), 4.99 (d, *J* = 10.0 Hz, 1H), 4.36 (d, *J* = 10.0 Hz, 1H), 3.40 (d, *J* = 2.0 Hz, 4H), 2.98 (s, 3H), 2.04 (p, *J* = 7.0 Hz, 4.0

Hz, 4H) ; ^{13}C NMR (125 MHz, $CDCl_3$): δ 152.2, 148.7, 128.7, 128.4, 127.9, 127.3, 127.2, 126.9, 107.7, 78.7, 47.1, 34.2, 25.3; IR ν_{max}^{neat} cm^{-1}: 3029, 2969, 2855, 1600, 1538, 1495, 1455, 1346, 1275, 1219, 1157, 1082, 1007, 813, 753; HRMS (EI) *m/z* calcd for $C_{25}H_{26}N_4$ $(M + H)^+$: 383.2236; found: 383.2248.

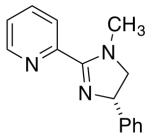

(S)-2-(1-Methyl-4-phenyl-4,5-dihydro-1*H*-imidzaole-2-yl)pyridine (108): Characterization materials match the data provided in the following publication: Malkov, A. V.; Stewart-Kiddon, A. J. P.; McGeoch, G. D.; Ramírez-López, P.; Kocovsky, P.; *Org. Biomol. Chem.*, **2012**, *10*, 4864-4877.

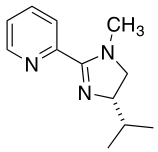

(S)-2-(4-Isopropyl-1-methyl-4,5-dihydro-1*H*-imidazole-2-yl)pyridine (109): General procedure B was followed by employing 185 μL picolinaldehyde (1.93 mmol), 214 mg (S)-N^1-3-dimethylbutane-1,2-diamine (1.84 mmol), and 327.8 mg N-bromosuccinimide (0.70 mmol) in CH_2Cl_2 (0.10 M relative to picolinaldehyde). The reaction mixture was purified by column chromatography (SiO_2, 5% MeOH/CH_2Cl_2 then 1% TEA/5% MeOH/CH_2Cl_2) to afford 185.0 mg (49%) of the title compound as a pale yellow oil: $[a]_D^{18}$ -10.796 (*c* 1.08, $CHCl_3$); ^{1}H NMR (500 MHz, $CDCl_3$): δ 8.61 (ddd, *J* = 5.0, 2.0, 1.0 Hz, 1H), 7.86 (dt, *J* = 8.0, 1.0 Hz, 1H), 7.73 (dt, 8.0, 2.0 Hz, 1H), 7.30 (ddd, *J* = 7.5, 4.5, 1.0 Hz, 1H), 3.89 (ddd, *J* = 10.5, 9.5, 6.5 Hz, 1H), 3.56 (dd, *J* = 10.5, 9.5 Hz, 1H), 3.12 (t, *J* = 9.5 Hz, 1H), 1.86 (dddd, *J* = 20.5, 14.5, 7.0 1H), 1.03 (d, *J* = 6.5 Hz, 3H), 0.92 (d, *J* = 6.5 Hz, 3H); ^{13}C NMR (125 MHz, $CDCl_3$): δ 164.3, 150.6, 148.6, 136.6, 124.4, 124.3, 70.3, 56.6, 35.7, 33.1, 19.7, 19.2; IR ν_{max}^{neat} cm^{-1}**:** 2957, 2871, 1589, 1563, 1498, 1467, 1387, 1266, 1077, 1044, 801, 747; HRMS (EI) *m/z* calcd for $C_{12}H_{17}N_3$ $(M + H)^+$: 204.1501; found: 204.1472.

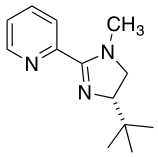

(S)-2-(4-*tert*-Butyl)-1-methyl-4,5-dihydro-1*H*-imidazol-2-yl)pyridine (110): General procedure B was followed by employing 83.0 μL picolinaldehyde (0.875 mmol), 114 mg (S)-N^1-3,3-trimethylbutane-1,2-diamine (0.875 mmol), and 163.5 mg N-bromosuccinimide (0.919 mmol) in CH_2Cl_2 (0.10 M relative to picolinaldehyde). The reaction mixture was purified by column chromatography (SiO_2, 5-20% MeOH/CH_2Cl_2 then 2% TEA/20% MeOH/CH_2Cl_2) to afford 36.0 mg (19%) of the title compound as a pale orange oil: $[\alpha]_D^{22}$ –14.733 (*c* 0.90, $CHCl_3$); ^{1}H NMR (500 MHz, $CDCl_3$); δ 8.59 (ddd, *J* = 5.0, 1.5, 1.0 Hz, 1H), 7.84 (dt, *J* = 8.0, 1.0 Hz, 1H), 7.70 (dt, *J* = 7.5, 1.5 Hz, 1H), 7.28 (ddd, *J* = 8.0, 5.0, 1.5 Hz, 1H), 3.83 (dd, *J* = 10.5, 10.0 Hz, 1H), 3.53 (dd, *J* = 11.0, 9.5 Hz, 1H), 3.13 (t, *J* = 10.0 Hz, 1H), 1.95 (s, 1H), 0.95 (s, 9H); ^{13}C NMR (125 MHz, $CDCl_3$): δ 164.2, 150.9, 148.5, 136.5, 124.4, 124.1, 74.1, 55.2, 35.7, 33.9, 26.1; IR ν_{max}^{neat} cm^{-1}: 2951, 2866, 1590, 1563, 1466, 1392, 1362, 1275, 1209, 1087, 800, 746.

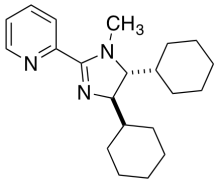

2-[(4*R*,5*R*)-4,5-Dicyclohexyl-1-methyl-4,5-dihydro-1*H*-imidazol-2-yl]pyridine (111): General procedure B was followed employing 83 μL picolinaldehyde (0.87 mmol), 186 mg (1R,2R)-dicyclohexylethylenediamine (0.83 mmol), and 155.2 mg N-bromosuccinimide (0.87 mmol) in 9 mL of CH_2Cl_2. After workup, 233.0 mg (0.75 mmol) of the crude product was recovered. Then the crude product was subjected to methylation employing 0.97 mL NaHMDS (1.0M in THF, 0.974 mmol) and 51.3 μL iodomethane (0.82 mmol) in 7 mL of THF. The reaction mixture was purified by column chromatography (SiO_2, 5-10% MeOH/CH_2Cl_2 gradient then 10% MeOH/2% Et_3N/8% CH_2Cl_2) to afford 202.0 mg (83%) the title product, an orange/brown viscous oil: $[a]_D^{18}$ +11.29 (*c* 1.15,

$CHCl_3$); ^1H NMR (500 MHz, $CDCl_3$): δ 8.64 (dd, *J* = 4.5, 0.5 Hz, 1H), 7.99 (d, *J* = 7.0 Hz, 1H), 7.75 (dt, *J* = 7.5, 1.5Hz, 1H), 7.32 (ddd, *J* = 7.5, 5.0, 1.0 Hz, 1H), 3.69 (t, *J* = 5.0 Hz, 1H), 3.14 (t, *J* = 4.0 Hz, 1H), 3.04 (s, 3H), 1.79-1.60 (m, 11H), 1.28-0.99 (m, 11H) ; ^{13}C NMR (125 MHz, $CDCl_3$): δ 162.7, 148.7, 136.7, 125.3, 124.6, 71.2, 43.4, 41.2, 34.7, 28.6, 28.5, 27.2, 26.6, 26.5, 26.4, 26.3, 26.2; IR ν_{max}^{neat} cm^{-1}: 2923, 2851, 1589, 1563, 1448, 1397, 1318, 1259, 1069, 1044, 799, 748; HRMS (EI) *m/z* calcd for $C_{21}H_{31}N_3$ $(M + H)^+$: 326.2596; found: 326.2588.

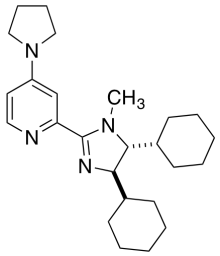

2-[(4R,5R)-4,5-Dicyclohexyl-1-methyl-4,5-dihydro-1*H*-imidazol-2-yl]-4-(pyrrolidin-1-yl)pyridine (112): 4-Chloro-2-[(4R,5R)-4,5-dicyclohexyl-1-methyl-4,5-dihydro-1*H*-imidazol-2-yl)pyridine, 203.0 mg (0.57 mmol) was added to a medium pressure reaction vessel along with 1.86 mL neat pyrrolidine (22.6 mmol). The vessel was sealed and heated to 90°C for 24 h. At this time the reaction vessel was removed from the oil bath and allowed to cool to ambient temperature and then concentrated in vacuo. The crude reaction mixture was purified by column chromatography (SiO_2, 5-8% MeOH/CH_2Cl_2 gradient) to afford 229.0 mg of the unmethylated HCl salt. The HCl salt was reexposed to the methylation procedure employing 187 mg of the salt (0.45 mmol), 1.12 mL NaHMDS (1.0 M in THF, 1.12 mmol), and 30.7 µL iodomethane (0.49 mmol) in 6 mL THF. The crude reaction mixture was purified by column chromatography (SiO_2, 5-10% MeOH/ CH_2Cl_2 gradient then 10% MeOH/1% Et_3N/9% CH_2Cl_2) to afford 157 mg (89%) of the title compound as a pale yellow oil: $[a]_D^{19}$ +7.07 (*c* 0.990, $CHCl_3$); ^1H NMR (500 MHz, $CDCl_3$): δ 8.18 (d, *J* = 6.0 Hz, 1H), 6.90 (br s, 1H), 6.31 (d, *J* = 5.5 Hz, 1H), 3.61 (t, *J* = 4.5 Hz, 1H), 3.30 (br s, 4H), 3.01 (br s, 1H), 2.94 (s, 3H), 1.96 (t, *J* = 6.0 Hz, 4H), 1.72-1.52 (m, 11H), 1.24-0.98 (m, 11H); ^{13}C NMR (125 MHz, $CDCl_3$): δ 164.0, 151.9, 150.8, 148.6, 107.5, 107.0, 71.5, 70.5, 46.9,

43.4, 41.2, 34.4, 28.6, 28.4, 28.3, 27.2, 26.7, 26.6, 26.4, 26.4, 26.3, 26.2, 25.2; IR ν_{max}^{neat} cm^{-1}: 2922, 2850, 1600, 1539, 1484, 1460, 1388, 1349, 1315, 1262, 1181, 1073, 1006, 811, 750; HRMS (EI) *m/z* calcd for $C_{25}H_{38}N_4$ $(M + H)^+$: 395.3175; found: 395.3201.

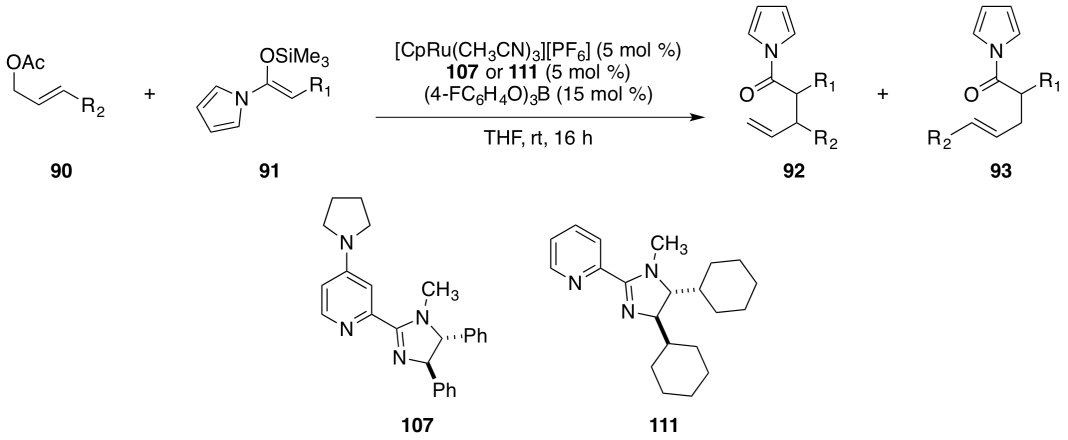

General Procedure C. Catalytic Asymmetric Enolate Allylic Alkylations: $[CpRu(CH_3CN)_3]PF_6$ (5 mol %) and ligand **107** or **111** (5 mol %) were combined in a 2 dram vial inside a nitrogen-filled glovebox. The THF (0.5 M final concentration of the allylic acetate substrate) was added and the reaction mixture was periodically shaken over 15 min. The resulting solution was then added to another 2 dram vial containing the allylic acetate (1 equiv), pyrrole silyl enol ether (1.05 equiv), $(4\text{-}FC_6H_4O)_3B$ (15 mol %) and a Teflon-coated stir bar. The vial was sealed with a threaded cap containing a rubber septum inlet. The vial was removed from the glovebox, and the mixture was stirred at ambient temperature for 16h. After this time, the vial was opened and the reaction mixture was concentrated under a stream of N_2. Pentanes (4x the reaction volume) were added and the resulting heterogeneous mixture was filtered through a Florisil® plug eluting with additional pentanes. The filtrate was concentrated and the resulting mixture of the *anti*/*syn* [3,3] products (**92a-92j**, **114**) and [1,3] regioisomer (**93a-93j**, **115**) was analyzed by ^1H NMR and chiral stationary phase GC.

Enantiomer ratio determination: Enantiomer ratios of the branched products (**92a-92j**) were determined by chiral stationary phase GLC (Varian Chirasil-Dex CB WCOT Fused Silica CP 7502 column, 25 m x 0.25 mm) or analytical high-performance liquid chromatography (HPLC) using a variable wavelength UV detector (deuterium lamp, 190-600 nm), a Chiracel OD-H column and HPLC-grade isopropanol and hexanes as the eluting solvents. Authentic samples of racemic *syn* and *anti* diastereomers of the products were used for comparison.

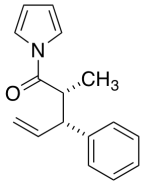

(2R,3R)-2-Methyl-3-phenyl-1-(1*H*-pyrrol-1-yl)pent-4-en-1-one (92a): General Procedure C was followed employing 75 mg (0.43 mmol) cinnamyl acetate, 87.3 mg (0.45 mmol) (Z)-1-[1-(trimethylsilyloxy)prop-1-en-1-yl]-1*H*-pyrrole (**91a**), 6.9 mg (0.021 mmol) ligand **111**, 9.2 mg (0.021 mmol) $[CpRu(CH_3CN)_3]PF_6$, 21.9 mg (0.064 mmol) $(4\text{-}FC_6H_4O)_3B$, and 0.80 mL THF. The reaction mixture was stirred for 16 h at which time it was concentrated under a stream of N_2, filtered through a plug of Florisil® and concentrated. The crude product was purified by column chromatography (SiO_2, 3% Et_2O/hexanes) to yield 90 mg (89%) as a mixture of diastereomers. Separating the stereoisomers of **92a** by GLC {flow rate 1.5 mL/min, method: 105 °C for 10 min, ramp @ 0.2 °C/min to 155 °C, hold for 5 min; T_r (min) = 116.5 [(2*S*,3*S*)-**92a**$_{anti}$], 117.2 [(2*R*,3*R*)-**92a**$_{anti}$], 134.3 (**92a**$_{syn1}$), 135.4 (**92a**$_{syn2}$), (ratio = 2.1:129.5:1:20.9)} provided the enantiomer ratio (2*S*,3*S*)-**92a**$_{anti}$:(2*R*,3*R*)-**92a**$_{anti}$ = 1.5:98.4 (97% ee), and (**92a**$_{syn1}$): (**92a**$_{syn2}$) = 4.5:95.4 (91% ee).

Anti diastereomer (white crystalline solid): mp 49-51 °C; $[\alpha]_D^{23}$ +6.67 (*c* 2.34, $CHCl_3$); ^1H NMR (500 MHz, $CDCl_3$): δ 7.26-7.20 (m, 6H), 7.16-7.12 (m, 1H), 6.22 (dd, *J* = 2.0 Hz, 2H), 6.00 (dt, *J* = 16.5, 9.5, Hz, 1H), 5.19 (m, 2H), 3.76 (t, *J* = 10.0 Hz, 1H), 3.51 (dq, *J* = 10.0, 7.0 Hz, 1H),

1.38 (d, J = 6.5 Hz, 3H); ^{13}C NMR (125 MHz, $CDCl_3$): δ 173.1, 142.0, 138.3, 128.6, 127.4, 126.7, 118.9, 117.3, 113.0, 53.3, 43.2, 16.8; IR ν_{max}^{neat} cm^{-1}: 3150, 3027, 1708, 1637, 1491, 1301, 1096, 915, 433; HRMS (EI) *m/z* calcd for $C_{16}H_{17}NO$ $(M + H)^+$: 240.1388; found: 240.1404.

Syn diastereomer (pale yellow oil): $[\alpha]_D^{23}$ +7.57 (*c* 1.06, $CHCl_3$); ^{1}H NMR (500 MHz, $CDCl_3$): δ 7.37-7.32 (m, 4H), 7.26-7.22 (m, 3H), 6.32 (app t, J = 2.0 Hz, 2H), 5.97 (ddd, J = 18.0, 10.0, 8.0 Hz, 1H), 5.02 (dt, J = 17.0, 1.0 Hz, 1H), 4.97 (d, J = 10.0 Hz, 1H), 3.72 (t, J = 10.0 Hz, 1H), 3.46 (dq, J = 10.5, 7.0 Hz, 1H), 1.08 (d, J= 7.0 Hz, 3H); ^{13}C NMR (125 MHz, $CDCl_3$): δ 173.5, 140.8, 138.9, 128.8, 128.3, 127.0, 119.0, 116.2, 113.3, 53.1, 43.3, 17.0; IR ν_{max}^{neat} cm^{-1}: 3027, 2930, 1711, 1600, 1467, 914, 742; HRMS (EI) *m/z* calcd for $C_{16}H_{17}NO$ $(M + H)^+$: 240.1388; found: 240.1373.

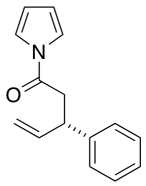

(S)-3-Phenyl-1-(1*H*-pyrrol-1-yl)pent-4-en-1-one (92b): General Procedure C was followed employing 75 mg (0.43 mmol) cinnamyl acetate, 81 mg (0.45 mmol) 1-[1-(trimethylsilyloxy)vinyl]-1*H*-pyrrole (**91b**), 6.9 mg (0.021 mmol) ligand **111**, 9.2 mg (0.021 mmol) $[CpRu(CH_3CN)_3]PF_6$, 21.9 mg (0.064 mmol) $(4\text{-}FC_6H_4O)_3B$, 0.80 mL THF. The reaction mixture was stirred for 16 h at which time it was concentrated under a stream of N_2, filtered through a plug of Florisil® and concentrated. The crude product was purified via column chromatography (SiO_2, 3% Et_2O/hexanes) to yield 78 mg (82%) of the product as a colorless oil. Separating the stereoisomers of **92b** by GLC {flow rate 1.5 mL/min, method: 105 °C for 10 min, ramp @ 0.3 °C/min to 175 °C, hold for 5 min; T_r (min) = 120.4 [(3S-(**92b**)], 120.9 [3R-(**92b**)], (ratio = 1:37.4)} provided an ee of 95%. $[\alpha]_D^{23}$ +0.940 (*c* 0.830, $CHCl_3$); ^{1}H NMR (500 MHz, $CDCl_3$): δ 7.33-7.29 (m, 4H), 7.27-7.21 (m, 3H), 6.28 (app t, J = 2.0 Hz, 2H), 6.06 (ddd, J =

24.0, 10.5, 7.0 Hz, 1H), 5.10 (m, 2H), 4.10 (dd, *J* = 14.5, 7.0 Hz, 1H), 3.24 (dq, *J* = 16.0, 7.5 Hz, 2H); ^{13}C NMR (125 MHz, $CDCl_3$): δ168.6, 142.3, 139.9, 128.7, 127.6, 126.9, 119.0, 115.3, 113.2, 44.8, 40.3; IR ν_{max}^{neat} cm^{-1}:3148, 3028, 2921, 1717, 1638, 1600, 1468, 1338, 1275, 1073, 922, 740; HRMS (EI) *m/z* calcd for $C_{15}H_{15}NO$ $(M + H)^+$ 226.1232; found: 226.1224.

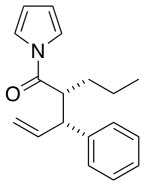

(2R,3R)-3-Phenyl-2-propyl-1-(1*H*-pyrrol-1-yl)pent-4-en-1-one (92c): General Procedure C was followed employing 75 mg (0.43 mmol) cinnamyl acetate, 100 mg (0.45 mmol) (Z)-1-[1-(trimethylsilyloxy)pent-1-en-1-yl]-1*H*-pyrrole (**91c**), 6.9 mg (0.021 mmol) ligand **111**, 9.2 mg (0.021 mmol) $[CpRu(CH_3CN)_3]PF_6$, 146 mg (0.43 mmol) $(4\text{-}FC_6H_4O)_3B$, 0.80 mL THF. The reaction mixture was stirred for 16 h at which time it was concentrated under a stream of N_2, filtered through a plug of Florisil® and concentrated. The crude product was purified via column chromatography (SiO_2, 3% Et_2O/hexanes) to yield 93 mg (82%) of the product as a mixture of diastereomers.

Anti diastereomer (white crystalline solid): mp 81-83 °C; $[\alpha]_D^{22}$ +6.40 (*c* 4.56, $CHCl_3$); ^{1}H NMR (500 MHz, $CDCl_3$): δ 7.20-7.15 (m, 5H), 7.10 (m, 1H), 6.16 (app t, *J* = 2.0 Hz, 2H), 6.02 (ddd, *J* = 17.0, 9.5 Hz, 1H), 5.17 (m, 2H), 3.71 (t, *J* = 9.5 Hz, 1H), 3.41 (dt, *J* = 10.0, 4.0 Hz, 1H), 3.14 (dt, *J* = 10.0, 4.0 Hz, 1H), 1.83-1.74 (m, 2H), 1.34-1.18 (m, 2H), 0.88 (t, *J* = 7.0 Hz, 3H); ^{13}C NMR (125 MHz, $CDCl_3$): δ 173.0, 141.8, 138.5, 128.6, 127.5, 126.7, 119.0, 117.2, 112.9, 53.3, 49.3, 33.7, 20.4, 14.1; IR ν_{max}^{neat} cm^{-1}: 3148, 3029, 2927, 1694, 1638, 1468, 1345, 1274, 1110, 1048, 924, 758; HRMS (EI) *m/z* calcd for $C_{18}H_{21}NO$ $(M + H)^+$: 268.1701; found: 268.1720.

Syn diastereomer (pale yellow oil): $[\alpha]_D^{22}$ +1.67 (*c* 1.28, $CHCl_3$); ^{1}H NMR (500 MHz, $CDCl_3$): δ 7.38 (br s, 2H), 7.34 (t, *J* = 7.5 Hz, 2H), 7.23 (dd, *J* = 10.0, 8.5 Hz, 3H), 6.31 (app t, *J* = 2.0 Hz, 2H), 5.93 (ddd, *J* = 19.0, 10.5, 8.3 Hz, 1H), 5.00 (d, *J* = 17.0 Hz, 1H), 4.92 (d, *J* = 10.0 Hz, 1H),

3.68 (t, J = 9.0 Hz, 1H), 3.42 (dt, J = 10.0, 3.5 Hz, 1H), 1.70-1.63 (m, 1H), 1.34-1.28 (m, 1H), 1.25-1.20 (m, 1H), 1.20-1.17 (m, 1H), 0.74 (t, J= 7.0 Hz, 3H); ^{13}C NMR (125 MHz, $CDCl_3$): δ173.3, 141.2, 138.5, 128.8, 128.0, 126.9, 119.0, 116.4, 113.3, 53.4, 49.3, 33.7, 20.5, 14.0; IR ν_{max}^{neat} cm^{-1}: 3150, 3027, 2924, 1709, 1466, 1371, 1114, 1073, 742; HRMS (EI) *m/z* calcd for $C_{18}H_{21}NO$ $(M + H)^+$: 268.1701; found: 268.1720.

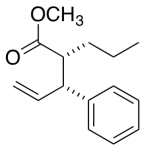

Methyl (2R,3R)-3-phenyl-2-propylpent-4-enoate (92c*): 92c was derivatized to the methyl ester **92c*** for ee determination. General procedure: To a solution of acyl pyrrole (**92c**, 1.0 equiv) in MeOH (0.1M) was added NaOMe(10.0 equiv). The reaction was allowed to stir at rt for 24 h, and then quenched with saturated ammonium chloride. The reaction was extracted 3 times with Et_2O, dried over $MgSO_4$, and concentrated. Separating the stereoisomers of **92c*** by GLC {flow rate 2.0 mL/min, method: 80 °C for 10 min, ramp @ 0.4 °C/min to 160 °C, hold for 5 min; T_r (min) = 60.0 [(2*R*,3*R*)-**92c***$_{anti}$], 60.7 [(2*S*,3*S*)-**92c***$_{anti}$], 81.2 (**92c***$_{syn1}$), 82.4 (**92c***$_{syn2}$), (ratio = 374:7.4:1:65.9)} provided the enantiomer ratio (2*R*,3*R*)-**92c***$_{anti}$:(2*S*,3*S*)-**92c***$_{anti}$ = 98.0:1.9 (96% ee), and (**92c***$_{syn1}$): (**92c***$_{syn2}$) = 1.5:98.5 (97% ee).

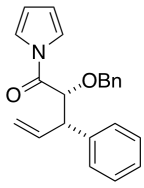

(2R,3S)-2-(Benzyloxy)-3-phenyl-1-(1*H*-pyrrol-1-yl)pent-4-en-1-one (92e): General Procedure C was followed employing 100 mg (0.57 mmol) cinnamyl acetate, 171 mg (0.59 mmol) (Z)-1-[2-(benzyloxy)-1-(trimethylsilyloxy)vinyl]-1*H*-pyrrole **91e**, 9.2 mg (0.028 mmol) ligand **111**, 12.3 mg (0.028 mmol) $[CpRu(CH_3CN)_3]PF_6$, 29 mg (0.085 mmol) $(4\text{-}FC_6H_4O)_3B$, 1.0 mL THF. The reaction mixture was stirred for 16 h at which time it was concentrated under a stream of N_2, filtered through a plug of Florisil® and

concentrated. The crude product was purified via column chromatography (SiO_2, 5% Et_2O/hexanes) to yield 141 mg (75%) of the product as a mixture of diastereomers.

Anti diastereomer (white solid): mp 77-79 °C; $[\alpha]_D^{22}$ +5.00 (*c* 0.280, $CHCl_3$); ^1H NMR (500 MHz, $CDCl_3$): δ 7.37 (br s, 2H), 7.32-7.16 (m, 10H), 6.30-6.23 (m, 3H), 5.20 (d, *J* = 10.5 Hz, 1H), 5.08 (d, *J* = 17.0 Hz, 1H), 4.70 (m, 2H), 4.41 (d, *J* = 11.5Hz, 1H), 3.90 (t, *J* = 7.0 Hz, 1H); ^{13}C NMR (125 MHz, $CDCl_3$): δ168.7, 139.2, 136.3, 136.1, 128.6, 128.4, 128.3, 128.1, 128.0, 127.3, 119.5, 117.9, 113.2, 83.3, 72.5, 53.4; IR ν_{max}^{neat} cm^{-1}: 3083, 3029, 2859, 1715, 1688, 1466, 1329, 1289, 1096, 1019, 926, 739; HRMS (EI) *m/z* calcd for $C_{22}H_{21}NO_2$ $(M + H)^+$: 332.1651; found: 332.1640.

Syn diastereomer (yellow oil): $[\alpha]_D^{18}$ +2.50 (*c* 0.08, $CHCl_3$); ^1H NMR (500 MHz, $CDCl_3$): δ 7.48 (t, *J* = 2.5 Hz, 2H), 7.33-7.28 (m, 3H), 7.23-7.20 (m, 5H), 6.97 (m, 2H), 6.28 (t, *J* = 2.5 Hz, 2H), 5.95 (ddd, *J* = 9.0, 10, 17 Hz, 1H), 4.98 (m, 2H), 4.63 (d, *J* = 9.0 Hz, 1H), 4.57 (d, *J* = 9.0 Hz, 1H), 4.23 (d, *J* = 9.0, 1H), 3.89 (t, *J* = 9 Hz, 1H); ^{13}C NMR (125 MHz, $CDCl_3$): δ169.4, 139.6, 136.3, 135.6, 128.5, 128.3, 127.9, 127.1, 119.5, 118.0, 113.3, 83.7, 72.4, 54.2; IR ν_{max}^{neat} cm^{-1}: 2956, 2926, 2867, 1712, 1602, 1505, 1468, 1409, 1344, 1255, 1088, 926, 820.0, 745; HRMS (EI) *m/z* calcd for $C_{18}H_{21}NO$ $(M + Na)^+$: 354.1470; found: 254.1467.e

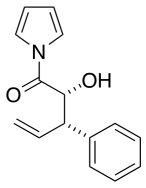

(2R,3S)-2-Hydroxy-2-phenyl-1-(1H-pyrrol-1-yl)pent-4-en-1-one (92e*): Compound **92e** was derivatized to the free alcohol **92e*** for ee determination. General procedure: To a -78 °C solution of compound **92e** (1.0 equiv.) in CH_2Cl_2 (0.1 M) was added a 1.0 M solution of BCl_3 in CH_2Cl_2 dropwise. The reaction was allowed to stir at a -78 °C for 3 h at which time it was quenched with an equal volume of MeOH. The reaction was allowed to warm to rt and then concentrated in vacuo to yield **92e*** as the free alcohol.

Separating the stereoisomers of **92e*** by GLC {flow rate 1.0 mL/min, method: 105 °C for 10 min, ramp @ 0.7 °C/min to 200 °C, hold for 5 min; T_r (min) = 99.3 (**92e***$_{syn1}$), 99.0 (**92e***$_{syn2}$), 100.9 [(2S,3S)-**92e***$_{ani}$], 101.5 [(2R,3R)-**92e***$_{anti}$, (ratio = 1:17:2:104)} provided the Enantiomer ratio (2S,3S)-**92e***$_{anti}$:(2R,3R)-**92e***$_{anti}$ = 1.9:98.1 (96% ee), and (**92e***$_{syn1}$):(**92e***$_{syn2}$) = 5.6:94.4 (89% ee).

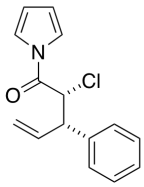

(2R,3S)-2-Chloro-3-phenyl-1-(1*H*-pyrrol-1-yl)pent-4-en-1-one (92f): General Procedure C was followed employing 100 mg (0.57 mmol) cinnamyl acetate, 128 mg (0.59 mmol) (Z)-1-[2-chloro-1-(trimethylsilyloxy)vinyl]-1*H*-pyrrole **91f**, 9.2 mg (0.028 mmol) ligand **111**, 12.3 mg (0.028 mmol) $[CpRu(CH_3CN)_3]PF_6$, 29 mg (0.085 mmol) $(4\text{-}FC_6H_4O)_3B$, 1.0 mL THF. The reaction mixture was stirred for 16 h at which time it was concentrated under a stream of N_2, filtered through a plug of Florisil® and concentrated. The crude product was purified via column chromatography (SiO_2, 3% Et_2O/hexanes) to yield 56 mg (38%) of the product as an inseparable mixture of diastereomers. In addition, 16mg (10%) of the OAc substituted product was collected eluting with 10% Et_2O/hexanes. Separating the stereoisomers of **92f** by GLC {flow rate 1.5 mL/min, method: 105 °C for 10 min, ramp @ 0.3 °C/min to 175 °C, hold for 5 min; T_r (min) = 140.6 [(2*S*,3*S*)-**92f**$_{anti}$], 141.2 [(2*R*,3*R*)-**92f**$_{anti}$], (ratio = 66.1:1)} provided an ee of 97%. The *syn* stereoisomers could not be separated. Diastereomer ratio*(anti:syn)* = 1.0: 0.80 (pale yellow oil); $[\alpha]_D^{23}$ +4.17 (*c* 5.72, $CHCl_3$); ^{1}H NMR (500 MHz, $CDCl_3$): δ 7.43-7.23 (m, 9H), 6.40 (t, *J*= 2.5 Hz, 2H), 6.29 (t, *J*= 2.0 Hz, 1.5H), 6.23 (ddd, *J* = 18.5, 10.5, 2.0 Hz, 0.8H), 6.01 (ddd, *J* = 17.5, 11.0, 6.5 Hz, 1H), 5.32 (d, *J* = 10.0 Hz, 0.8H), 5.25 (dt, *J* = 17.0, 10.0 Hz, 0.8H), 5.18 (d, *J* = 1.0 Hz, 1H), 5.15 (d, *J* = 6.5 Hz, 1H), 5.12 (d, *J* = 10.0 Hz, 0.8H), 5.09 (d, *J* = 10.5 Hz, 1H), 4.21 (dd, *J* = 17.5, 7.5 Hz, 1.8H); ^{13}C NMR

(125 MHz, $CDCl_3$): δ 164.5, 165.1, 138.9, 138.6, 136.2, 135.8, 128.9, 128.8, 128.5, 128.1, 127.6, 127.6, 119.4, 119.3, 119.1, 118.9, 114.2, 113.9, 57.4, 57.1, 53.1, 52.8; IR ν_{max}^{neat} cm^{-1}: 3150, 3063, 3029, 1638, 1600, 1547, 1411, 1364, 1318, 1265, 1233, 1076, 988, 860, 742; HRMS (EI) *m/z* calcd for $C_{15}H_{14}ClNO$ $(M + H)^+$: 260.0842; found: 260.0825.

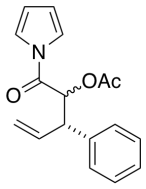

(3*S*)-1-oxo-3-Phenyl-1-(1*H*-pyrrol-1-yl)pent-4-en-2-yl acetate (92f'): Separating the stereoisomers of **90f'** by GLC {flow rate 1.5 mL/min, method: 105 °C for 10 min, ramp @ 0.2 °C/min to 155 °C, hold for 5 min; T_r (min) = 172.7 [(2*R*,3*S*)-**92f'**$_{syn}$], 174.1 [(2*S*,3*R*)-**92f'**$_{syn}$], 176.3 (**92f'**$_{anti1}$), 178.9 (**92f'**$_{anti2}$), (ratio = 1.1:112.6:79.9:1)} provided the enantiomer ratio (2*R*,3*S*)-**92f'**$_{syn}$:(2*S*,3*R*)-**92f'**$_{syn}$ = 1.0:99.0 (98% ee), and (**92f'**$_{syn1}$):(**92f'**$_{syn2}$) = 1.5:98.7 (97% ee). *Anti* diastereomer: *Syn* diastereomer = 1.0: 0.80 (pale yellow oil); $[\alpha]_D^{23}$ +3.31 (*c* 1.16, $CHCl_3$); ^{1}H NMR (500 MHz, $CDCl_3$): δ 7.38-7.20 (m, 13H), 6.33 (app t, *J* = 2.5 Hz, 1.4H), 6.25 (app t, *J* = 2.5 Hz, 2H), 6.17 (ddd, *J* = 17.0, 10.0, 8.5 Hz, 1.3H), 5.99 (ddd, *J* = 17.0, 10.0, 8.5 Hz, 0.8H), 5.94 (m, 0.8H), 5.92 (s, 1H), 5.22 (d, *J* = 10.0 Hz, 1.1H), 5.12 (m, 2.8H), 4.02 (m, 1.8H), 2.16 (s, 3H), 1.96 (s, 2H); ^{13}C NMR (125 MHz, $CDCl_3$): δ170.2, 170.0, 166.5, 166.1, 138.3, 138.1, 135.0, 134.6, 128.8, 128.6, 128.4, 128.1, 127.6, 127.5, 119.2, 119.1, 118.7, 118.6, 113.9, 113.7, 74.1, 73.9, 51.9, 51.7, 20.6, 20.3; IR ν_{max}^{neat} cm^{-1}: 3150, 3030, 2923, 1722, 1640, 1601, 1470, 1415, 1373, 1323, 1294, 1234, 1123, 1073, 926, 817, 744; HRMS (EI) *m/z* calcd for $C_{15}H_{14}ClNO$ $(M + Na)^+$: 306.1106; found: 306.1124.

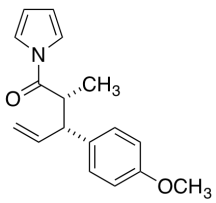

(2R,3R)-3-(4-Methoxyphenyl)-2-methyl-1-(1*H*-pyrrol-1-yl)pent-4-en-1-one (92g): General Procedure C was followed employing 100 mg (0.49

mmol) (E)-3-(4-methoxyphenyl)allyl acetate, 99 mg (0.51 mmol) (Z)-1-[1-(trimethylsilyloxy)prop-1-en-1-yl]-1*H*-pyrrole **91a**, 7.9 mg (0.024 mmol) ligand **111**, 10.5 mg (0.024 mmol) $[CpRu(CH_3CN)_3]PF_6$, 25 mg (0.073 mmol) $(4\text{-}FC_6H_4O)_3B$, 1.0 mL THF. The reaction mixture was stirred for 16 h at which time it was concentrated under a stream of N_2, filtered through a plug of Florisil® and concentrated. The crude product was purified via column chromatography (SiO_2, 5% Et_2O/hexanes) to yield 103 mg (79%) of the product as a mixture of diastereomers. *Anti* diastereomer (white crystalline solid): mp 56-59 °C; $[\alpha]_D^{22}$ +0.291 (*c* 1.10, $CHCl_3$); ^{1}H NMR (500 MHz, $CDCl_3$): δ 7.22 (br s, 2H), 7.11 (d, *J* = 9 Hz, 2H), 6.76 (d, *J*= 8.5 Hz, 2H), 6.22 (app t, *J* = 2.0 Hz, 2H), 5.97 (ddd, *J* = 18.0, 16.5, 9.0 Hz, 1H), 5.15 (m, 2H), 3.73 (s, 3H), 3.71 (m, 1H), 3.46 (dq, *J* = 9.5, 7.0 Hz, 1H), 1.36 (d, *J* = 7.0 Hz, 3H); ^{13}C NMR (125 MHz, $CDCl_3$): δ 173.1, 158.2, 138.5, 134.2, 128.4, 118.9, 116.9, 114.0, 113.0, 55.1, 52.4, 43.4, 16.9; IR ν_{max}^{neat} cm^{-1}: 3149, 3074, 2935, 2836, 1714, 1636, 1491, 1467, 1366, 1273, 1125, 1072, 995, 896, 742; HRMS (EI) *m/z* calcd for $C_{17}H_{19}NO_2$ $(M + H)^+$: 270.1494; found: 270.1501.

Syn diastereomer (clear colorless oil): $[\alpha]_D^{22}$ +9.74 (*c* 0.310, $CHCl_3$); ^{1}H NMR (500 MHz, $CDCl_3$): δ 7.38 (br s, 2H), 7.14 (d, *J* = 8.5 Hz, 2H), 6.89 (d, *J* = 8.5 Hz, 2H), 6.32 (app t, *J* = 2.5 Hz, 2H), 5.96 (ddd, *J* = 17.5, 10.5, 8.0 Hz, 1H), 4.98 (m, 2H), 3.81 (s, 3H), 3.68 (t, *J* = 8.0 Hz, 1H), 3.41 (dq, *J* = 10.0, 3.5 Hz, 1H), 1.08 (d, *J* = 7.0 Hz, 3H); ^{13}C NMR (125 MHz, $CDCl_3$): δ173.6, 158.5, 139.1, 132.8, 129.2, 119.0, 115.8, 114.2, 113.3, 55.3, 52.2, 43.4, 16.9; IR ν_{max}^{neat} cm^{-1}: 2930, 2360, 1709, 1492, 1466, 1371, 1274, 1120, 1073, 914, 743; HRMS (EI) *m/z* calcd for $C_{17}H_{19}NO_2$ $(M + H)^+$: 270.1494; found: 270.1479.

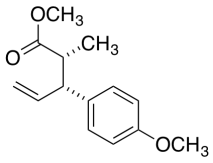

Methyl-(2R,3R)-3-(4-methoxyphenyl)-2-methylpent-4-enoate (92g*): Compound **92g** was derivatized to the corresponding methyl ester **92g*** for ee determination. General procedure: To a solution of acyl pyrrole **92g** (1.0 equiv.) in MeOH (0.1 M) was added NaOMe (10.0 equiv.). The reaction was allowed to stir at rt for 24 h and then quenched with saturated ammonium chloride. The reaction was extracted 3 time with Et_2O, dried over $MgSO_4$, and concentrated to yield product **92g*** as the methyl ester. Separating the stereoisomers of **92g*** by GLC {flow rate 2.0 mL/min, method: 80 °C for min, ramp @ 0.4 °C/min to 160 °C, hold for 5 min; T_r (min) = 112.9 [(2S,3S)-**92g***$_{anti}$], 113.9 [(2R,3R)-**92g***$_{anti}$], 123.4 (**92g***$_{syn1}$), 123.7 (**92g***$_{syn2}$), (ratio = 2.2:66.8:1:16.6)} provided the Enantiomer ratio (2S,3S)-**92g***$_{anti}$:(2R,3R)-**92g***$_{anti}$ = 3.2:96.8 (94% ee) and (**92g***$_{syn1}$):(**92g***$_{syn2}$) = 5.6:94.3 (89% ee).

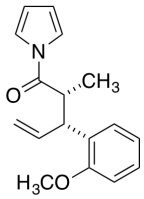

(2R,3R)-3-(2-Methoxyphenyl)-2-methyl-1-(1H-pyrrol-1-yl)pent-4-en-1-one (92h): General Procedure C was followed employing 100 mg (0.49 mmol) (E)-3-(2-methoxyphenyl)allyl acetate, 99 mg (0.51 mmol) (Z)-1-[1-(trimethylsilyloxy)prop-1-en-1-yl]-1*H*-pyrrole **91a**, 7.9 mg (0.024 mmol) ligand **111**, 10.5 mg (0.024 mmol) $[CpRu(CH_3CN)_3]PF_6$, 25 mg (0.073 mmol) $(4\text{-}FC_6H_4O)_3B$, 1.0 mL THF. The reaction mixture was stirred for 16 h at which time it was concentrated under a stream of N_2, filtered through a plug of Florisil® and concentrated. The crude product was purified via column chromatography (SiO_2, 5% Et_2O/hexanes) to yield 104 mg (80%) of the product as a mixture of diastereomers. Separating the stereoisomers of **92h** by GLC {flow rate 1.5 mL/min, method: 105 °C for 10 min, ramp @ 0.2 °C/min to 155 °C, hold for 5 min; T_r (min) = 170.9 [(2*S*,3*S*)-**92h**$_{anti}$], 172.4 [(2*R*,3*R*)-**92h**$_{anti}$], 186.4 (**92h**$_{syn1}$), 187.9 (**92h**$_{syn2}$), (ratio = 1:84.2:19.0:1.5)} provided the

enantiomer ratio (2*S*,3*S*)-**92h**$_{anti}$:(2*R*,3*R*)-**92h**$_{anti}$ = 1.2:98.8 (98% ee), and (**92h**$_{syn1}$): (**92h**$_{syn2}$) = 92.7:7.3 (85% ee).

Anti diastereomer (white crystalline solid): mp 50-52 °C; $[\alpha]_D^{22}$ +7.83 (*c* 2.84, $CHCl_3$); ^{1}H NMR (500 MHz, $CDCl_3$): δ 7.36 (dd, *J* = 2.0 Hz, 2H), 7.17-7.14 (m, 2H), 6.86 (app t, *J* = 7.0, 7.0 Hz, 1H), 6.82 (d, *J* = 8.0 Hz, 1H), 6.24 (t, *J*= 2.0 Hz, 2H), 6.21 (m, 1H), 5.10 (m, 2H), 4.03 (t, *J* = 9.0Hz, 1H), 3.87 (s, 3H), 3.81 (ddd, *J* = 7.0 Hz, 1H), 1.25 (d, *J* = 7.0 Hz, 3H); ^{13}C NMR (125 MHz, $CDCl_3$): δ 173.3, 156.5, 136.4, 129.9, 129.2, 127.8, 120.7, 119.1, 117.6, 112.6, 110.8, 55.2, 49.1, 41.1, 15.0; IR ν_{max}^{neat} cm^{-1}: 3151, 3004, 2905, 2835, 1701, 1611, 1513, 1469, 1376, 1278, 1179, 835, 743 ; HRMS (EI) *m/z* calcd for $C_{17}H_{19}NO_2$ $(M + Na)^+$: 292.1313; found: 292.1310.

Syn diastereomer (clear colorless oil): $[\alpha]_D^{22}$ +5.74 (*c* 0.380, $CHCl_3$); ^{1}H NMR (500 MHz, $CDCl_3$): δ 7.38 (br s, 2H), 7.23 (dt, *J*= 8.0, 1.5 Hz, 1H), 7.16 (dd, *J* = 7.5, 1.5 Hz, 1H), 6.93 (dt, *J* = 7.5, 1.0 Hz, 1H), 6.89 (d, *J* = 8.5 Hz, 1H), 6.30 (app t, *J* = 2.0 Hz, 2H), 6.10 (ddd, *J* = 18.5, 10.0, 8.0 Hz, 1H), 5.04 (dt, *J* = 17.0, 1.0 Hz, 1H), 4.94 (dd, *J* = 10.0, 0.5 Hz, 1H), 4.04 (t, *J* = 9.0 Hz, 1H), 3.85 (s, 3H), 3.75 (dq, *J*= 9.5, 7.0 Hz, 1H), 1.08 (d, *J* = 6.5 Hz, 3H); ^{13}C NMR (125 MHz, $CDCl_3$): δ 173.9, 157.2, 138.0, 129.7, 129.0, 128.0, 120.8, 119.1, 116.2, 113.0, 111.0, 55.4, 48.9, 41.5, 16.5; IR ν_{max}^{neat} cm^{-1}: 2930, 2835, 1711, 1637, 1511,1466, 1408, 1320, 1269, 1178, 1115, 1073, 993, 828, 742; HRMS (EI) *m/z* calcd for $C_{17}H_{19}NO_2$ $(M + H)^+$: 270.1494; found: 270.1531.

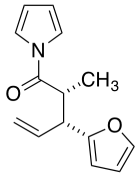

(2R,3R)-3-(Furan-2-yl)-2-methyl-1-(1*H*-pyrrol-1-yl)pent-4-en-1-one (92i): General Procedure C was followed employing 100 mg (0.60 mmol) (E)-3-(furan-2-

yl)allyl acetate, 123 mg (0.63 mmol) (Z)-1-[1-(trimethylsilyloxy)prop-1-en-1-yl]-1*H*-pyrrole **91a**, 9.8 mg (0.030 mmol) ligand **111**, 13.1 mg (0.030 mmol) $[CpRu(CH_3CN)_3]PF_6$, 31 mg (0.090 mmol) $(4\text{-}FC_6H_4O)_3B$, 1.2 mL THF. The reaction mixture was stirred for 16 h at which time it was concentrated under a stream of N_2, filtered through a plug of Florisil® and concentrated. The crude product was purified via column chromatography (SiO_2, 3% Et_2O/hexanes) to yield 136 mg (99%) of the product as a mixture of diastereomers. Separating the stereoisomers of **92i** by GLC {flow rate 2.0 mL/min, method: 80 °C for 10 min, ramp @ 0.4 °C/min to 160 °C, hold for 5 min; T_r (min) = 105.3 [(2*S*,3*S*)-**92i**$_{anti}$], 106.0 [(2*R*,3*R*)-**92i**$_{anti}$], 108.0 (**92i**$_{syn1}$), 109.2 (**92i**$_{syn2}$), (ratio = 1.1:43.1:1:28.9)} provided the enantiomer ratio (2*S*,3*S*)-**92i**$_{anti}$:(2*R*,3*R*)-**92i**$_{anti}$ = 2.4:97.5 (95% ee), and (**92i**$_{syn1}$): (**92i**$_{syn2}$) = 3.3:96.7 (93% ee)

Anti diastereomer (off white, waxy solid): mp 26-28 °C; $[\alpha]_D^{22}$ +3.24 (*c* 4.64, $CHCl_3$); ^{1}H NMR (500 MHz, $CDCl_3$): δ 7.31 (br s, 2H), 7.25 (m, 1H), 6.27 (app t, *J* = 2.5 Hz, 2H), 6.21 (dd, *J* = 3.0, 2.0 Hz, 1H), 6.01 (d, *J* = 3.5 Hz, 1H), 5.92 (ddd, *J* = 17.0, 10.0, 9.5 Hz, 1H), 5.24 (dd, *J* = 10.0, 1.0 Hz, 1H), 5.18 (d, *J* = 17.0Hz, 1H), 3.88 (t, *J* = 9.0 Hz, 1H), 3.57 (dq, *J* = 8.5, 7.0 Hz, 1H), 1.29 (d, *J* = 7.0 Hz, 3H); ^{13}C NMR (100 MHz, $CDCl_3$): δ 172.9, 154.6, 141.5, 134.7, 119.1, 118.7, 113.1, 110.2, 106.0, 46.7, 41.5, 15.4; IR ν_{max}^{neat} cm^{-1}: 3149, 2980, 1714, 1503, 1468, 1364, 1321, 1272, 1096, 994, 734; HRMS (EI) *m/z* calcd for $C_{14}H_{15}NO_2$ $(M + H)^+$: 230.1181; found: 230.1183.

Syn diastereomer (light yellow oil): $[\alpha]_D^{22}$ +3.03 (*c* 1.79, $CHCl_3$); ^{1}H NMR (500 MHz, $CDCl_3$): δ 7.37 (dd, *J* = 2.0, 1.0 Hz, 1H), 7.35 (br s, 2H), 6.32 (m, 3H), 6.15 (d, *J* = 3.0 Hz, 1H), 5.95 (ddd, *J* = 18.5, 10.5, 8.0 Hz, 1H), 5.08 (dt, *J* = 17.0, 1.0 Hz, 1H), 5.04 (d, *J* = 10.0 Hz, 1H), 3.85 (t, *J* = 9.0 Hz, 1H), 3.56 (dq, *J* = 9.5, 6.5 Hz, 1H), 1.16 (t, *J* = 7.0 Hz, 3H); ^{13}C NMR (125 MHz, $CDCl_3$): δ 172.9, 153.8, 141.8, 135.9, 119.1, 117.4, 113.3, 110.2, 107.3, 46.5, 42.1, 16.8; IR

ν_{max}^{neat} cm^{-1}: 2978, 2929, 1712, 1639, 1503, 1467, 1409, 1318, 1274, 1148, 1073, 1010, 994, 909, 806, 737; HRMS (EI) *m/z* calcd for $C_{14}H_{15}NO_2$ $(M + H)^+$: 230.1181; found: 230.1183.

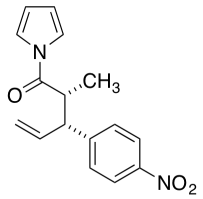

(2R,3R)-2-Methyl-3-(4-nitrophenyl)-1-(1*H*-pyrrol-1-yl)pent-4-en-1-one (92j): General Procedure C was followed employing 100 mg (0.45 mmol) (E)-3-(4-nitrophenyl)allyl acetate, 93 mg (0.48 mmol) (Z)-1-[1-(trimethylsilyloxy)prop-1-en-1-yl]-1*H*-pyrrole **91a**, 7.4 mg (0.023 mmol) ligand **111**, 9.8 mg (0.023 mmol) $[CpRu(CH_3CN)_3]PF_6$, 23 mg (0.068 mmol) $(4\text{-}FC_6H_4O)_3B$, 0.90 mL THF. The reaction mixture was stirred for 16 h at which time it was concentrated under a stream of N_2, filtered through a plug of Florisil® and concentrated. The crude product was purified via column chromatography (SiO_2, 6% Et_2O/hexanes) to yield 112 mg (88%) of the product as a mixture of diastereomers. Separating the enantiomers by chiral HPLC [Daicel Chiralpak OD-H column, flow rate 1.0 ml/min, 1% *i*PrOH, 99% hexane; T_r (min) = 13.3 [(2*S*,3*S*)-**92j**$_{anti}$], 14.3 [(2*R*,3*R*)-**92j**$_{anti}$], 15.9 (**92j**$_{syn1}$), 17.0 (**92j**$_{syn2}$), (ratio = 1:30.4:6.7:220.9)} provided the enantiomer ratio (2*S*,3*S*)-**92j**$_{anti}$:(2*R*,3*R*)-**92j**$_{anti}$ = 3.2:96.8 (94% ee), and (**92j**$_{syn1}$): (**92j**$_{syn2}$) = 2.9:97.1 (94% ee).

Anti diastereomer (off white solid): mp 93-95 °C; $[\alpha]_D^{22}$ +8.71 (*c* 1.84, $CHCl_3$); ^1H NMR (500 MHz, $CDCl_3$): δ 8.09 (d, *J* = 8.5 Hz, 2H), 7.36 (d, *J* = 9.0 Hz, 2H), 7.18 (m, 2H), 6.24 (dd, *J* = 2.5 Hz, 2H), 5.94 (m, 1H), 5.23 (m, 2H), 3.86 (t, *J* = 10.0 Hz, 1H), 3.50 (dq, *J* = 10.0, 7.0 Hz, 1H), 1.42 (d, *J* = 7.0 Hz, 3H); ^{13}C NMR (125 MHz, $CDCl_3$): δ 172.4, 149.8, 146.7, 137.0, 128.4, 123.9, 118.8, 118.7, 113.6, 53.1, 43.1, 17.3; IR ν_{max}^{neat} cm^{-1}: 3148, 3078, 2927, 1709, 1638, 1598, 1467, 1408, 1298, 1235, 1094, 994, 919, 893, 822, 743, 704; HRMS (EI) *m/z* calcd for $C_{16}H_{16}N_2O_3$ $(M + H)^+$: 285.1239; found: 285.1211.

Syn diastereomer (clear, colorless oil): $[\alpha]_D^{22}$ +2.63 (*c* 0.950, $CHCl_3$); ^1H NMR (500 MHz, $CDCl_3$): δ 8.22 (d, *J* = 9.0 Hz, 2H), 7.41 (d, *J* = 8.5 Hz, 2H), 7.36 (br s, 2H), 6.35 (app t, *J* = 2.0 Hz, 2H), 5.96 (ddd, *J* = 18.0, 10.5, 7.5 Hz, 1H), 5.07 (m, 2H), 3.90 (t, *J* = 9.5 Hz, 1H), 3.50 (dq, *J* = 10.0, 7.0 Hz, 1H), 1.10 (t, *J* = 7.0 Hz, 3H); ^{13}C NMR (100 MHz, $CDCl_3$): δ 172.5, 148.5, 147.1, 137.3, 129.2, 124.0, 119.0, 117.8, 113.7, 52.7, 43.0, 16.9; IR ν_{max}^{neat} cm^{-1}: 2927, 1711, 1602, 1519, 1467, 1409, 1346, 1322, 1273, 1113, 1073, 914, 852, 740, 702; HRMS (EI) *m/z* calcd for $C_{16}H_{16}N_2O_3$ $(M + H)^+$: 285.1239; found: 285.1241.

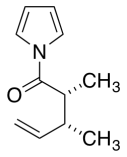

(2R,3R)-2,3-Dimethyl-1-(1*H*-pyrrol-1-yl)pent-4-en-1-one (111): General Procedure C was followed employing 50 mg (0.44 mmol) (E)-but-2-en-1-yl acetate, 90 mg (0.46 mmol) (Z)-1-[1-(trimethylsilyloxy)prop-1-en-1-yl]-1*H*-pyrrole **91a**, 8.7 mg (0.022 mmol) ligand **112**, 9.5 mg (0.022 mmol) $[CpRu(CH_3CN)_3]PF_6$, 23 mg (0.066 mmol) $(4\text{-}FC_6H_4O)_3B$, 0.8 mL THF. The reaction mixture was stirred for 16 h at which time it was concentrated under a stream of N_2, filtered through a plug of Florisil® and concentrated. The crude product was purified via column chromatography (SiO_2, 1% Et_2O/hexanes) to yield 29 mg (37%) of the product as an inseparable mixture of diastereomers and regioisomers. The mixture of products was saponified to the carboxylic acid [to a solution of 11 mg compound **114** (0.061 mmol) in 0.60 mL THF was added a solution of 0.60 mL of 1.0M NaOH. The solution was allowed to stir overnight. The THF was evaporated and the aqueous layer was made basic with the addition of an equal volume of saturated sodium bicarbonate. The aqueous layer was extracted 3x CH_2Cl_2 and discarded. The aqueous layer was then acidified to pH = 1 with 1 M HCl and extracted 3x CH_2Cl_2, dried over $MgSO_4$ and concentrated] which matched literature data. For *Anti* product see: Metz, P.; Hungerhoff, B. *J. Org. Chem.* **1997**, *62*, 4442-4448, for *Syn*

product see: Rye, C. E.; Barker, D. *J. Org. Chem.* **2011**, *76*, 6636-6648, and for linear product see: Deyo, D. T.; Aebi, J. D.; Rich, D. H. *Synthesis* **1988**, *8*, 608-610.

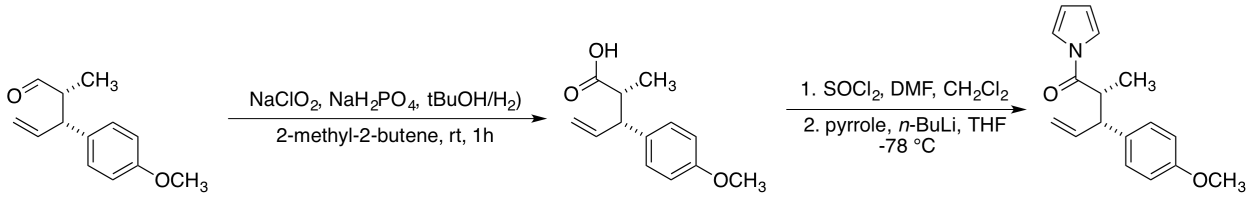

92g

Stereochemical Proof for Products (92a-92j): (2*R*,3*R*)-3-(4-Methoxyphenyl)-2-methylpent-4-enal was prepared according to the catalytic asymmetric Claisen rearrangement[25] in which the absolute stereochemistry was determined via X-ray crystallography.

To a magnetically-stirred solution of aldehyde 64 mg (0.32 mmol) and 2-methyl-2-butene 0.48 mL (4.5 mmol) in 1.0 mL *t*-BuOH (0.3 M) was added a solution of $NaClO_2$ 85 mg (0.94 mmol) and NaH_2PO_4 113 mg (0.94 mmol) in 1 mL H_2O (1 M in $NaClO_2$) dropwise via syringe at ambient temperature. The reaction was stirred for 3 h whereupon a saturated aqueous solution of NH_4Cl (100% v/v to reaction volume) was added and the resulting mixture was extracted with Et_2O (3x). The combined organic extracts were combined, dried ($MgSO_4$) and concentrated to provide 85 mg of the corresponding carboxylic acid that was used without purification in the next reaction.

To a rt solution of carboxylic acid 50 mg (0.23 mmol) in 1 mL CH_2Cl_2 was added thionyl chloride 30 mL (0.34 mmol) dropwise followed by 1 drop DMF. The reaction was allowed to stir for 1h until evolution of gas ceased. The reaction was then concentrated and redissolved in 0.5 mL of THF. The THF solution was added dropwise to a -78 °C solution of pyrrole 16 mL (0.23 mmol) and 0.18 mL of 1.4M *n*-BuLi (0.25 mmol) in 0.5 mL of THF. The reaction was

allowed to gradually warm to rt and stir overnight. The reaction was quenched with H_2O (100% v/v to reaction volume), extracted with Et_2O (3x), dried over $MgSO_4$ and concentrated.

The product of this reaction matched the 1H NMR and GLC of compound **92g**$_{anti}$. The absolute stereochemistry of compounds **92a-92j** was assigned by analogy to this determination.

4.2 EFFORTS TOWARDS THE SYNTHEIS OF ACTINORANONE

General Information: Unless otherwise indicated, all reactions were performed in dry glassware under an atmosphere of oxygen-free nitrogen using standard inert atmosphere techniques for the manipulation of both solvents and reagents. Anhydrous solvents were obtained by passage through successive alumina- and Q5-packed columns on a solvent purification system. $[CpRu(CH_3CN)_3]PF_6$ was synthesized according to the published procedure[87] and was stored and weighed out in a nitrogen-filled glove box. NMR spectra were recorded at the indicated magnetic field strengths with chemical shifts reported relative to residual C**H**Cl_3 (7.26 ppm) for ^{1}H and **C**DCl_3 (77.0 ppm) for ^{13}C spectra. Analytical thin layer chromatography (TLC) was performed on 0.25 mm silica gel 60-F plates. Flash chromatography was performed over silica gel (230-240 mesh). Analytical gas chromatography (GC) was performed using a flame ionization detector and split mode capillary injection system using Varian Chirasil-Dex CB WCOT fused silica 25 m x 0.25 mm column (CP 7502). Analytical high-performance liquid chromatography (HPLC) was performed using a variable wavelength UV detector (deuterium lamp, 190-600 nm) using a Chiracel OD-H column and HPLC-grade isopropanol and hexanes as the eluting solvents. Melting points were obtained on a Laboratory Devices Mel-Temp apparatus and are uncorrected.

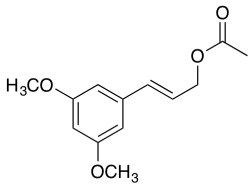

(*E*)-3-(3,5-Dimethoxyphenyl)allyl acetate (131): (*E*)-3-(3,5-dimethoxyphenyl)-2-propen-1-ol,[88] 6.61 g (34.0 mmol) was added to a solution of pyridine (102 mmol) in diethyl ether (0.5 M relative to the alcohol) at 0°C. To this solution was added acetyl chloride (55.1 mmol) drop-wise. The reaction was allowed to warm to room temperature and stirred for 16 h. The reaction was quenched with an equivalent volume of H_2O and extracted with diethyl ether (3x the reaction volume). The resultant organics were washed with saturated $CuSO_4$ (1x equivalent volume), dried over $MgSO_4$ and concentrated in vacuo. The product mixture was purified by column chromatography (SiO_2 5% ethyl acetate:hexanes) to afford 7.10 g (88%) as a colorless crystalline solid: mp 31.2-32.4 °C; ^{1}H NMR (500 MHz, $CDCl_3$): δ 6.58 (d, J = 16.0, 1H), 6.54 (s, 2H), 6.39 (s, 1H), 6.27 (apt dt, *J* = 6.5, 15, 1H), 4.72 (d, *J* = 6.5, 2H), 3.79 (s, 6H), 2.10 (s, 3H); ^{13}C NMR (125 MHz, $CDCl_3$): δ 170.8, 160.9, 138.2, 134.1, 123.7, 104.7, 100.4, 64.9, 55.4, 21.0; IR ν_{max}^{neat} cm^{-1}: 3002, 2940, 2839, 1738, 1592, 1458, 1427, 1347, 1299, 1240, 1205, 1153, 1064, 1025, 965, 682; HRMS (TOF AP$^+$) *m/z* for $C_{13}H_{17}O_4$ $(M + H)^+$: 237.1127; found: 237.1126.

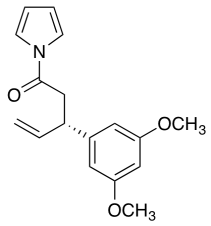

(3S)-(3,5-Dimethoxyphenyl)-1-(1*H*-pyrrol-1-yl)pent-4-en-1-one (130): General procedure C was followed employing 1.00 g (4.24 mmol) (*E*)-3-(3,5-dimethoxyphenyl)allyl acetate **131**, 1.00 g (5.48 mmol) 1-[1-(trimethylsilyloxy)vinyl]-1*H*-pyrrole **91b**, 82 mg (0.211 mmol) ligand **107**, 92 mg (0.211 mmol) [$CpRu(CH_3CN)_3PF_6$, 230 mg (0.633 mmol) $(4\text{-}FC_6H_4O)_3B$, 6.3 mL THF (0.67M). The reaction mixture was stirred for 16 h at which time it was dissolved onto SiO_2 and dried overnight in vacuo. The product was purified by column chromatography (SiO_2, 5%

EtOAc/Hexanes) to yield 1.04 g (86%) as a white crystalline solid. [α] +8.37 (*c* 0.023, $CHCl_3$); mp 72.9-74.3 °C; ^{1}H NMR (400 MHz, $CDCl_3$): δ 7.30 (b s, 2H), 6.41 (d, *J* = 2.4, 2H), 6.34 (apt t, *J* = 2.4, 1H), 6.28 (apt t, *J* = 2.4, 1H), 6.03 (ddd, *J* = 6.8, 10.8, 16.0, 1H), 5.13 (d, *J* = 1.2, 1H), 5.10 (apt dt, *J* = 1.2, 7.6, 1H), 4.03 (q, *J* = 6.8, 1H), 3.78 (s, 6H), 3.21 (ddd, *J* = 7.6, 16.0, 27.2, 1H); ^{13}C NMR (100 MHz, $CDCl_3$): δ 168.6, 161.0, 144.8, 139.5, 119.0, 115.5, 113.2, 105.8, 98.5, 55.3, 45.0, 40.1; IR ν_{max}^{neat} cm^{-1}: 3159, 3074, 2937, 2837, 1717, 1596, 1469, 1287, 1261, 1205, 1155, 1069, 923, 834, 744; HRMS (TOF MSES+) *m/z* for $C_{17}H_{20}NO_3$ $(M + H)^+$: 286.1443; found 286.1439.

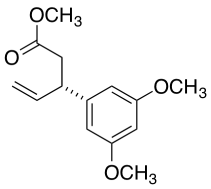

(S)-Methyl 3-(3,5-dimethoxyphenyl)pen-4-enonate (139): (3S)-(3,5-dimethoxyphenyl)-1-(1*H*-pyrrol-1-yl)pent-4-en-1-one **130**, 510 mg (1.78 mmol) in MeOH (0.1 M relative to the acyl pyrrole) at room temperature was added sodium methoxide (17.8 mmol as a 25% wt/wt solution in MeOH). The reaction was monitored by TLC for consumption of starting material. The reaction was quenched with and equivalent volume of H_2O and extracted with Et_2O (3x equivalent volume), dried over $MgSO_4$, and concentrated in vacuo. The product was purified by column chromatography (SiO_2 5% EtOAc/hexanes) to afford 385 mg (87%) as a colorless oil. [α] -3.90 (*c* 0.049 $CHCl_3$); ^{1}H NMR (400 MHz, $CDCl_3$): δ 6.37 (d, *J* = 2.4, 2H), 6.32 (t, *J* = 2.4, 1H), 5.95 (ddd, *J* = 7.2, 10.4, 17.2, 1H), 5.10 (apt dt, *J* = 1.2, 10.4, 1H), 5.06 (m, 1H), 3.87 (q, *J* = 7.2, 15.2, 1H), 3.77 (s, 6H), 3.64 (s, 3H), 2.71(dddd, *J* = 2.1, 15.6, 22.4, 23.6, 2H); ^{13}C NMR (100 MHz, $CDCl_3$): δ 172.5, 161.2, 145.1, 140.0, 115.2, 106.0, 105.8, 98.7, 55.5, 51.8, 45.9, 40.2; IR ν_{max}^{neat} cm^{-1}: 3081, 3001, 2953, 2838, 1737, 1596, 1461, 1431, 1357, 1205, 1067, 922, 835; HRMS (TOF MSES+) *m/z* for $C_{14}H_{19}O_4$ $(M + H)^+$: 251.1283; found 251.1285.

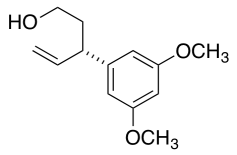

(S)-3-(3,5-Dimethoxyphenyl)pent-4-en-1-ol (139*): Compound **139** was derivatized to the corresponding alcohol **139*** for ee determination. General procedure: To a solution of **139** (308 mg, 1.22 mmol) in DCM (0.3 M relative to the ester) at -78°C was added to DiBAlH (3.05 mmol as a 1.0 M solution in DCM) drop-wise. The reaction was stirred at -78°C for 2 h and subsequently quenched with MeOH (3.1 mL) followed by saturated sodium potassium tartrate solution. The reaction mixture was allowed to warm to room temperature and stir for 16 h. The resulting clear solution was extracted with DCM (3x equivalent volume), dried over $MgSO_4$, and concentrated in vacuo. The product mixture was purified by column chromatography (5% EtOAc/Hexanes) to afford 231 mg (85%) as a colorless oil. Separating the stereoisomers of **139*** by GC {flow rate 2.0 mL/min, method: 120 °C for 10 min, ramp @ 0.1 °C/min to 160 °C hold for 15 min; T_r (min) = 136.8 (3R-(**139***)), 138.0 (3S-(**139***)), (ratio = 1:6.1)} provided an ee of 72%.: [α] +22.27 (*c* 0.043 $CHCl_3$); ^1H NMR (500 MHz, $CDCl_3$): δ 6.37(d, *J* = 2.0, 2H), 6.32 (dd, *J*= 2.0, 1H), 5.95 (ddd, *J* = 8.0, 10.5, 17.5, 1H), 5.10 (apt dt, *J* = 1.0, 17.0, 1H), 5.05 (d, *J* = 10, 1H), 3.78 (s, 6H), 3.63 (m, 2H), 3.40 (dd, *J* = 8.0, 15.0, 1H), 1.96 (m, 2H); ^{13}C NMR (100 MHz, $CDCl_3$): δ 160.9, 146.2, 141.4, 114.5, 105.7, 98.1, 61.0, 60.9, 55.3, 46.6, 37.8; IR ν_{max}^{neat} cm^{-1}: 3369, 3000, 2938, 2838, 1597, 1463, 1430, 1346, 1292, 1205, 1155, 1059, 995, 835, 717, 695; HRMS (ESI) *m/z* for $C_{13}H_{19}O_3$ $(M + H)^+$: 223.13287; found 223.13141.

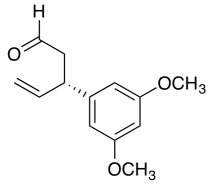

(S)-3-(3,5-Dimethoxyphenyl)pent-4-enal (129): (S)-methyl 3-(3,5-dimethoxyphenyl)pen-4-enonate **139**, 536 mg (2.14 mmol) in DCM (0.3 M relative to the ester) at -78°C was subjected to DiBAlH (3.21 mmol as a 1.0 M

solution in DCM) dropwise. The reaction was stirred at -78°C for 2 h and subsequently quenched with MeOH (3.2 mL) followed by saturated sodium potassium tartrate solution. The reaction mixture was allowed to warm to room temperature and stir for 16 h. The resulting clear solution was extracted with DCM (3x equivalent volume), dried over $MgSO_4$, and concentrated in vacuo. The product mixture was purified by column chromatography (5% EtOAc/hexanes) to afford 370 mg (71%) as a colorless oil. [α] -1.27 (*c* 0.078 $CHCl_3$); ^{1}H NMR (400 MHz, $CDCl_3$): δ 9.72 (t, *J* = 2.0, 1H), 6.37 (d, *J* = 2.4, 2H), 6.33 (t, *J* = 2.0, 2H), 5.96 (ddd, *J* = 6.8, 10.4, 17.2, 1H), 5.29 (s, 6H), 5.12 (apt dt, *J* = 1.2, 8.0, 1H), 5.08 (apt dt, *J* = 1.2, 14.4, 1H), 3.88 (q, *J* = 7.2, 14.4, 1H), 3.78 (s, 6H), 2.81 (m, 2H); ^{13}C NMR (100 MHz, $CDCl_3$): δ 201.2, 161.0, 144.6, 139.7, 115.2, 105.7, 98.4, 53.4, 48.3, 43.6; IR ν_{max}^{neat} cm^{-1}: 3080, 3001, 2938, 2838, 2756, 1721, 1595, 1459, 1429, 1347, 1292, 1204, 1152, 1062, 923, 835, 737, 697; HRMS (TOF MSES+) *m/z* for $C_{13}H_{17}O_3$ $(M + H)^+$: 222.1178; found 221.1183.

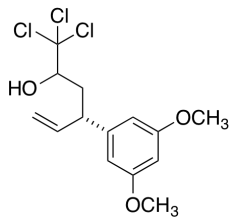

(4S)-1,1,1-trichloro-4-(3,5-dimethoxyphenyl)hex-5-en-2-ol (154): To a solution of (S)-3-(3,5-Dimethoxyphenyl)pent-4-enal (**129**, 1.40 g, 6.36 mmol) in DMF (8.5 mL) was added trichloroacetic acid (1.56 g, 9.54 mmol), followed by sodium trichloroacetate (1.77 g, 9.54 mmol). Vigorous evolution of CO_2 was observed and the reaction was allowed to stir overnight. The volume was doubled upon the addition of ether and the reaction was washed with 3x mL sat. $NaHCO_3$. The organic layer was dried over an. $MgSO_4$, concentrated in vacuo and columned in 5% EtOAc in hexanes to yield 1.1 g (51 %) of a colorless oil as a mix of diastereomers. ^{1}H NMR (500 MHz, $CDCl_3$): δ 6.42 – 6.40 (2H), 6.38 – 6.33 (1H), 6.04 – 5.88 (1H), 5.25 – 5.06 (2H), 4.15 (ddd, J = 15.3, 5.3, 2 Hz, 0.5H), 3.79 – 3.76 (6.5 H),3.63 – 3.60 (1H), 2.75 – 2.73 (1H), 2.47 – 2.38 (1H) ,2.08 – 1.97 (1H),

1.55 (s. 1H); ^{13}C NMR (125 MHz, $CDCl_3$): δ 161.3, 161.2, 146.4, 144.6, 141.6, 140.0, 116.7, 114.5, 106.3, 105.7, 104.4, 104.3, 98.8, 98.5. 81.1, 80.7, 55.5, 55.5, 46.6, 46.3, 37.4, 36.5;IR ν_{max}^{neat} cm^{-1}: 3458, 3001, 2938, 2828, 1597, 1462, 1430, 1346, 1293, 1205, 1155, 1094, 1063, 924, 809, 629. HRMS (ESI) *m/z* for $C_{13}H_{17}O_3$ $(M + H)^+$: 339.03160; found 339.03034.

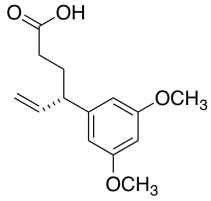

(S)-4-(3,5-Dimethoxyphenyl)hex-5-enoic acid (128): To a solution of **154** (975 mg, 2.87 mmol) in *tert*-butyl alcohol (0.1 M relative to the carbinol) at 30 °C was subjected to freshly powdered NaOH (9.4 mmol). After 10 minutes, $NaBH_4$ (4.5 mmol) was added to the slurry and the temperature increased to 55 ^oC. After 18 h the solvent was removed in vacuo and the slurry was dissolved in 15 mL Et_2O and 15 ml H_2O. The pH of the mixture was adjusted to 1 using 1 M HCl and extracted with 5 x 20 mL. dried with an. $MgSO_4$, and then concentrated by rotary evaporator. The crude material was purified by flash chromatography 1:4 EtOAc: hexanes to furnish 250 mg of the homologated acid as a colorless oil (35%). [α] +11.01(*c* 0.051 $CHCl_3$); ^1H NMR (500 MHz, $CDCl_3$) δ 10.18 (s, 1H), 6.35 (d, J = 2.5, 2H), 6.32 (t, J = 2.5, 1H), 5.91 (ddd, J = 7.5, 10.0, 17.0, 1H), 5.09 (apt dt, J = 1.0, 14.5, 1H), 5.07 (apt dt, J = 1.0, 7.5, 1H), 3.78 (s, 6H), 3.22 (q, J = 7.5, 2H), 2.33 (m, 2H), 2.03 (m, 2H); ^{13}C NMR (125 MHz, $CDCl_3$) 178.3, 160.9, 145.7, 140.8, 115.0, 105.7, 98.3 55.3, 49.2, 31.7, 29.8; IR ν_{max}^{neat} cm^{-1}: 3229, 2082, 3000, 2936, 2838, 1708, 1596, 1461, 1429, 1292, 1204, 1155, 1063, 920, 834; HRMS (ESI) *m/z* for $C_{14}H_{19}O_4$ $(M + H)^+$: 251.12779; found 251. 12683.

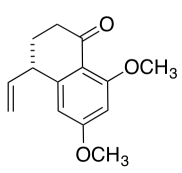

(S)-6,8-Dimethoxy-4-vinyl-3,4-dihydronaphthalen-1(2H)-one (127): To a solution of (S)-4-(3,5-dimethoxyphenyl)hex-5-enoic acid (**128**, 250 mg (1.0 mmol) in nitromethane (0.5 M relative to the acid) at room temperature was

added triflic anhydride (0.20 mL, 1.2 mmol). The reaction was complete after 60 min. The mixture was quenched with saturated $NaHCO_3$ solution (equivalent volume) and the organics were extracted with EtOAc (3x equivalent volume), dried over $MgSO_4$, and concentrated en vacuo. The crude product mixture was purified by column chromatography (25% EtOAc/Hexanes) to afford 175 mg (75%) of a pale yellow solid. [α] +59.34 (*c* 0.052 $CHCl_3$); mp 74.0-75.7 °C; ^{1}H NMR (500 MHz, $CDCl_3$) δ 6.38 (d, J = 2.0, 1H), 6.36 (d, J = 2.0, 1H), 5.93 (ddd, J = 7.5, 10.5, 17.5), 5.19 (d, J = 10, 1H), 5.02 (dd, J = 1.5, 17.0, 1H), 3.89 (s, 3H), 3.85 (s, 3H), 3.56 (dd, J = 5.5, 6.5, 1H) 2.61 (dddd, J = 5.0, 9.5, 14.5, 77.0, 2H), 2.18 (m, 1H), 1.98 (m, 1H); ^{13}C NMR (125 MHz, $CDCl_3$) δ 196.2, 164.2, 162.8, 150.1, 140.2, 117.2, 116.3, 105.3, 97.7, 56.2, 55.6, 44.8, 37.7, 28.6; IR ν_{max}^{neat} cm^{-1}: 3066, 3004, 2939, 2834, 1670, 1596, 1570, 1455, 1419, 1324, 1253, 1201, 1160; HRMS (ESI) *m/z* for $C_{14}H_{17}O_3$ $(M + H)^+$: 233.11722; found 233.11642.

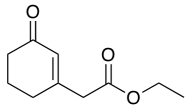

Ethyl 2-(3-oxocylohex-1-en-1-yl)acetate (175a): Characterization materials match the data provided in the following publication s: Liu, H.; Zhu, B; *Can. J. Chem.* **1991**, *69*, 2008-2013; Eidman, K. F.; MacDougall, B. S.; *J. Org. Chem.* **2006**, *71*, 9513-9516.

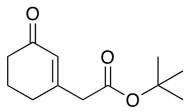

***tert*-Butyl 2-(3-oxocyclohex-1-en-1-yl)acetate (175b):** Pyridinium chlorochromate (4.61 g, 21.4 mmol) was added to a solution of *tert*-Butyl 2-(1-hydroxycyclohex-2-en-1-yl)acetate (1.81 g, 8.54 mmol) in DCM (0.2 M relative to the alcohol) and reacted for 5 h. The reaction mixture was diluted with Et_2O and the resultant solution was plugged through Florisil®. The column was washed with Et_2O (3x 50 mL) and the combined

organics were concentrated in vacuo. The crude reaction mixture was purified by column chromatography (SiO_2 10% EtOAc/hexanes) to afford the product 1.270 g (71%) as a yellow oil: ^{1}H NMR (500 MHz, $CDCl_3$) δ 5.93 (s, 1H), 3.14 (s, 2H), 2.39 (t, *J* = 7, 4H), 2.02 (dd, *J* = 6.5, 13.0, 2H), 1.49 (s, 9H); ^{13}C NMR (125 MHz, $CDCl_3$) δ 199.7, 168.8, 158.1, 128.8, 81.9, 45.0, 37.4, 29.9, 28.2, 22.9; IR ν_{max}^{neat} cm^{-1}: 2978, 2930, 2865, 1730, 1674, 1456, 1370, 1153, 973.12, 888; HRMS (TOF AP+) *m/z* for $C_{12}H_{18}O_3$ $(M + H)^+$: 211.1334; found 211.1335.

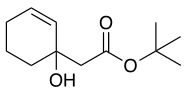

tert*-Butyl 2-(1-hydroxycyclohex-2-en-1-yl)acetate (175b*):** The synthesis of **175b** required to synthesis of novel tertiary alcohol **175b. The material was prepared according to the following procedures: Liu, H.; Zhu, B; *Can. J. Chem.* **1991**, *69*, 2008-2013; Eidman, K. F.; MacDougall, B. S.; *J. Org. Chem.* **2006**, *71*, 9513-9516. Eidman, K. F.; MacDougall, B. S.; *J. Org. Chem.* **2006**, *71*, 9513-9516. To a stirred solution of lithium hexamethyldisilazide (10.8 mmol) in THF (0.2 M relative to the tert-butyl acetate) at -78 °C was added *tert*-butyl acetate (2.80 mL, 20.8 mmol) and the reaction was stirred for 2 h. To this solution was added anhydrous $CeCl_3$ (5.13 g, 20.8 mmol) as a solid and the resulting suspension was stirred for an additional 2 h at -78 °C. Cyclohexenone (1.07 mL, 10.4 mmol) was then added to the reaction and stirring continued at -78 °C for 2 h. The reaction was quenched with 10% acetic acid solution (250 mL) and extracted with EtOAc (3x equivalent volume). The resultant organics were sequentially washed with saturated sodium bicarbonate solution (equivalent volume) and brine (equivalent volume), dried over $MgSO_4$, and concentrated in vacuo. The crude reaction mixture was purified by column chromatography (SiO_2, 10% EtOAc/Hex) to afford the product (2.201 g, quantitative yield) as a yellow oil.[80] ^{1}H NMR (500 MHz, $CDCl_3$) δ 5.81 (apt dt, *J* = 3.5, 10.0, 1H), 5.65 (d, *J* = 10.5, 1H), 3.82 (b s, 1H), 2.46 (dd, *J* = 15.0, 26.5, 2H), 2.04 (m,

1H), 1.94 (m, 1H), 1.81 (m, 2H), 1.61 (m, 2H), 1.48 (s, 9H); ^{13}C NMR (125 MHz, $CDCl_3$) δ 172.1, 131.1, 130.1, 81.6, 68.3, 46.4, 35.7, 28.1, 25.0, 18.9; IR ν_{max}^{neat} cm^{-1}: 3498, 2978, 2936, 2872, 1710, 1456, 1393, 1369, 1255, 1151, 1070, 998, 953, 735; HRMS (ESI) *m/z* for $C_{12}H_{20}O_3Na$ $(M + Na)^+$: 235.13047; found 235.13066.

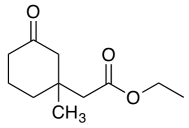

Ethyl 2-(1-methyl-3-oxocyclohexyl)acetate (166a): In a glovebox, a flask was charged with $(CuOTf)_2$•PhH (11.1 mg, 0.022 mmol) and (3,5-dioxa-4-phospha-cyclohepta[2,1-a;3,4-a']dinaphthalene-4-yl)bis(1-phenylmethyl]amine (**180**, 45.0 mg, 0.088 mmol). The flask was pumped out of the inert atmosphere and Et_2O was added to the solids and the mixture was stirred at room temperature for 30 min, resulting in a cloudy suspension. To this was added ethyl 2-(3-oxocyclohex-1-en-1-yl)acetate (200 mg, 1.10 mmol) and the reaction was cooled to -10 °C. After 30 min, Me_3Al (1.10 mL of a 2.0 M solution in heptanes, 2.20 mmol) was added and the resultant yellow solution was allowed to stir for 16h. The reaction was carefully quenched with MeOH (2 mL) and then saturated ammonium chloride solution (equivalent volume) and extracted with Et_2O (3x equivalent volume), dried over $MgSO_4$, and concentrated in vacuo. The reaction mixture was purified by column chromatography (SiO_2 10% EtOAc/hexanes) to yield the product (177 mg, 81%) as a colorless oil. ^{1}H NMR (500 MHz, $CDCl_3$) δ 4.13 (q, *J* = 7.0, 2H), 2.42 (d, *J* = 13.5, 1H), 2.31 (m, 2H), 2.27 (d, *J* = 3.5, 2H), 2.20 (apt dt, *J* = 2.0, 14.0, 1H), 1.91 (m, 2H), 1.81 (m 1H), 1.66 (m, 1H), 1.26 (t, *J* = 7.0, 3H), 1.06 (s, 3H); ^{13}C NMR (125 MHz, $CDCl_3$) δ 211.0, 171.1, 60.3, 53.3, 46.1, 40.8, 38.2, 35.7, 25.2, 21.9, 14.3; IR ν_{max}^{neat} cm^{-1}: 2961, 2931, 2880, 1730, 1710, 1458, 1370, 1228, 1180, 1146, 1034; HRMS (ESI) *m/z* for $C_{11}H_{19}O_3$ $(M + H)^+$: 199.13287; found 199.13344

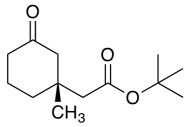

(R)-*tert*-Butyl 2-(1-methyl-3-oxocylohexyl)acetate (166b): In a glovebox, a flask was charged with $(CuOTf)_2$•PhH (4.8 mg, 0.01 mmol) and (S)-(+)-(3,5-dioxa-4-phospha-cyclohepta[2,1-a;3,4-a']dinaphthalene-4-yl)bis[(1R)-1-phenylethyl]amine (**30**, 20.7 mg, 0.04 mmol). The flask was pumped out of the inert atmosphere and Et_2O (1 mL, 0.4 M relative to acetate) was added to the solids and the mixture was stirred at room temperature for 30 min, resulting in a cloudy suspension. To this was added *tert*-butyl 2-(3-oxocyclohex-1-en-1-yl)acetate (100 mg, 0.48 mmol) and the reaction was cooled to -10 °C. After 30 min, Me_3Al (0.48 mL of a 2.0 M solution in heptanes, 0.96 mmol) was added and the resultant yellow solution was allowed to stir for 16h. The reaction was carefully quenched with MeOH (2 mL) and then saturated ammonium chloride solution (equivalent volume) and extracted with Et_2O (3x equivalent volume), dried over $MgSO_4$, and concentrated in vacuo. The reaction mixture was purified by column chromatography (SiO_2 10% EtOAc/hexanes) to yield the product (73.5 mg, 68%) as a colorless oil. Separating the stereoisomers of **166b** by GC {flow rate 0.6 mL/min, method: 105 °C for 10 min, ramp @ 0.7 °C/min to 160 °C hold for 5 min; T_r (min) = 62.095 (R-(**166b**)), 63.006 (S-(**166b**)), (ratio = 4.56:1)} provided an ee of 64%. ^{1}H NMR (500 MHz, $CDCl_3$) δ 2.40 (d, *J* = 13.5, 1H), 2.29 (m, 2H), 2.19 (m, 1H), 2.18 (dd, *J* = 14.0, 20.0, 2H), 1.87 (m, 3H), 1.65 (m, 1H), 1.45 (s, 9H), 1.06 (s, 3H); ^{13}C NMR (125 MHz, $CDCl_3$) δ 211.2, 170.6, 80.6, 53.4, 47.2, 40.8, 38.3, 35.7, 28.1, 25.3, 21.9; IR ν_{max}^{neat} cm^{-1}: 2967, 2942, 2876, 1716, 1457, 1367, 1333, 1252, 1142, 1109, 958, 842; HRMS (ESI) *m/z* for $C_{13}H_{23}O_3$ $(M + H)^+$: 227.16417; found 227.16442.

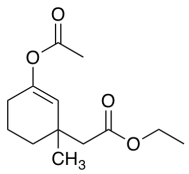

Ethyl-2-(3-acetoxy-1-methylcyclohex-2-en-1-yl)acetate (165a): In a glovebox, a flask was charged with $(CuOTf)_2$•PhH (80.5 mg, 0.16 mmol) and

(3,5-dioxa-4-phospha-cyclohepta[2,1-a;3,4-a']dinaphthalene-4-yl)bis(1-phenylmethyl]amine (**180**, 321 mg, 0.63 mmol). The flask was removed from the glovebox, Et_2O was added to the solids and the mixture was stirred at room temperature for 30 min, resulting in a cloudy suspension. To this was added ethyl 2-(3-oxocyclohex-1-en-1-yl)acetate (1.430 g, 7.84 mmol) and the reaction was cooled to -10 °C. After 30 min, Me_3Al (7.84 mL of a 2.0 M solution in heptanes, 15.68 mmol) was added and the resultant yellow solution was allowed to stir for 16h. Acetic anhydride (3.0 mL, 31.4 mmol) was added and the reaction was warmed to room temperature and stirred for 72 h. The reaction mixture was quenched by carefully pouring over and equal volume of saturated ammonium chloride and ice solution. The organics were extracted with Et_2O (3x equal volume), dried over $MgSO_4$, and concentrated in vacuo. The crude reaction mixture was purified by column chromatography (SiO_2 5% EtOAc/Hexanes) to afford 1.282 g (68%) of the product as a yellow oil. ^{1}H NMR (500 MHz, $CDCl_3$) δ 5.31 (s, 1H), 4.12 (q, J = 7.0, 2H), 2.32 (s, 2H), 2.12 (m, 2H), 2.10 (s, 3H), 1.76 (m 2H), 1.66 (m, 1H), 1.47 (m, 1H), 1.25 (t, J = 7.0, 2H), 1.15 (s, 3H); ^{13}C NMR (125 MHz, $CDCl_3$) δ 171.5, 169.1, 148.1, 121.8, 60.1, 46.6, 34.5, 27.1, 26.7, 21.1, 19.2, 14.3, 14.1; IR ν_{max}^{neat} cm^{-1}: 2939, 2884, 1756, 1732, 1456, 1366, 1218, 1135, 1115, 1053, 1088, 1035; HRMS (TOF AP+) *m/z* for $C_{13}H_{21}O_4$ $(M + H)^+$: 241.1440; found 241.1434.

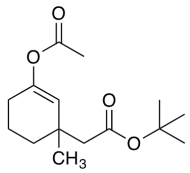

***tert*-Butyl 2-(3-acetoxy-1-methylcyclohex-2-en-1-yl)acetate (165a'):** In a glovebox, a flask was charged with $(CuOTf)_2$•PhH (10.1 mg, 0.02 mmol) and (3,5-dioxa-4-phospha-cyclohepta[2,1-a;3,4-a']dinaphthalene-4-yl)bis(1-phenylmethyl]amine (**182**, 38.9 mg, 0.08 mmol). The flask was removed from the glove box, Et_2O was added to the solids, and the mixture was stirred at room temperature for 30 min,

resulting in a cloudy suspension. To this was added ethyl 2-(3-oxocyclohex-1-en-1-yl)acetate (200 mg, 0.95 mmol) and the reaction was cooled to -10 °C. After 30 min, Me_3Al (0.95 mL of a 2.0 M solution in heptanes, 1.90 mmol) was added and the resultant yellow solution was allowed to stir for 16 h. Acetic anhydride (0.36 mL, 3.80 mmol) was added and the reaction was warmed to room temperature and stirred for 72 h. The reaction mixture was quenched by carefully pouring over and equal volume of saturated ammonium chloride and ice solution. The organics were extracted with Et_2O (3x equal volume), dried over $MgSO_4$, and concentrated in vacuo. The crude reaction mixture was purified by column chromatography (SiO_2 5% EtOAc/hexanes) to afford 165 mg (65%) of the product as a pale yellow oil. ^{1}H NMR (500 MHz, $CDCl_3$) δ 5.30 (s, 1H), 2.22 (s, 2H), 2.11 (m, 1H), 2.09 (s, 3H), 1.75 (apt dq, J = 6.5, 12.0, 2H), 1.66 (m, 1H), 1.56 (d, J = 1.0, 1H), 1.47 (m, 1H), 1.44 (s, 9H), 1.14 (s, 2H); ^{13}C NMR (125 MHz, $CDCl_3$) δ 171.0, 169.2, 147.8, 122.1, 80.3, 47.8, 34.5, 34.5 28.1, 27.1, 26.7, 21.1, 19.2; IR ν_{max}^{neat} cm^{-1}: 2969, 2937, 2872, 1757, 1726, 1457, 1367, 1219, 1135, 1087, 1053, 1010, 961, 903, 841, 760; HRMS (ESI) *m/z* for $C_{15}H_{24}O_4Na$ $(M + Na)^+$: 291.15668; found 291.15656.

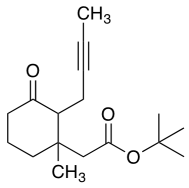

***tert*-Butyl 2-(2-(but-2-yn-1-yl)-1-methyl-3-oxocyclohexyl)acetate (186b):** To a solution of *tert*-butyl 2-(3-acetoxy-1-methylcyclohex-2-en-1-yl)acetate **165a'**, 300 mg (1.12 mmol) in THF (2.0 M relative to the vinyl acetate) at -78 °C was added MeLi•LiBr (0.82 mL of a 1.5 M solution in THF, 1.23 mmol). After 30 min, 1-iodobut-2-yne (221.4 mg, 1.23 mmol) was added to the reaction and then protected from light by with aluminum foil. The reaction was then allowed to warm to room temperature and stir for 16 h. The reaction was quenched with saturated ammonium chloride (equivalent volume) and the organics extracted with EtOAc (3x equivalent volume), dried over $MgSO_4$, and concentrated in

vacuo. The crude reaction mixture was purified by column chromatography (SiO_2, 5% EtOAc/Hexanes) to yield the product, 243 mg (78%) as a yellow oil. Separating the stereoisomers of **186b** by GC {flow rate 0.6 mL/min, method: 105 °C for 10 min, ramp @ 0.7 °C/min to 200 °C hold for 5 min; T_r (min) =102.717, 103.192, 109.051, 109.640 (ratio = 1.0:1.0:1.4:1.4)}; ^{1}H NMR (500 MHz, $CDCl_3$) δ 2.53 (apt dtd, *J* = 2.5, 5.0, 16.5, 1H), 2.48 (2, *J* = 13.0, 1H), 2.38 (m, 1H), 2.28 (m, 1H), 2.24 (d, *J* = 2.5, 1H), 2.22 (s, 2H), 2.15 (m, 1H), 1.85 (apt dt, J = 4.0, 13.5, 1H), 1.77 (t, J = 2.5, 3H), 1.73 (m, 1H), 1.59 (m, 1H), 1.46 (s, 9H), 0.97 (s, 3H); ^{13}C NMR (125 MHz, $CDCl_3$) δ 210.2, 170.5, 80.7, 52.8, 49.5, 49.0, 38.9, 35.9, 29.7, 28.2, 23.4, 18.8, 3.47; IR ν_{max}^{neat} cm^{-1}: 2965, 2925, 2853, 2360, 1716, 1456, 1368, 1255, 1152; HRMS (ESI) *m/z* for $C_{17}H_{26}O_3Na$ $(M + Na)^+$: 301.17742; found 301.17756.

BIBLIOGRAPHY

1. Tsuji, J.; Takshashi, H.; Morikawa, M. Organic Syntheses by means of Nobel Metal Compounds XVII. Reaction of π-Allylpalladium Chloride with Nucleophiles. *Tetrahedron Lett*. **1965**, *49*, 4387-4388.

2. Atkins, K. E.; Walker, W. E.; Manyik, R. M. Palladium Catalyzed Transfer of Allylic Groups. *Tetrahedron Lett*. **1970**, *43*, 3821-3824.

3. Hata, G.; Takahashi, K.; Miyake, A. Palladium-catalyzed Exchange of Allylic Groups of Ethers and Esters with Active-hydrogen Compounds. *J. Chem. Soc. Chem. Comm*. **1970**, 1392-1393.

4. Trost, B. M.; Dietsche, T. J. New Synthetic Reactions. Asymmetric Induction in Allylic Alkylations. *J. Am. Chem. Soc.* **1973**, *95*, 8200-8201.

5. Trost, B. M. Pd Asymmetric Allylic Alkylations (AAA). A Powerful Synthetic Tool. *Chem. Pharm. Bull.* **2002**, *50*, 1-14.

6. Trost, B. M. Asymmetric Allylic Alkylation, an Enabling Methodology. *J. Org. Chem*. **2004**, *69*, 5813-5837.

7. Lu, M.; Ma, S. Metal-Catalyzed Enantioselective Allylation in Asymmetric Synthesis. *Angew. Chem. Int. Ed.* **2008**, *47*, 258-297.

8. Trost, B. M.; Crawley, M. L. Asymmetric Transition-Metal-Catalyzed Allylic Alkylations: Applications in Total Synthesis. *Chem. Rev.* **2003**, *103*, 2921-2943.

9. Engelin, C. J.; Fristrup, P. Palladium Catalyzed Allylic C-H Alkylation: A Mechanistic Perspective. *Molecules* **2011**, *16*, 951-969.

10. Trost, B. M.; Weber, L.; Strege, P. E.; Fullerton, T. J.; Dietsche, T. J. New Synthetic Reactions. Allylic Alkylation. *J. Am. Chem. Soc.* **1978**, *100*, 3416-3426. See also: Trost. B. M.; Fullerton, T. J. *J. Am. Chem. Soc.* **1973**, *95*, 292-294.

11. van Haaren, R. J.; Goubitz, K.; Fraanje, J.; van Strijdonck, G. P. F.; Oevering, H.; Coussens, B.; Reek, J. N. H.; Kamer, P. C. J.; van Leeuwen, Piet W. N. M. An X-ray Study of the Effect of the Bite Angle of Chelating Ligands on the Geometry of the Palladium(allyl)

Complexes: Implications for the Regioselectivity in the Allylic Alkylation. *Inorg. Chem*. **2001**, *40*, 3363-3372.

12. Trost, B. M. Pd- and Mo-Catalyzed Asymmetric Allylic Alkylation. *Org. Process Res. Dev.* **2012**, *16*, 185-194.

13. Belda, O.; Moberg, C. Molybdenum-Catalyzed Asymmetric Allylic Alkylations. *Acc. Chem. Res.* **2004**, *37*, 159-167.

14. Yorimitsu, H.; Oshima, K. Recent Progress in Asymmetric Allylic Substitutions Catalyzed by Chiral Copper Complexes. *Angew. Chem. Int. Ed.* **2005**, *44*, 4435-4439.

15. Tosatti, P.; Nelson, A.; Marsden, S. P. Recent Advances and Applications in Iridium-catalyzed Asymmetric Allylic Substitution. *Org. Biomol. Chem.* **2012**, *10*, 3147-3160.

16. Kazmaier, U.; Stolz, D. Regio- and Stereoselective Rhodium-Catalyzed Allylic Alkylations of Chelated Enolates. *Angew. Chem. Int. Ed.* **2006**, *45*, 3072-3075.

17. Bruneau, C.; Renaud, J.-L.; Bemerseman, B. Pentamethylcyclopentadienyl-Ruthenium Catalysts for Regio- and Enantioselective Allylation of Nucleophiles. *Chem. Eur. J.* **2006**, *12*, 5178-5187.

18. Bruneau, C.; Achard, M. Allylic Ruthenium(IV) Complexes in Catalysis. *Coordin. Chem. Rev.* **2012**, *256*, 525-536.

19. Bruneau, C.; Renaud, J.-L.; Demerseman, B. Ruthenium Catalysis for Selective Nucleophilic Allylic Substitution. *Pure Appl. Chem.* **2008**, *80*, 861-871.

20. Kanbayashi, N.; Hosoda, K.; Kato, M.; Takii, K.; Okamura, T.; Onitsuka, K. Enantio- and Diastereoselective Asymmetric Allylic Alkylation Catalyzed by a Planar-chiral Cyclopentadienyl Ruthenium Complex. *Chem. Commun.* **2015**, *51*, 10895-10898.

21. Trost, B. M.; Schroeder, G. M. Palladium-Catalyzed Asymmetric Alkylation of Ketone Enolates. *J. Am. Chem. Soc.* **1999**, *121*, 6759-6760.

22. Chen, M.; Hartwig, J. F. Iridium-Catalyzed Enantioselective Allylic Substitution of Unstablilized Enolates Derived from α,β-Unsaturated Ketones. *Angew. Chem. Int. Ed.* **2014**. *53*, 8691-8695.

23. Evans, P. A.; Oliver, S.; Chae, J. Rhodium-Catalyzed Allylic Substitution with an Acyl Anion Equivalent: Stereospecific Construction of Acyclic Quaternary Carbon Stereogenic Centers. *J. Am. Chem. Soc.* **2012**, *134*, 19314-19317.

24. Geherty, M. E.; Dura, R. D.; Nelson, S. G. Catalytic Asymmetric Claisen Rearrangement of Unactivated Allyl Vinyl Ethers. *J. Am. Chem. Soc.* **2010**, *132*, 11875-11877.

25. Geherty, M. E. Catalytic Asymmetric Claisen Rearrangements. The Development of Ru(II)-catalyzed Formal [3,3] Sigmatropic Rearrangements and Related Enolate Allylic Alkylations. Ph. D. Dissertation, University of Pittsburgh, Pittsburgh, PA, 2012.

26. Hermatschweiler, R.; Fernández, I.; Pregosin, P. S.; Watson, E. J.; Albinati, A.; Rizzato, S.; Veiros, L. F.; Calhorda, M. J. X-ray, 13C NMR, and DFT Studies of a Ruthenium(IV) Allyl Complex. Explanation for the Observed Control of Regioselectivity in Allylic Alkylation Chemistry. *Organometallics* **2005**, *24*, 1809-1812.

27. Zaitsev, A. B.; Gruber, S. Plüss, P. A.; Pregosin, P. S.; Veiros, L. F.; Wörle, M. Fast and Highly Regioselective Allylation of Indole and Pyrrole Compounds by Allyl Alcohols Using Ru-Sulfonate Catalysts. *J. Am. Chem. Soc.* **2008**, *130*, 11604-11605.

28. Kawatsura, M.; Ata, F.; Wada, S.; Hayase, S.; Uno, H.; Itoh, T. Ruthenium-catalyzed Linear-Selective Allylic Alkylation of Allyl Acetates. *Chem. Commun.* **2007**, 298-300. See also: Kawatsura, M.; Ata, F.; Kirakawa, T.; Hayase, S.; Itoh, T. Ruthenium-catalyzed Linear Selective Allylic Aminations of Monosubstituted Allyl Acetates. *Tetrahedron Lett.* **2008**, *49*, 4873-4875.

29. Trost, B. M.; Fraisse, P. L.; Ball, Z. T. A Stereospecific Ruthenium-catalyzed Allylic Alkylation. *Angew. Chem. Int. Ed.* **2002**, *41*, 1059-1061.

30. Linder, D.; Buron, F.; Constant, S.; Lacour, J. Enantioselective CpRu-Catalyzed Carroll Rearrangement – Ligand and Metal Source Importance. *Eur. J. Chem.* **2008**, 5778-5785. See also: Constant, S.; Tortoioli, S.; Müller, J.; Lacour, J. An Enantioselective CpRu-Catalyzed Carroll Rearrangement. *Angew. Chem. Int. Ed.* **2007**, *46*, 2082-2085; Burger, E. C.; Tunge, J. A. Ruthenium-Catalyzed Decarboxylative Allylation of Nonstabilized Ketone Enolates. *Org. Lett*. **2004**, *6*, 2603-2605.

31. Trost, B. M.; Miller, J. R.; Hoffman, Jr., C. M. A Highly Enantio- and Diastereoselective Molybdenum-Catalyzed Asymmetric Allylic Alkylation of Cyanoesters. *J. Am. Chem. Soc.* **2011**, *133*, 8165-8167.

32. Liu, W.-B.; Reeves, C. M.; Stoltz, B. M. Enantio- Diastereo- and Regioselective Iridium-Catalyzed Asymmetric Allylic Alkylation of Acyclic β-Ketoesters. *J. Am. Chem. Soc.* **2013**, *135*, 17298-17301.

33. Liu, W.-B.; Reeves, C. M.; Virgil, S. C.; Stoltz, B. M. Construction of Vicinal Tertiary and All-Carbon Quaternary Stereocenters via Ir-Catalyzed Regio-, Diastereo-, and Enantioselective Allylic Alkylation and Application in Sequential Pd Catalysis. *J. Am. Chem. Soc.* **2013**, *135*, 10626-10629.

34. Krautwald, S.; Sarlah, D.; Schaforth, M.; Carreira, E. M. Enantio- and Diastereodivergent Dual Catalysis: α-Allylation of Branched Aldehydes. *Science* **2013**, *340*, 1065-1068.

35. Krautwald, S.; Schaforth, M.; Sarlah, D.; Carreira, E. M. Stereodivergent α-Allylation of Linear Aldehydes with Dual Iridium and Amine Catalysis. *J. Am. Chem. Soc.* **2014**, *136,* 3020-2023.

36. Chandra, B.; Fu, D.; Nelson, S. G. Catalytic Asymmetric Synthesis of Complex Propionates: Lewis Base Catalyzed Aldol Equivalents in the Synthesis of Erthronolide B. *Angew. Chem. Int. Ed.* **2010**, *49*, 2591-2594.

37. Evans, D. A.; Johnson, D. S. Catalytic Enantioselective Amination of Enolsilanes Using C2-Symmetric Copper(II) Complexes as Chiral Lewis Acids. *Org. Lett.* **1999**, *1*, 595-598.

38. Goldys, A. M.; McErlean, C. S. P. Acyl Pyrroles: More than Amides. *Eur. J. Org. Chem.* **2012**, *134*, 1877-1888.

39. Graening, T.; Hartwig, J. F. Iridium-Catalyzed Regio- and Enantioselective Allylation of Ketone Enolates. *J. Am. Chem. Soc.* **2005**, *127*, 17192-17193.

40. Mao, B.; Ji, Y.; Fañanás-Mastral, M.; Caroli, G.; Meetsma, A.; Feringa, B. L. Highly Enantioselective Synthesis of 3-Substituted γ-Butenolides by Palladium-Catalyzed Kinetic Resolution of Unsymmetrical Allyl Acetates. *Angew. Chem. Int. Ed.* **2012**, *51*, 3168-3173.

41. Hou, D.; Reibenspies, J. H.; Burgess, K. New, Optically Active Phosphine Oxazoline (JM-Phos) Ligands: Syntheses and Application in Allylation Reactions. *J. Org. Chem.* **2001**, *66*, 206-215.

42. Agenet, N.; Amatore, C.; Gamez, S.; Gerardin, H.; Jutand, A.; Meyer, G.; Orthwein, C. Effect of the Leaving Group and the Allylic Structure on the Kinetics and Thermodynamics of the Reaction of Allylic Carboxylates with Palladium(0) Complexes. *ARKIVOC* **2002**, *5*, 92-101.

43. Bastero, A.; Claver, C.; Ruiz, A.; Castillón, Daura, E.; Bo, C.; Zangrando, E. Insights into CO/styrene Copolymerization by Using Pd(II) Catalysts Containing Modular Pyridine-imidazoline Ligands. *Chem. Eur. J.* **2004**, *10*, 3747-3760.

44. Bastero, A.; Bella, A. F.; Fernández, F.; Jansat, S.; Claver, C.; Gómez, M.; Muller, G.; Ruiz, A.; Font-Bardía, M.; Solans, X. First Allylpalladium Systems Containing Chiral Imidazolylpyridine Ligands – Structural Studies and Catalytic Behavior. *Eur. J. Inorg. Chem.* **2007**, 132-139.

45. Fujioka, H.; Murai, K.; Ohba, Y.; Hiramatsu, A.; Kita, Y. A Mild and Efficient One-pot Synthesis of 2-Dihydroimidazolines from Aldehydes. *Tetrahedron Lett.* **2005**, *46*, 2197-2199.

46. Fujioka, H.; Murai, K. Kubo, O.; Ohba, Y.; Kita, Y. One-pot Synthesis of Imidazolines from Aldehydes: Detailed Study about Solvents and Substrates. *Tetrahedron* **2007**, *63*, 638-643.

47. Jencks, W. P.; Regenstein, J. Ionization Constants of Acids and Bases. In *Handbook of Biochemistry and Molecular Biology*; Lundblad, R. L.; Macdonald, F., Eds.; CRC Press; pp. 305-351. Accessed via: http://www.sas.upenn.edu/~marisa/documents/pkatables.pdf

48. Sundberg, R. J.; Jiang, S. Improved Procedures for Preparation of 4-Hydroxy- and 4-Methoxy-2-aminopyridines. *Org. Prep. Proced. Int.* **1997**, *29*, 117-122.

49. Mono-substitued ethylenediamines were synthesized using procedures found in the following: a) Campbell, C. D.; Concellon, C.; Smith, A. D. Catalytic Enantioselective Steglich Rearrangements Using Chiral *N*-Heterocyclic Carbenes. *Tetrahedron Asymmetry* **2011**, *22*, 797-811. b) Liu, Z.; Hu, J.; Sun, J.; He, G.; Li, Y.; Zhange, G. Preparation of Thermoresponsive Polymers Bearing Amino Acid Diamide Derivatives via RAFT Polymerization. *J. Polym. Sci. A1* **2010**, *48*, 3573-3586. c) Malkov, A. V.; Stewart-Liddon, A. J. P.; McGeoch, G. D.; Ramierz-López, P.; Kocovsky, P. Catalyst Development for Organocatalytic Hydrosilylation of Aromatic Ketones and Ketimines. *Org. Biomol. Chem.* **2012**, *10*, 4864-4877.

50. Anslyn, E. V.; Dougherty, D. A.; *Modern Physical Organic Chemistry*; University Science Books: Sausalito, CA, 2006; p 104.

51. Kim, H.; Nguyen, Y.; Yen, C. P.; Chagal, L.; Lough, A. J.; Kim, B. M.; Chin, J. Stereospecific Synthesis of C2 Symmetric Diamines from the Mother Diamine by Resonance-Assisted Hydrogen-Bond Directed Diaza-Cope Rearrangement. *J. Am. Chem. Soc.* **2008**, *130*, 12184-12191. See also: Kim, H.; Staikova, M.; Lough, A. J.; Chin, J. Stereospecific Synthesis of Alkyl-Substituted Vicinal Diamines from the Mother Diamine: Overcoming the "Intrinsic Barrier" to the Diaza-Cope Rearrangement Reaction. *Org. Lett.* **2009**, *11*, 157-160.

52. a) Mbaye, M, D.; Demerseman, B.; Renaud, J.-L.; Toupet, L.; Bruneau, C. [Cp*(η^2-bipy)(MeCN)RuII][PF_6] Catalysts for Regioselective Allylic Substitution and Characterization of Dicationic [Cp*(η^2-bipy)(η^3-allyl)RuIV][PF_6]$_2$ Intermediates. *Angew. Chem. Int. Ed.* **2003**, *42*, 5066-5068. b) Zhang, H.-J.; Demerseman, B.; Toupet, L.; Xi, Z.; Bruneau, C. Novel [Ruthenium(Substituted-tetramethylcyclopentadiene)(2-Quinolinecarboxylato)(allyl)] Hexafluorophosphate Complexes as Efficient Catalysts for Highly Regioselective Nucleophilic Substitution of Aliphatic Allylic Substrates. *Adv. Synth. Catal.* **2008**, *350*, 1601-1609.

53. Fujisawa, H.; Mukaiyama, T. A Catalytic Aldol Reaction Between Ketene Silyl Acetals and Aldehydes Promoted by Lithium Amide Under Non-acidic Conditions. *Chem. Lett*. **2002**, *2*, 182-183.

54. Evans, P. A.; Nelson, J. D. Conservation of Absolute Configuration in the Acyclic Rhodium-Catalyzed Allylic Alkylation Reaction: Evidence for an Enyl(σ + π) Organorhodium Intermediate. *J. Am. Chem. Soc.* **1998**, *120*, 5581-5582.

55. Nam, S.-J.; Kauffman, C. A.; Paul, L. A.; Jensen, P. R.; Fenical, W. Actinoranone, a Cyctotoxic Meroterpenoid of Unprecedented Structure from a Marine Adapted Streptomyces sp. *Org. Lett*. **2013**, *15*, 5400-5403.

56. a) American Cancer Society: Colorectal Cancer. Colorectal Cancer. http://www.cancer.org/cancer/colonandrectumcancer/detailedguide/colorectal-cancer-

key-statistics. (accessed Aug 28, 2015). b) World Health Organization: Cancer. http://www.who.int/mediacentre/factsheets/fs297/en/. (accessed Sep 18, 2015).

57. a) Vishchuk, O. S.; Ermakova, S. P.; Zvyagintseva, T. N. The Effect of Sulfated (1→3)-α-Fucan from Brown Alga Saccharina Cichorioides Miyabe on Resveratrol-induced Apoptosis in Colon Carcinoma Cells. *Mar. Drugs* **2013**, *11*, 194-212. b) Lee, D. E.; Lee, K. W.; Jung, S. K.; Lee, E. J.; Hwang, J. A.; Lim, T.-G.; Kim, B. Y.; Bode, A. M.; Lee, H. J.; Dong, Z. 6, 7, 4'- Trihydroxyisoflavone Inhibits HCT-116 Human Colon Cancer Cell Proliferation by Targeting CDK1 and CDK2. *Carcinogenesis*, **2011**, *32*, 629-635.

58. a) Chuang, C.-H.; Cheng, T.-C.; Leu, Y.-L.; Chuang, K.-H.; Tzou, S.-C.; Chen, C.-S. Discovery of Akt Kinase Inhibitors Through Structure-based Virtual Screening and Their Evaluation as Potential Anticancer Agents. *Int. J. Mol. Sci*. **2015**, *16*, 3202-3212. b) Sun, Q.; Weber, C. R.; Sohail, A.; Bernardo, M. M.; Toth, M.; Zhao, H.; Turner, J. R.; Fridman, R. MMP25 (MT6-MMP) Is Highly Expressed in Human Colon Cancer, Promotes Tumor Growth, and Exhibits Unique Biochemical Properties. *J. Biol. Chem.* **2007**, *282*, 21998-22010. c) Coumar, M. S.; Chu, C.-Y.; Lin, C.-W.; Shiao, H.-Y.; Ho, Y.-L.; Reddy, R.; Lin W.-H.; Chen, C.-H.; Peng, Y-H.; Leou, J.-S.; Lien, T.-W.; Huang, C.-T.; Fang, M.-Y.; Wu, S.-H.; Wu, J.-S.; Chittimalla, S. K.; Song, J.-S.; Hsu, J. T.-A.; Wu, S.-Y.; Liao, C.-C.; Chao, Y.-S.; Hsiech, H.-P. Fast-Forwarding Hit to Lead: Aurora and Epidermal Growth Factor Receptor Kinase Inhibitor Lead Identification. *J. Med. Chem.* **2010**, *53*, 4980-4988.

59. Levine, S. G. A New Aldehyde Synthesis. *J. Am. Chem. Soc.* **1958**, *80*, 6150-6151.

60. Van Schaik, T. A.; Henzen, A. V.; van der Gen, A. A Horner-Wittig Solution to the Synthesis of Ketene O,O-acetals. *Tetrahedron Lett.* **1983**, *24*, 1303.

61. a) Katritzky, A. R.; Jiang, R.; Somment, G. L.; Singh, S. K. One-carbon Homologation of Aryl and Alkyl Aldehydes to Amides Using $BtCH_2P^+Ph_3C^-$. *ARKIVOC*, **2004**, *9*, 44-51. b) Katrizky, A. R.; Yang, Z.; Moutou, J.-L. Conversion of Aldehydes to α-Acetoxymethyl Ketones: One-carbon Homologation with (Benzotriazol-1-yl)phenoxymethane. *Tetrahedron Lett.* **1995**, *36*, 841-844. c) Katritzky, A. R.; Yang, Z.; Cundy, D. J. (Benzotriazol-1-yl)methoxymethyl Anion: A Novel Methlal Anion Equivalent. *Synth. Commun.* **1993**, *23*, 3061-71. d) Dinizo, S. E.; Freerksen, R. W.; Pabst, W. E.; Watt, D. S. A One-Carbon Homolgation of Carbonyl Compounds to Carboxylic Acids , Esters, and Amides. *J. Am. Chem. Soc.* **1977**, *99*, 182-186.

62. a) Cafiero, L. R.; Snowden, T. S. General and Practical Conversion of Aldehydes to Homologated Carboxylic Acids. *Org. Lett.* **2008**, *10*, 3853-3856. b) Li, Z.; Gupta, M. K.; Snowden, T. S. *Eur. J. Org. Chem.* **2015**, 7009-7019. c) Corey, E. J.; Link, J. O.; Shao, Y. Two Effective Procedures for the Synthesis of Trichloromethyl Ketones, Useful Precursors of Chiral α-Amino and α-Hydroxy Acids. *Tetrahedron Lett.* **1992**, *33*, 3435-3438.

63. a) Schäfer, A.; Wellner, A.; Strauss, M.; Schäfer, A.; Wolber, G.; Gust, R. Influence of Chlorine or Fluorine Substitution on the Estrogenic Properties of 1-Allyl-2,3,5,-tris(4-

hydroxyphenyl)-1H-pyrroles. *J. Med. Chem.* **2012**, *55*, 9607-9618. b) Schrittwieser, J. H.; Resch, V.; Wallner, S.; Lienhart, W.-D.; Sattler, J. H.; Resch, J.; Macheroux, P.; Kroutil, W. Biocatalytic Organic Synthesis of Optically Pure (S)-Scoulerine and Berbine and Benzylisoquinoline Alkaloids. *J. Org. Chem.* **2011**, *76*, 6703-6714.

64. Khodaei, M. M.; Alizadeh, A.; Nazari, E. Tf2O as a Rapid and Efficient Promoter for the Dehydrative Friedel-Crafts Acylation of Aromatic Compounds with Carboxylic Acids. *Tetrahedron Lett.* **2007**, *48*, 4199-4202.

65. Parker, K. A.; Fokas, D. The Radical Cyclization Approach to Morphine. Models for Highly Oxygenated Rin-III Synthons. *J. Org. Chem.* **1994**, *59*, 3933-3988.

66. Tallman, K. A.; Roschek, B.; Porter, N. A. Factors Influence the Autoxidation of Fatty Acids: Effects of Olefin Geometry of the Nonconjugated Diene. *J. Am. Chem. Soc.* **2004**, *126*, 9240-9247.

67. Lee, J. H.; Deng, L. Asymmetric Approach toward Chiral Cyclohex-2-enones from Anisoles via an Enantioselective Isomerization by a New Chiral Diamine Catalyst. *J. Am. Chem. Soc.* **2012**, *134*, 18209-18212.

68. Nammalwar, B.; Bunce, R. A. Friedel-Crafts Cyclzation of Tertiary Alcohols Using Bismuth(III)triflate. *Tetrahedron Lett.* **2013**, *54*, 4330-4332.

69. Bunce, R. A.; Cox, A. N. Tetrahydronaphthalene Derivatives by Amberlyst 15-promoted Friedel-Crafts Cyclization. *Org. Prep. Proced. Int.* **2010**, *42*, 83-93.

70. Parlow, J. J. Syntheses of Tetrahydronaphthalenes. Part II. *Tetrahedron* **1994**, *50*, 3297-3314.

71. Braude, E. A.; Webb, A. A.; Sultanbawa, M. Studies in the Vitamin D Field. Part III. Approaches to Derivatives of 5-Hydroxy-2-methylcyclohexanone. *J. Chem. Soc.* **1958**, 3328-3336.

72. Nelson, S. G.; Bungard, C. J.; Wang, K. Catalytic Olefin Isomerization Leading to Highly Stereoselective Claisen Rearrangements of Aliphatic Allyl Vinyl Ethers. *J. Am. Chem. Soc.* **2003**, *125*, 13000-13001.

73. Acharya, H. P.; Miyoshi, K.; Kobayashi, Y. Mercury-Free Preparation and Selective Reactions of Propargyl (and Propargylic) Grignard Reagents. *Org. Lett*. **2007**, *9*, 3535-3538.

74. Reetz, M. T.; Westermann, J.; Kyung, S.-H. Direct Geminal Dimethylation of Ketones and Exhaustive Methylation of Carboxylic Acid Chlorides Using Dichlorodimethyltitanium. *Chem. Ber.* **1985**, *118*, 1050-1057.

75. a) Liu, Y.; Xu, W.; Wang, X. Gold(I)-Catalyzed Tandem Cyclization Approach to Tetracyclic Indolines. *Org. Lett.* **2010**, *12*, 1448-1451. b) Barabé, F.; Bétournay, G.; Bellavance, G.; Barriault, L. Gold-Catalyzed Synthesis of Carbon-Bridged Medium-Sized Rings. *Org. Lett.* **2009**, *11*, 4236-4238. c) Staben, S. T.; Kennedy-Smith, J. J.;

Huang, D.; Corkey, B. K.; LaLonde, R. L.; Toste, F. D. Gold(I)-Catalyzed Cyclizations of Silyl Enol Ethers: Application to the Synthesis of (+)-Lycopladine A. *Angew. Chem. Int. Ed.* **2006**, *45*, 5991-5994.

76. Ngoc, D. T.; Albicker, M.; Schneider, L.; Cramer, N. Enantioselective Assembly of the Benzo[d]xanthene Tetracyclic Core of Anti-influenza Active Natural Products. *Org. Biomol. Chem.* **2010**, *8*, 1781-1784. See also: Jarugumilli, G. K.; Zhu, C.; Cook, S. P. Re-evaluating the Nucleophilicity of Zinc Enolates in Alkylation Reactions. *Eur. J. Org. Chem.* **2012**, 1712-1715.

77. a) Vuagnoux-d'Augustin, M.; Alexakis, A. Copper-catalyzed Asymmetric Conjugate Addition of Trialkylaluminium Reagents to Trisubstituted Enones: Construction of Chiral Quaternary Centers. *Chem. Eur. J.* **2007**, *13*, 9647-9662. b) Alexakis, A.; Bäckvall, J. E.; Krause, N.; Pàmies, O.; Diéguez, M. Enantioselective Copper-Catalyzed Conjugation Addition and Allylic Substitution Reactions. *Chem. Rev.* **2008**, *108*, 2796-2823. See also: Germain, N.; Guénée, L.; Mauduit, M.; Alexakis, A. Asymmetric Conjugate Addition to α-Substituted Enones/Enolate Trapping. *Org. Lett.* **2014**, *16*, 118-121.

78. a) Liu, H.-J.; Zhu, B.-Y. Efficient Addition of Cerium(III) Enolate of Ethyl Acetate to Ketones: Application to the Synthesis of β-Ethoxycarbonylmethyl α,β-Unsaturated Ketones. *Can. J. Chem.* **1991**, *69*, 2008-2013. b) Eidman, K. F.; MacDougall, B. S. Synthesis of Loliolide, Actinidiolide, Dihydroactinidiolide, and Aeginetolide via Cerium Enolate Chemistry. *J. Org. Chem.* **2006**, *71*, 9513-9516.

79. Teichert, J. F.; Feringa, B. L. Phosphoramidites: Privileged Ligands in Asymmetric Catalysis. *Angew. Chem. Int. Ed.* **2010**, *49*, 2486-2528.

80. Baldwin, J. E. Rules for Ring Closure. *J. Chem. Soc., Chem. Commun.* **1976**, 734-736.

81. Brown, C. A.; Yamashita, A. The Acetylene Zipper. Exceptionally Facile "Contrathermodynamic" Multipositional Isomerization of Alkynes with Potassium 3-Aminopropylamide. *J. Am. Chem. Soc.* **1975**, *97*, 891-892.

82. a) Valeev, R.; Bikzhanov, R. F. Yagafarov, N. Z.; Niftakhov, M. S. Synthesis of the Northern Fragment of an Epothilone D Analog from (-)-Carvone. *Tetrahedron* **2012**, *68*, 6868-6872 b) Rubottom, G. M., Vazques, M. A., Pelegrina, D. R. Peracid Oxidation of Trimethylsilyl Enol Ethers. Facile α-Hydroxylation Procedure. *Tetrahedron Lett.* **1974**, 4319-4322. c) Zoretic, P. A.; Wang, M.; Zhang, Y.; Shen, Z. Total Synthesis of *d/l*-Isospongiadiol: An Intramolcular Radical Cascade Approach to Furanoditerpenes. *J. Org. Chem.* **1996**, *61*, 1806-1813.

83. Netherton, M. R.; Dai, C.; Neuschuetz, K.; Fu, G. Room-Temperature Alkyl-Alkyl Suzuki Cross-Coupling of Alkyl Bromides that Possess β-Hydrogens. *J. Am. Chem. Soc.* **2001**, *123*, 10099-10100.

84. Clary, J. W.; Rettenmaier, T. J.; Snelling, R.; Bryks, W.; Banwell, J.; Wipke, W. T.; Singaram, B. Hydride as a Leaving Group in the Reaction of Pinacolborane with Halides

under Ambient Grignard and Barbier Conditions. One-Pot Synthesis of Alkyl, Aryl, Heteroaryl, Vinyl, and Allyl Pinacolborane Esters. *J. Org. Chem.* **2011**, *76*, 9602-9610. See also: Ito, H.; Kubota, K. Copper(I)-Catalyzed Boryl Substitution of Unactivated Alkyl Halides. *Org. Lett.* **2012**, *14*, 890-893.

85. a) Laube, T.; Schröder, J.; Stehle, R.; Seifert, K. Total Synthesis of Yahazunol, Zonarone and Isozonarone. *Tetrahedron*, **2002**, *58*, 4299-4309. b) Pollini, G. P.; Bianchi, A.; Casolari, A.; De Risi, C.; Zanirato, V.; Bertolasi, V. An Efficient Approach to Chiral Nonracemic trans- and cis-Decalin Scaffolds for Drimane and Labdane Synthesis. *Tetrahedron: Asymmetry* **2004**, *15*, 3223-3231.

86. Markwell-Heys, A. W.; Kuan, K. K. W.; George, J. H. Total Synthesis and Structure Revision of (-)-Siphonodictyal B and Its Biomimetic Conversion into (+)-Liphagal. *Org. Lett.* **2015**, *17*, 4228-4231. For a review, see: Frija, L. M. T.; Frade, R. F. M.; Afonso, C. A. M. Isolation, Chemical, and Biotransformation Routes of Labdane-type Diterpenes. *Chem. Rev.* **2011**, *111,* 4418-4452.

87. a) Mercier, A. M.; Yeo, W. C.; Chou, J.; Chaudhuri, P. D.; Bernardinelli, G.; Kündig, E. P. Synthesis of Highly Enantiomerically Enriched Planar Chiral Ruthenium Complexes via Pd-catalyzed Asymmetric Hydrogenolysis. *Chem. Commun.* **2009**, *35*, 5227-5229. b) Kuendig, E. P.; Monnier, F. R. Efficient Synthesis of Tri(acetonitrile)-(η^5-cyclopentadienyl)-ruthenium(II) Hexafluorophosphate via Ruthenocene. *Adv. Synth. Catal.* **2004**, *346*, 901-904.

88. Klemm, L. H.; Klemm, R. A.; Santhanam, P. S.; White, D. V. Intramolecular Diels-Alder Reactions. VI. Syntheses of 3-Hydroxymethyl-2-naphthoic Acid Lactiones. *J. Org. Chem.* **1971**, *36*, 2169-2172.